

DOPAMINE-MEDIATED ALTERATIONS IN BRAIN-WIDE FUNCTIONAL DYNAMICS  
MEASURED BY fMRI

Heather Kaye Decot

A dissertation submitted to the faculty at the University of North Carolina at Chapel Hill in partial fulfillment of the requirements for the degree of Doctor of Philosophy in the Biological and Biomedical Sciences Program (Neuroscience Curriculum) in the Graduate School.

Chapel Hill  
2017

Approved by:

Garret D. Stuber

Yen-Yu Ian Shih

John H. Gilmore

Joyce Besheer

Fulton T. Crews

Regina M. Carelli

© 2017  
Heather Kaye Decot  
ALL RIGHTS RESERVED

## **ABSTRACT**

Heather Kaye Decot: Dopamine-Mediated Alterations in Brain-Wide Functional Dynamics  
Measured by fMRI  
(Under the direction of Garret D. Stuber)

Drug addiction is a complex, multifaceted disease characterized by compulsive drug-seeking and drug-taking behavior despite adverse consequences. In accordance with its complex nature, several neural systems are likely to be dysregulated to promote maladaptive behaviors associated with addiction. For instance, dopaminergic signaling within the mesolimbic dopamine (DA) system is thought to be critical for reward prediction, an adaptive process that likely goes awry in addiction. While it is well known that DA release events occur in mesolimbic terminal fields such as the nucleus accumbens (NAc) in response to reward predictive cues, including those associated with drugs of abuse, how DA release events affect network adaptation across the entire brain has largely been unexplored. To address this, we selectively activated ventral tegmental area (VTA) dopaminergic ( $TH^{VTA}$ ) neurons in transgenic rats and measured resulting changes in whole-brain activity using stimulus-evoked functional magnetic resonance imaging (fMRI). We demonstrated DAergic modulation activates several anatomically distinct regions throughout the brain, many of which receive little to no direct dopaminergic input. We also showed that explicit pairing of midbrain dopamine neuron activity and a sensory stimulus can dramatically enhance the brain-wide representation of that specific sensory stimulus. Next, since drugs of abuse increase extracellular DA in the mesolimbic pathway of the brain, we utilized a rodent model of addiction to explore whether functional connectivity is altered after self-administration of cocaine. We found that cocaine self-

administration orchestrates dynamic shifts in functional connectivity across many anatomically defined neuronal network nodes. Overall, these findings suggest that DA not only controls plasticity in direct target regions, but may effectively modulate brain-wide network plasticity as well. This research may provide critical insight into the circuit-level maladaptations that underlie compulsive drug-seeking behavior, and the chronic cycles of abstinence and relapse that characterize addiction in humans.

I dedicate this work to my Grandma, Grandpa, Grammy and Grandpa Schmidt. Thank you for your guidance, protection and for always cheering me on. I am so proud to be your granddaughter. I love you so much.

## **ACKNOWLEDGEMENTS**

I would first like to thank my thesis mentor, Garret Stuber. It has been an incredible honor being a member of your lab. Thank you for your guidance and support and for allowing me to bridge optogenetics and fMRI through my experiments. Your fearlessness and abilities to adapt and grow in the ever-changing world of scientific research are unmatched and it has been so neat to be able to be a part of the evolution of this lab over these past 6 years. I have learned so much from you, and will walk with confidence and pride into the next stage of my career because of it.

To Ian, your lab was a second home to me. Thank you for allowing me to be a part of your lab. Your generosity and kindness have meant so much to me. Some of my fondest memories from graduate school are from the ISMRM conferences that I had the privilege to attend.

To my lab mates past and present, thank you for always being there for me and for assisting me whenever I have needed help or guidance. I have learned so much from each of you and have loved talking both science and life together over these past 6 years. To Manasmita, your constant support and encouragement has meant more than you will ever know. You were there every step of the way. Thank you for your friendship and sisterhood. To Oksana, thank you for always being there for me and for all of your help and encouragement. To Vijay and SungHo, thank you for your data analysis expertise and friendships. You have taught me so much and it was such a pleasure being able to work with you. To Jill and Hsin-yi, thank you for your warmth and kindness and dedicating so much of your time to teaching me about MRI acquisition when I first started in lab. Your support over the years has meant so much to me.

To my entire committee, Gina, Ian, Joyce, Dr. Gilmore and Dr. Crews, thank you for your

unwavering support. To Gina, thank you so much for opening your lab to me and for always supporting me and my endeavors, it has meant so much to me. To Dr. Gilmore, thank you for being my clinical co-mentor for the HHMI translational medicine program and for allowing me to shadow you in the clinic, I truly enjoyed those experiences. To Joyce, thank you for supporting me and for always e-mailing me after my departmental talks with kind and encouraging words. To Dr. Crews, thank you for your guidance and for your insightful comments and enthusiasm related to my work.

Finally, to my family. To my sister Lauren, I have looked up to you every day of my life. Thank you for always been there for Brian and me, guiding and protecting us. To my brother Brian, my Irish Twin, you inspire me every day with everything you have accomplished, I am so proud of you. To my parents, your unyielding love, support, and encouragement has been the root to all of my achievements. I would not be the woman I am today without you and could not have done this without you. I love you so much.

## TABLE OF CONTENTS

LIST OF FIGURES .....	xi
LIST OF ABBREVIATIONS AND SYMBOLS .....	xiii
CHAPTER 1: GENERAL INTRODUCTION .....	1
HISTORY OF DOPAMINE AS A NEUROTRANSMITTER.....	1
CELLULAR COMPOSITION OF THE VTA .....	2
VTA CIRCUITRY .....	5
Connectivity within the VTA .....	5
Afferent Projections to the VTA.....	6
Efferent Projections of the VTA.....	10
EVIDENCE FOR THE ROLE OF DOPAMINE IN REWARD AND MOTIVATION .....	15
ROLE OF DOPAMINE IN DRUG ADDICTION .....	17
OVERVIEW OF OPTOGENETICS .....	19
OPTOGENETIC fMRI .....	22
OVERVIEW OF FUNCTIONAL MRI (fMRI): TASK-BASED VERSUS RESTING STATE fMRI .....	23
DISSERTATION .....	24
CHAPTER 2: COORDINATION OF BRAIN-WIDE ACTIVITY DYNAMICS BY DOPAMINERGIC NEURONS .....	26
INTRODUCTION .....	26
METHODS .....	29
Experimental Subjects and Stereotactic Surgery .....	29
fMRI Procedures.....	30



Data Processing and Statistical Analysis .....	32
Histology, Immunohistochemistry, and Microscopy.....	38
RESULTS .....	38
Viral Targeting of VTA Dopaminergic Neurons in TH-Cre Rats .....	38
Whole Brain Analysis of the Effect of $TH^{VTA}$ Neuron Stimulation .....	39
Whole Brain Analysis of Forepaw Stimulation Pre and Post Pairing with $TH^{VTA}$ Neuron Stimulation .....	43
DISCUSSION .....	44
FIGURES .....	51
CHAPTER 3: BRAIN-WIDE FUNCTIONAL CONNECTIVITY CHANGES FOLLOWING SELF-ADMINISTRATION OF COCAINE AND ABSTINENCE .....	59
INTRODUCTION .....	59
METHODS .....	61
Experimental Subjects .....	61
fMRI Procedures.....	61
Cocaine Self-Administration .....	62
Data Pre-Processing.....	63
Functional Connectivity Analysis.....	63
Dual Regression Analysis.....	64
RESULTS .....	65
DISCUSSION .....	67
FIGURES .....	72
CHAPTER 4: GENERAL DISCUSSION .....	80
SUMMARY OF FINDINGS .....	80
GENERAL IMPLICATIONS OF FINDINGS.....	81
TECHNICAL CONSIDERATIONS AND LIMITATIONS.....	84

Anesthesia.....	84
Light and Heating Artifacts During Opto-fMRI Experiments .....	85
Imaging Resolution.....	85
FUTURE DIRECTIONS .....	86
To Explore the Permanence of our Findings .....	86
To Explore Sex- and Age-Based Brain Functional Connectivity Differences Following Cocaine Exposure. ....	87
APPENDIX 1: SUPPLEMENTAL MATERIALS FOR CHAPTER 2.....	90
APPENDIX 2: SUPPLEMENTAL MATERIALS FOR CHAPTER 3.....	99
REFERENCES .....	101

## LIST OF FIGURES

Figure 1.1: Afferent projections to the VTA. ....	8
Figure 2.1: Viral targeting of VTA dopaminergic neurons in TH-cre rats. ....	51
Figure 2.2: Optical fiber placement in the VTA of TH-cre rats. ....	52
Figure 2.3: Whole brain analysis of the effect of TH <sup>VTA</sup> neuron stimulation. ....	53
Figure 2.4: Map of defined regions of interest. ....	55
Figure 2.5: Whole brain analysis of forepaw stimulation pre and post pairing with TH <sup>VTA</sup> neuron stimulation. ....	56
Figure 2.6: Evolution of forepaw stimulation pairing response over the course of pairings. ....	58
Figure 3.1: Experimental timing diagram and self-administration training data. ....	72
Figure 3.2: Resting state networks derived from the multi-subject ICA analysis. ....	73
Figure 3.3: Cocaine exposure causes a significant increase in functional activity between the visual network and the anterior cingulate cortex in drug naïve rats. ....	75
Figure 3.4: Cocaine exposure causes a significant increase in functional connectivity between the sensorimotor network and the primary somatosensory cortex in drug naïve rats. ....	76
Figure 3.5: Cocaine exposure causes an increase in functional connectivity between the somatosensory network and the anterior cingulate cortex in drug naïve rats. ....	77
Figure 3.6: Cocaine exposure causes a decrease in functional connectivity between the hippocampal network and the insular cortex in drug naïve rats. ....	77
Figure 3.7: Seed-based whole brain connectivity maps of pre-cocaine and post-cocaine rsfMRI data. ....	78
Figure 3.8: Functional connectivity changes following cocaine exposure in drug naïve rats. ....	79
Figure A.1: Optical fiber placements in the VTA of TH-cre rats. ....	90
Figure A.2: Activation of VTA dopaminergic neurons increases CBV signals in striatal target regions. ....	91
Figure A.3: Additional results for the TH <sup>VTA</sup> stimulation experiment. ....	93

Figure A.4: Whole brain analysis of the effect of 1 s TH <sup>VTA</sup> neuron stimulation. ....	95
Figure A.5: Optical fiber placements in the VTA of TH-cre rats for the pairing experiments. ....	96
Figure A.6: Pairing VTA dopamine neuronal activity with somatosensory stimuli enhances the neuronal representation of the sensory stimulus. ....	97
Figure A.7: Additional results for the forepaw stimulation pre and post pairing with THVTA stimulation. ....	98
Figure A.8: The independent components derived from the multi-subject ICA analysis that were excluded from further analysis due to noise artifacts. ....	99
Figure A.9: Seed-based whole brain connectivity maps of pre-cocaine and post-cocaine rsfMRI data. ....	100

## **LIST OF ABBREVIATIONS AND SYMBOLS**

AAV	Adeno-associated virus
AFNI	Analysis of Functional NeuroImages
ANOVA	Analysis of variance
BLA	Basolateral amygdala
BNST	Bed nucleus of the stria terminalis
BOLD	Blood-oxygen-level dependent
CBV	Cerebral blood volume
CDC	Centers for disease control and prevention
CeA	Central nucleus of the amygdala
ChR2	Channelrhodopsin-2
CPu	Caudate putamen
D1R	D1-receptor
D2R	D2-receptor
DA	Dopamine
DAT	Dopamine transporter
DBS	Deep brain stimulation
DIO	Double-floxed inverted open reading frame
DMS	Dorsomedial striatum
EF1 $\alpha$	Elongation factor 1-alpha
EPI	Echo-planar imaging
EtCO <sub>2</sub>	End-tidal carbon dioxide
eYFP	Enhanced yellow fluorescent protein
FDR	False discovery rate

fMRI	Functional magnetic resonance imaging
FOV	Field of view
GABA	Gamma-aminobutyric acid
GLM	Generalized linear model
HPC	Hippocampus
HRF	Hemodynamic response function
$I_h$	Hyperpolarization-activated cation current
IPN	Interpeduncular nucleus
LH	Lateral hypothalamus
LHb	Lateral habenula
L-DOPA	Levodopa
NAc	Nucleus accumbens
mPFC	Medial prefrontal cortex
MION	Monocrystalline iron oxide nanoparticles
NpHR	Halorhodopsin
opto-fMRI	Optogenetic-functional magnetic resonance imaging
OVX	Ovariectomized
PBS	Phosphate buffered saline
PC	Principal component
PCA	Principal component analysis
pCO <sub>2</sub>	Partial pressure of carbon dioxide
RARE	Rapid imaging with refocused echoes
RMTg	Rostromedial tegmental nucleus

ROI	Region of interest
RF	Radio frequency
rsfMRI	Resting state functional magnetic resonance imaging
rTMS	Repetitive transcranial magnetic stimulation
S1	Primary somatosensory cortex
SEM	Standard error of the mean
SNc	Substantia nigra pars compacta
SPM	Statistical parametric mapping
SpO <sub>2</sub>	Oxygen saturation
TH	Tyrosine hydroxylase
TH <sup>VTA</sup>	Ventral tegmental area dopaminergic neurons
TE	Echo time
TR	Repetition time
VMAT	Vesicular monoamine transporter
VTA	Ventral tegmental area

## **CHAPTER 1: INTRODUCTION**

### **HISTORY OF DOPAMINE AS A NEUROTRANSMITTER**

Although first synthesized in 1910, our modern understanding of dopamine (DA) function in the brain began in the late 1950s when Arvid Carlsson discovered that DA not only serves as a precursor for norepinephrine and epinephrine but is also a neurotransmitter itself (Carlsson, Lindqvist, Magnusson, & Waldeck, 1958). In a set of seminal experiments, Carlsson and colleagues measured catecholamine expression across the dog brain and reported high concentrations of DA in the striatum, despite norepinephrine levels being low in this region (Bertler & Rosengren, 1959; Carlsson, 1959). Furthermore, reserpine, a vesicular monoamine transport (VMAT) inhibitor which causes the depletion of monoamine neurotransmitters in the synapse, caused a loss of movement control in mice and rabbits, a core symptom of Parkinson's disease (Carlsson, Lindqvist, & Magnusson, 1957). Notably, injecting levodopa (L-DOPA), the precursor to DA, reversed the reserpine-induced immobility. Carlsson initially hypothesized this effect was due to the ability of L-DOPA to restore norepinephrine in the basal ganglia, however found a resurgence of DA instead. In 1960, Oleh Hornykiewicz would provide a critical translational complement to Carlsson's preclinical work by being the first to report substantially low DA levels within the striatum in postmortem brain tissue derived from human patients with Parkinson's disease (Ehringer & Hornykiewicz, 1960). The following year, Hornykiewicz and neurologist Walther Birkmayer gave intravenous application of L-DOPA to patients with



Parkinson's disease and observed significant and rapid alleviation of symptoms (Birkmayer & Hornykiewicz, 1961). More than 50 years later, L-DOPA is still considered the most effective drug treatment for the management of Parkinson's disease.

Taken together, these discoveries provided the first evidence that, contrary to the prevailing notion of the first half of the 20<sup>th</sup> century that DA had limited function beyond being an intermediate for norepinephrine and epinephrine, dopaminergic signaling within the basal ganglia is critical for the control of motor function and its loss plays a significant role in the pathogenesis of Parkinson's disease. The scope of the diversity and complexity of the role of DA signaling in the brain, beyond motor control, would begin to widen greatly in subsequent decades.

## **CELLULAR COMPOSITION OF THE VTA**

It is now well established that midbrain dopaminergic neurons are essential not only in motor control, but in the expression of other diverse behavioral states including motivation, reinforcement, and associative learning (discussed in detail in the section titled 'Evidence for the role of dopamine in reward and motivation'), and maladaptive changes in their activity are associated with several neuropsychiatric disorders (Salamone, Correa, Farrar, & Mingote, 2007; W. Schultz, 2001; Roy A. Wise, 2004). Although paradoxical in regards to what is now known regarding the complexities of DA function in the brain, there are only estimated to be ~400,000-600,000 DA neurons in the human brain, which account for less than 1% of the total neuronal population (Björklund & Dunnett, 2007; German, Schlusberg, & Woodward, 1983). The main sources of DA in the brain originate from midbrain DA neurons located in the ventral tegmental area (VTA) and substantia nigra pars compacta (SNc). Situated adjacent to each other, the SNc is comprised almost entirely of DA neurons (~90%) and sends dense projections to the dorsal striatum, deterioration of these cells leads to the loss of motor control seen in Parkinson's

disease, whereas the VTA is heterogeneous in cell type composition and projects to the ventral striatum, and to other limbic and cortical structures including the amygdala, septum, hippocampus, and prefrontal cortex (Swanson, 1982). The VTA is comprised of DA (~65%), GABA (~30%), and glutamate (<5%) neurons (Dobi, Margolis, Wang, Harvey, & Morales, 2010; Margolis, Lock, Hjelmstad, & Fields, 2006; Nair-Roberts et al., 2008). Notably, however, several studies using slice electrophysiology have now explicitly shown that a subset of VTA DA neurons co-release DA with glutamate or GABA which are also capable of postsynaptic signaling (Chuhma et al., 2004; Hnasko et al., 2010; Lavin et al., 2005; Stuber, Hnasko, Britt, Edwards, & Bonci, 2010; Tecuapetla et al., 2010; Tritsch, Ding, & Sabatini, 2012; Tritsch, Oh, Gu, & Sabatini, 2014). Future work investigating the effects of coincidental signaling by glutamate and GABA will need to be performed to further our understanding of the functional significance of neurotransmitter co-release from VTA DAergic neurons.

The electrophysiological properties of VTA DA neurons are also diverse. Although initial reports specified a large hyperpolarization-activated inwardly rectifying cation current ( $I_h$ ) as physiological criteria for the identification of midbrain dopaminergic neurons, this is no longer accurate (Johnson & North, 1992; Mercuri, Bonci, Calabresi, Stefani, & Bernardi, 1995). It has now been well documented that several non-dopaminergic VTA neurons exhibit  $I_h$  current (Margolis, Hjelmstad, Bonci, & Fields, 2003; Margolis et al., 2006; T. A. Zhang, Placzek, & Dani, 2010), and furthermore a subset of dopaminergic neurons that project to the mPFC lack  $I_h$  current altogether (Lammel et al., 2008). Thus, coupling electrophysiology with retrograde neuronal labeling and immunohistochemistry staining techniques (i.e. for *tyrosine hydroxylase* (TH), the rate-limiting enzyme in DA biosynthesis) is important to aid in the proper identification of these neurons. Recent work suggests  $I_h$  magnitude of midbrain DA neurons can

vary based on the positioning of these neurons within the VTA as well as their projection targets (Ford, Mark, & Williams, 2006; Lammel et al., 2008). DA neurons situated more laterally within the VTA exhibit larger amplitude  $I_h$  relative to those positioned in the medial VTA (T. A. Zhang et al., 2010). Consistent with this, a retrograde tracing study found that VTA DA neurons that project to the BLA exhibit large  $I_h$  amplitudes and are situated primarily in the anterior/lateral portions of the VTA whereas projection fibers to the NAc have significantly smaller  $I_h$  and originate in the posterior/medial regions (Ford et al., 2006).

Finally, several studies also indicate a high degree of molecular heterogeneity among midbrain DA neurons. The biosynthetic pathway of DA begins with the conversion of phenylalanine to tyrosine by phenylalanine hydroxylase. Tyrosine is converted to L-DOPA by the enzyme tyrosine hydroxylase (TH) and L-DOPA is then converted to DA through the removal of its carboxyl group by DOPA-decarboxylase. After DA is synthesized or has undergone reuptake via DAT transporters, it is packaged into vesicles by vesicular monoamine transporter 2 (VMAT2) where it is then stored until release. Levels of expression of these signature molecular markers of DA neurons (i.e. TH, DAT, VMAT2) show variation within the VTA. For example, DAT mRNA expression, as well as DAT/TH and DAT/VMAT2 mRNA expression ratios is very low in mPFC projecting VTA DA neurons (Lammel et al., 2008). Glycosylated DAT, the active form of the transporter, has also been shown to have variable expression across the rodent VTA, with expression highest within the dorsolateral region (Afonso-Oramas et al., 2009). Comprehensive findings from past and future studies utilizing reverse transcription quantitative PCR (qRT-PCR) and RNA-seq techniques on a single cell level will be critical in advancing our understanding of the heterogeneity of gene expression profiles

of individual DA neurons within the midbrain (Lammel et al., 2008; Poulin et al., 2014; Stamatakis et al., 2013).

## **VTA CIRCUITRY**

### **Connectivity within the VTA**

Within the VTA, GABA neurons form local, direct synaptic connections onto VTA DA neurons (Johnson & North, 1992; van Zessen, Phillips, Budygin, & Stuber, 2012). VTA GABA neuron stimulation both *in vitro* and *in vivo* have shown to reduce the activity and excitability of VTA DA neurons (Tan et al., 2012; van Zessen et al., 2012). Indeed, van Zessen and colleagues demonstrated that DA release in the NAc in response to electrical stimulation of VTA DA neurons is significantly attenuated by coincidental VTA GABA neuron activation. Furthermore, VTA GABA neuron activation disrupts reward consumption (van Zessen et al., 2012) and causes a conditioned place aversion (Tan et al., 2012). Conversely, optogenetic inhibition of VTA GABA neurons leads to an increase in VTA DA activity (Bocklisch et al., 2013). Taken together, these findings suggest that local VTA GABA neurons are a potent modulator of DAergic output and their drive onto VTA DA neurons may be critical for the initiation of aversion-related behavior.

It has also recently been discovered that VTA glutamatergic neurons establish local excitatory synapses with VTA DAergic neurons that project to the NAc (H.-L. Wang, Qi, Zhang, Wang, & Morales, 2015). Local synaptic glutamate release from VTA glutamatergic neurons through the activation of glutamate receptors on neighboring DA neurons was shown to promote rewarding behavioral phenotypes including optical self-stimulation and place preference.

Finally, VTA DAergic neurons are themselves capable of local somatodendritic release of DA within the VTA (Adell & Artigas, 2004; Beart & McDonald, 1982). DA released within the VTA has been shown to be an important regulator of VTA DA neuron activity, as it binds to

D2 autoreceptors causing autoinhibition of these cells (Bernardini, Gu, Viscardi, & German, 1991; White & Wang, 1984).

### **Afferent Projections to the VTA**

The VTA receives several excitatory and inhibitory inputs from both cortical and subcortical structures which are discussed in detail below (**Figure 1.1**). Recent advances in anatomical mapping experiments using rabies virus-based transsynaptic retrograde tracing have greatly expanded our understanding of the synaptic connectivity within the VTA, by validating previously known anatomical inputs to the VTA as well as identifying new inputs (Beier et al., 2015; Faget et al., 2016; Watabe-Uchida, Zhu, Ogawa, Vamanrao, & Uchida, 2012). Building a comprehensive map that identifies the specific inputs onto VTA DAergic and non-DAergic neurons, as well as determining how they modulate the activity of these cells is critical for our understanding of how the midbrain regulates adaptive behaviors such as reward prediction but also how maladaptive alterations within these circuits can lead to the manifestation of neuropsychiatric disease such as drug addiction.

#### *Lateral hypothalamus (LH)*

The lateral hypothalamus (LH) is composed of diverse genetically distinct cell types, sending glutamatergic, GABAergic, and peptidergic projections to the VTA involved in homeostatic physiology and motivated behavior. In fact, the LH provides one of the largest subcortical inputs to the VTA (Geisler, Derst, Veh, & Zahm, 2007; Nieh et al., 2015; Phillipson, 1979; Watabe-Uchida et al., 2012). Rodents that have received lesions of the LH exhibit profound lack of goal-directed behavior, including severe deficits in feeding and drinking, notably similar to the phenotypes observed in DA-deficient mice (Anand & Brobeck, 1951a; Grossman, Dacey, Halaris, Collier, & Routtenberg, 1978; Stricker, Swerdloff, & Zigmond, 1978; Zhou & Palmiter, 1995). Conversely, non-specific electrical stimulation of the LH causes

insatiable food intake behavior (Anand & Brobeck, 1951b; Delgado & Anand, 1953) and persistent intracranial self-stimulation (Olds & Milner, 1954). Furthermore, LH self-stimulation has been found to cause release of DA in the NAc (Hernandez & Hoebel, 1988; You, Chen, & Wise, 2001). Taken together, these findings suggest that LH input to the VTA, possibly via drive onto VTA DA neurons, is an important pathway in the activation of brain reward circuits as well as reinforcing behavioral responding.

The immense heterogeneity of the LH has been an obstacle for elucidating the exact circuit mechanisms underlying its role in motivated behavior. A recent study by Nieh and colleagues demonstrated that both glutamatergic and GABAergic LH fibers functionally innervate both VTA GABA neurons and VTA DA neurons (Nieh et al., 2015). GABAergic projection fibers from the LH preferentially innervate VTA GABA neurons, reducing local activity-dependent GABA release onto VTA DA neurons and thus causing disinhibition of these cells. More cell-type specific optogenetic targeting approaches will need to be performed to further disentangle the functional heterogeneity of the LH and its projection targets.

#### *Medial Prefrontal Cortex (mPFC)*

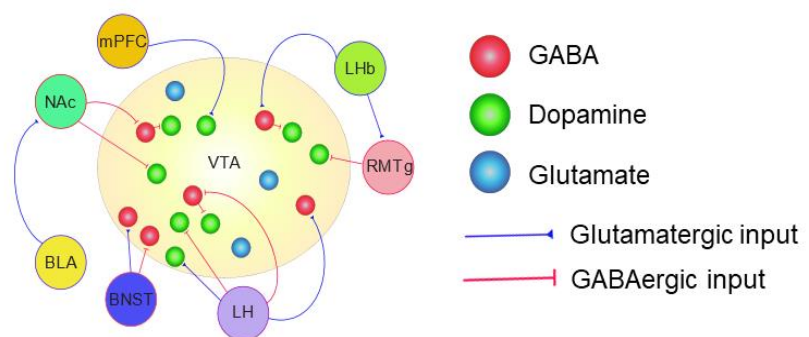
The medial prefrontal cortex (mPFC) provides another main source of glutamatergic input to the VTA (Geisler, Derst, Veh, & Zahm, 2007). VTA-projecting mPFC neurons are found predominantly in layer 5 of the cortex (Gabbott, Warner, Jays, Salway, & Busby, 2005) and through the use of electron microscopy, Carr and Sesack found that they preferentially synapse onto mPFC-projecting VTA dopaminergic neurons and NAc-projecting VTA GABAergic neurons (Carr & Sesack, 2000b). Activation of prelimbic cortex layer 5 pyramidal neurons has been shown to promote synchronized oscillatory activity across limbic projection target regions, including the NAc, BLA and VTA (Kumar et al., 2013). However, future studies using optogenetic tools to selectively target mPFC afferents to the VTA will need to be

performed to provide more insight on the specific synaptic connectivity between these two regions and the role this circuit plays on complex behavioral and affective states.

### *Lateral Habenula (LHb)*

The lateral habenula (LHb) provides another important source of glutamatergic drive into the VTA. The LHb encodes negative reward prediction error and is activated by aversive stimuli/reward omission and inhibited by unexpected rewards (Matsumoto & Hikosaka, 2007, 2009). Activation of the LHb almost completely abolishes the activity of midbrain DA neurons (Christoph, Leonzio, & Wilcox, 1986) and leads to reduced DA release in the NAc (Lisoprawski, Herve, Blanc, Glowinski, & Tassin, 1980). The LHb sends direct glutamatergic inputs to the VTA that are confirmed to form synapses predominantly onto GABAergic neurons (Brinschwitz et al., 2010; Lammel et al., 2012; Stamatakis & Stuber, 2012) that inhibit DA VTA activity. Consistent with this, local application of the GABA<sub>A</sub> receptor antagonist bicuculline into the VTA attenuates LHb-induced suppression of DA neuron activity (Ji & Shepard, 2007). In addition to modulating VTA DAergic activity through its glutamatergic drive onto VTA GABAergic neurons, the LHb also sends glutamatergic inputs onto the rostromedial tegmental nucleus (RMTg), a GABAergic

structure just posterior to the VTA, that directly inhibits VTA DA neurons (Jhou, Fields, Baxter, Saper, & Holland, 2009; Jhou, Geisler, Marinelli, Degarmo, & Zahm, 2009). Exposure to acute



**Figure 1.1: Afferent projections to the VTA.**

The VTA is comprised of DA (~65%), GABA (~30%), and glutamate (<5%) neurons. The VTA receives several excitatory and inhibitory inputs from both cortical and subcortical structures. The afferents discussed in this dissertation are illustrated above.

unpredictable footshock in mice increased LHb excitatory drive onto RMTg neurons and optogenetic stimulation of this pathway promoted behavioral avoidance (Stamatakis & Stuber, 2012). Taken together, the LHb is a critical node of the reward circuit by providing negative value signals to DAergic neurons of the midbrain, and thus important for survival by promoting punishment avoidance behaviors.

#### *Nucleus Accumbens (NAc)*

The nucleus accumbens (NAc) sends a major GABAergic projection to the VTA (Heimer, Zahm, Churchill, Kalivas, & Wohltmann, 1991; P. W. Kalivas, Churchill, & Klitenick, 1993; Nauta, Smith, Faull, & Domesick, 1978). D1-receptor expressing medium spiny neurons (MSNs) of the NAc preferentially target VTA GABA neurons (Bocklisch et al., 2013; Hjelmstad & Fields, 2003). Furthermore, activating GABA<sub>A</sub> receptors in the VTA increases DA release in the NAc (Xi & Stein, 1998). Taken together, these results suggest that activation of GABAergic afferents from the NAc and other regions may cause a transient increase in VTA DA activity via a disinhibitory mechanism and may provide a putative mechanism for the persistent reinforcement behavior induced by optogenetic stimulation of D1-receptor expressing MSNs of the NAc (Kravitz, Tye, & Kreitzer, 2012). GABAergic inputs from the NAc also form synapses directly onto VTA DA neurons (Watabe-Uchida et al., 2012), however the inhibitory projection onto VTA GABA neurons is much more robust (Bocklisch et al., 2013).

#### *Bed Nucleus of the Stria Terminalis (BNST)*

The bed nucleus of the stria terminalis (BNST) sends a dense projection to the VTA (Geisler & Zahm, 2005; Jalabert, Aston-Jones, Herzog, Manzoni, & Georges, 2009; Kudo et al., 2012). Known for playing an essential role in modulating sustained fear and anxiety states (Michael Davis, Walker, Miles, & Grillon, 2010; Walker & Davis, 2008), understanding the BNST and its precise functional connectivity with regions across the brain has become an



important question to unravel. Jennings, Sparta and colleagues found that the BNST sends both glutamatergic and GABAergic inputs to the VTA that preferentially synapse onto VTA GABAergic neurons (Jennings et al., 2013). This work revealed that these two distinct neuronal cell type projections have opposing roles. VTA projecting glutamatergic neurons displayed an enhancement in activity following exposure to an aversive stimulus, whereas BNST GABAergic neurons were inhibited. Furthermore, *in vivo* optogenetic stimulation of BNST glutamatergic inputs to the VTA caused aversion and anxiety, whereas stimulating BNST GABAergic inputs produced reward-related behaviors and anxiolytic effects. Finally, it was found that concurrent stimulation of BNST GABAergic inputs to the VTA during an unpredictable foot-shock session could reduce the development of subsequent anxiety-like behaviors. Taken together, these data reveal how two distinct BNST neuronal projections onto a shared target region can promote very opposing behavioral effects. This may provide new insight as to a potential circuit mechanism underlying neuropsychiatric disorders, especially those related to anxiety, where proper glutamatergic and GABAergic drive from the BNST onto VTA GABAergic neurons is critical and if one becomes altered, maladaptive behavior ensues.

### **Efferent Projections of the VTA**

As previously stated, the VTA is heterogeneous in cell type composition and projects to several forebrain targets including the NAc, basolateral amygdala (BLA), hippocampus, and prefrontal cortex (Swanson, 1982). Several pioneering studies using optogenetic tools (discussed in detail in ‘Overview of Optogenetics’) to directly activate VTA DAergic neurons in freely behaving rodents have found that phasic activation of these neurons promotes behavioral conditioning (Tsai et al., 2009; Witten et al., 2011) and positive reinforcement (Adamantidis et al., 2011; Steinberg et al., 2014). Notably, the stimulation parameters used to selectively activate midbrain DA neurons that mediated behavioral conditioning as measured by conditioned place

preference (Tsai et al., 2009) also caused transient DA release in the NAc, suggesting that associative learning is driven by stimulation frequencies that cause observable DA transients in limbic terminal fields such as the NAc. These projections, as well as the studies that have demonstrated their significance in the expression of motivated behavior are discussed in detail below.

### *Nucleus Accumbens (NAc)*

The NAc receives DAergic, GABAergic, and glutamatergic inputs from the VTA (Brown et al., 2012; Hnasko, Hjelmstad, Fields, & Edwards, 2012; Margolis et al., 2006; Qi et al., 2016; Van Bockstaele & Pickel, 1995; van Zessen et al., 2012). The NAc, commonly referred to as the limbic-motor interface, is a critical node for the manifestation of learned associations between environmental stimuli and primary reinforcers, and in translating this information into conditioned approach behavior (Mogenson, Jones, & Yim, 1980). DAergic projections from the VTA to the NAc comprise the mesolimbic DA system. During reward-seeking behavior, burst firing of these neurons results in phasic DA release in the NAc (Day, Roitman, Wightman, & Carelli, 2007; P. E. M. Phillips, Stuber, Heien, Wightman, & Carelli, 2003; Stuber et al., 2008). Depletion of DA in the NAc or antagonism of DA receptors leads to impairments in acquisition and performance in a Pavlovian conditioning task (Di Ciano & Everitt, 2001). Collectively, these data indicate that activation of midbrain DA neurons, followed by the subsequent release of DA in the NAc, is critical for the expression of learned associations.

As mentioned previously, VTA GABA neurons provide local inhibition through their direct synaptic connections onto VTA DA neurons (Johnson & North, 1992; van Zessen et al., 2012) but also provide long-distance inhibition through their projections to forebrain targets including the NAc (Van Bockstaele & Pickel, 1995). Long-range VTA GABAergic inputs to the NAc selectively target cholinergic interneurons and optogenetic activation of this projection

enhanced discrimination of a conditioned stimulus that had previously been associated with an aversive outcome during a fear conditioning task (Brown et al., 2012).

VTA glutamatergic neurons, in addition to providing local excitatory drive onto VTA DA neurons that project to the NAc and cause rewarding behavioral effects (H.-L. Wang et al., 2015), also send direct, long-range projections to the NAc. A recent study by Qi et al. found that VTA glutamatergic inputs to the NAc preferentially synapse onto parvalbumin GABAergic interneurons and activation of this pathway promotes conditioned place aversion (Qi et al., 2016). Thus, these data demonstrate that VTA glutamatergic neurons, depending on their postsynaptic target, can regulate two functionally opposing motivational states.

#### *Medial Prefrontal Cortex (mPFC)*

The VTA also sends an assortment of DAergic, GABAergic and glutamatergic afferents to the mPFC. Midbrain dopaminergic neurons projecting to the mPFC are thought to modulate cognitive function, including executive functioning, working memory and attentional control (Ridderinkhof, Ullsperger, Crone, & Nieuwenhuis, 2004). A recent study investigating the functional and behavioral relevance of VTA DA neurons that project to the mPFC found that unexpected rewards and cues that predict them cause an increase in their phasic firing activity, however optogenetic stimulation (both tonic and phasic activation) of this pathway does not elicit conditioned place preference (Ellwood et al., 2017). Interestingly, however, it was found that tonic firing activity of mPFC-projecting VTA DA neurons is involved in the maintenance of previously learned cue-reward associations, whereas phasic firing causes deviation from previously learned associations.

Dysfunction of DA signaling within the mPFC has also been implicated in several neuropsychiatric disorders including schizophrenia, depression and drug addiction (Davey,

Yücel, & Allen, 2008; Goldman-Rakic & Selemon, 1997; Goldstein & Volkow, 2011). Several studies have used optogenetic tools to understand the role of this circuit in social behavior and the onset of maladaptive behavioral states in rodents. Optogenetic inhibition of mPFC-projecting DA VTA neurons in mice that had previously undergone subthreshold social defeat, promoted susceptibility to depression-related behaviors and caused reduced social interaction (Chaudhury et al., 2013). Consistent with these findings, optogenetic activation of these neurons reversed social avoidance in depression-susceptible mice following chronic social defeat stress (Friedman et al., 2014). Interestingly, contradictory effects were observed in another report using similar optogenetic methods but in naïve mice. Gunaydin and colleagues found that activation of DA VTA neurons projecting to the mPFC had no effect on social interaction and caused anxiety-like effects and conditioned place aversion (Gunaydin et al., 2014). These paradoxical findings may reflect the difference in the motivational and behavioral states of these mice immediately preceding optogenetic stimulation of this pathway. Still, these findings provide new insights into the neural circuit mechanisms underlying depression, and may in turn advance effective circuit-based treatments for this disease.

As previously mentioned, the VTA also sends glutamatergic projections to the prefrontal cortex and a subset of mesocortical midbrain dopaminergic neurons express vesicular glutamate transporters (vGLUTs), an indicator for their ability to co-release DA and glutamate in their target regions. A recent report demonstrated that non-selective optogenetic stimulation of mesocortical projections to the PFC mediate glutamatergic excitation of mPFC fast-spiking GABAergic interneurons, that in turn inhibit prefrontal cortical pyramidal neurons (Kabanova et al., 2015).

VTA GABA neurons also send long-range projections to the prefrontal cortex (Carr &

Sesack, 2000a; Taylor et al., 2014), however functional and behavioral relevance of this circuit is currently unknown.

### *Hippocampus*

It is well established that the hippocampus is critically involved in episodic and spatial memory formation (Burgess, Maguire, & O'Keefe, 2002; Squire, 1992). Several studies suggest that DA neurotransmission influences hippocampal plasticity and function (Kulla & Manahan-Vaughan, 2000; Rossato, Bevilacqua, Izquierdo, Medina, & Cammarota, 2009; Sajikumar & Frey, 2004). Anterograde tracing studies have established that the VTA sends fibers that synapse onto several regions of the hippocampus, with CA1 subregion receiving the majority and CA3 subregion and dentate gyrus receiving fewer (Gasbarri, Sulli, & Packard, 1997; Gasbarri, Verney, Innocenzi, Campana, & Pacitti, 1994; Swanson, 1982). Currently, there is not a clear consensus as to how much of the projection from the VTA to hippocampus is DAergic, but these studies report relatively low percentages, ranging from 6-18%. Although the function of VTA drive onto the hippocampus is not well characterized, it has been suggested that DAergic neurons of the VTA form a loop with the hippocampus regulating the conversion of new, salient information into long term memory storage (Lisman & Grace, 2005). Future studies using afferent-specific optogenetic stimulation of VTA DA fibers to hippocampus will further elucidate the functional connectivity between these regions and their role in complex behaviors, specifically in spatial learning tasks.

### *Basolateral Amygdala (BLA)*

The basolateral amygdala (BLA) is critically involved in forming learned associations between neutral stimuli in the environment and aversive or appetitive outcomes (M. Davis, 1992; Everitt, Cador, & Robbins, 1989; Gallagher & Chiba, 1996; LeDoux, 2000). Notably, the BLA has been implicated in the learned associations that occur with exposure to natural rewards as well as with drugs of abuse. For example, lesioning of the BLA impairs the formation of cocaine conditioned place preference (Fuchs, Weber, Rice, & Neisewander, 2002) and abolishes the ability of drug associated cues to reinstate lever pressing for cocaine following extinction (Meil & See, 1997). While it is known that the BLA receives DAergic input from the VTA (Sadikot & Parent, 1990), functional significance of this circuit has not been extensively explored. However, it has been found that inactivating the BLA attenuates terminal DA release in the NAc following exposure to a cue that predicts a sucrose reward (Jones et al., 2010). These results provide clear evidence that afferents from the BLA to the NAc are capable of modulating DAergic signaling, thus providing a functional mechanism as to how the BLA facilitates associative learning between environmental stimuli and a salient event.

### **EVIDENCE FOR THE ROLE OF DOPAMINE IN REWARD AND MOTIVATION**

Dopaminergic signaling is now known to be critically involved not only in motor control, but many diverse emotional, cognitive, and motivational states. One of the first theories to attribute DA function within the brain to something other than motor function was described by Wise et al. in the late 1970s. It became known as the ‘dopamine hypothesis of anhedonia’ and suggested that DAergic signaling in the brain mediates the pleasure produced by a hedonic reward (R. A. Wise, 1978). The findings that lead to the proposal of this hypothesis included those that showed pharmacological blockade of DA signaling and selective ablation of DA neurons results in a significant reduction in motivated output to obtain natural rewards (K. C.

Berridge, Venier, & Robinson, 1989; Gerber, Sing, & Wise, 1981; Ungerstedt, 1971; R. A. Wise & Raptis, 1986; R. A. Wise, Spindler, deWit, & Gerberg, 1978) and to engage in intracranial self-stimulation (Fouriez, Hansson, & Wise, 1978; Fouriez & Wise, 1976). Furthermore, several studies in the early to mid-1990s showed that midbrain DA neurons become excited by primary rewards including food, sex, and drugs of abuse which results in phasic DA release in cortical and limbic terminal fields such as the mPFC and NAc (Apicella, Ljungberg, Scarnati, & Schultz, 1991; Hoebel, Mark, & West, 1992; Pfaus et al., 1990; Pfaus, Damsma, Wenkstern, & Fibiger, 1995; R. A. Wise, Newton, et al., 1995; R. A. Wise, Leone, Rivest, & Leeb, 1995).

The ‘dopamine hypothesis of anhedonia’ would be challenged by several studies including the pioneering work led by Wolfram Schultz and colleagues when they showed that while midbrain DA neurons are initially activated by primary rewards, when an animal learns to associate a stimulus with the receipt of a reward, DA neurons will shift their activation response to the cue that predicts the reward (conditioned stimulus) (W. Schultz, Dayan, & Montague, 1997). These findings would lead to their proposal that midbrain DA neurons encode reward prediction errors – signaling the discrepancy between the predicted reward and actual reward received. They found that DA neurons not only responded to a conditioned stimulus that predicts reward but fail to respond to the unconditioned hedonic stimulus if it occurs according to prediction (zero prediction error). Consistent with this, when a conditioned stimulus predicts a reward, but the reward is smaller than predicted or omitted completely, DA neurons are phasically inhibited (negative prediction error). Furthermore, *in vivo* voltammetry studies show phasic DA release in the NAc in response to stimuli that become associated with rewards (Day et al., 2007; A. G. Phillips, Atkinson, Blackburn, & Blaha, 1993; P. E. M. Phillips et al., 2003; Roitman, Stuber, Phillips, Wightman, & Carelli, 2004).

Midbrain dopaminergic neurons have not only been reported to encode reward prediction errors but also signal the incentive salience of sensory cues (K. C. Berridge & Robinson, 1998). The ‘incentive salience hypothesis’ states that dopamine signaling transforms the neural representation of a conditioned stimulus from neutral to a cue worthy of attention. In congruence to this hypothesis, research has shown that putative and identified VTA DA neurons respond to salient, but non-rewarding experiences including aversive stimuli and stress (Anstrom & Woodward, 2005; Brischoux, Chakraborty, Brierley, & Ungless, 2009; Herman et al., 1982; Thierry, Tassin, Blanc, & Glowinski, 1976; Tidey & Miczek, 1996). For instance, veterans with post traumatic stress disorder (PTSD) show activity in limbic terminal fields including the amygdala and NAc in response to hearing trauma-related stimuli including gunshots, explosions and other combat sounds (Liberzon et al., 1999). Taken together, these data suggest that DA signaling not only promotes learned associations between rewards and cues that predict them but also between aversive stimuli and their predictive cues. These learned associations will either promote approach or avoidance behavior towards rewarding (i.e. food and sex) and aversive stimuli (i.e. predators) respectively, both of which are critical for the survival of an organism and ultimately its species.

## **ROLE OF DOPAMINE IN DRUG ADDICTION**

In 2016, the U.S. Department of Health and Human Services released the first ever Surgeon General’s report on Alcohol, Drugs, and Health, a comprehensive statement on the addiction crisis in America (Substance Abuse and Mental Health Services Administration (US) & Office of the Surgeon General (US), 2016). Providing an extensive review of the scientific evidence accumulated thus far for the neurobiological basis of this disease, a primary aim of this report is to shift the way our society thinks about drug addiction and to outline ideas for effective prevention and treatment strategies. In an interview with NPR last year, former U.S. Surgeon



General Dr. Vivek Murthy when speaking on the prevalence of substance abuse in this country stated that an estimated 20.8 million people in our country have met the diagnostic criteria for a substance use disorder, which is 1.5 times the number of people who have all cancers combined (“Surgeon General Murthy Wants America To Face Up To Addiction,” 2016). In the U.S., 52,404 people died from drug overdose in 2015, an average of 143 deaths per day (Rudd, Seth, David, & Scholl, 2016). Furthermore, the number of infants being born dependent on drugs is also rising dramatically. A recent report from the Centers for Disease Control and Prevention (CDC) estimates that nearly 24,000 babies were born dependent on drugs in 2013, meaning that roughly one infant is born every twenty minutes in the U.S. dependent on drugs (Ko et al., 2016). It is clear that the consequences of drug addiction and substance misuse are becoming increasingly grave.

Drug addiction is a chronically relapsing disease characterized by compulsive drug-seeking and drug-taking behavior despite severe adverse consequences. Several preclinical research studies that have identified specific maladaptations in neurocircuit function following drug exposure may help us elucidate why certain individuals are more susceptible to progressing to addiction while others do not. For example, exposure to natural rewards and drugs of abuse has been shown to potentiate glutamatergic synaptic transmission onto VTA DA neurons (Borgland, Malenka, & Bonci, 2004; B. T. Chen et al., 2008; Lammel, Ion, Roeper, & Malenka, 2011; Mameli, Balland, Luján, & Lüscher, 2007; Saal, Dong, Bonci, & Malenka, 2003; Stuber et al., 2008; Ungless, Whistler, Malenka, & Bonci, 2001). It has also been shown that having higher expression levels of the DA D2 receptor in the NAc could protect against maladaptive behaviors associated with addiction. Macaque monkeys with higher expression levels of the DA D2 receptor showed a significant reduction in their propensity to self-administer cocaine

compared to subjects with lower expression levels (Morgan et al., 2002). Likewise, in rodents, Bock et al. found that potentiation of glutamatergic drive onto DA D2 receptor-expressing medium spiny neurons (MSNs) in the NAc promotes resilience towards compulsive cocaine intake and *in vivo* optogenetic stimulation of these neurons inhibits cocaine self-administration (Bock et al., 2013). Taken together, these results suggest that neuroadaptations following drug exposure as well as individual gene expression profiles that may render an individual more susceptible/resilient to the onset and progression of addiction are very important to continue to investigate and understand.

While the effects of cocaine at the cellular and molecular levels have advanced, how exposure to drugs of abuse and modulation of midbrain DAergic neurons affect network adaptation across the entire brain has largely been unexplored. The experiments outlined in this dissertation will determine whether large-scale neuronal network dynamics, measured across many distinct neuroanatomical circuit nodes, are directly regulated by activity of VTA dopaminergic neurons.

## **OVERVIEW OF OPTOGENETICS**

Understanding the precise circuit function that underlies behavior is critical in order to identify new therapeutic targets of neuropsychiatric disease, as several of these disorders are characterized exclusively by behavioral output. Due to the heterogeneity of neuronal cell types and complexity of their interactions and connections across the brain, behavioral outcomes observed during experiments that utilize more traditional methods to probe neuronal circuit function (i.e. lesioning and electrical stimulation techniques) are generally very difficult to interpret. Through the emergence of optogenetic technologies, it is now possible to selectively perturb specific neuronal cell types within the intact brain with fast temporal precision (Boyden, Zhang, Bamberg, Nagel, & Deisseroth, 2005). This is achieved through viral or transgenic

techniques that selectively integrate light-gated opsins into the membranes of genetically defined neurons. There are several light-sensitive proteins available for modulating neural circuits both *in vitro* and *in vivo* (Yizhar, Fenno, Davidson, Mogri, & Deisseroth, 2011). Channelrhodopsin-2 (ChR2), a light-gated cation channel derived from the green algae, *Chlamydomonas reinhardtii* permits  $\text{Na}^+$  and other cations to enter the cell in response to blue light (~470 nm), causing optical excitation of the cell. Alternatively, optical inhibition is achieved by the integration of the bacteria-derived light sensitive chloride pump, Halorhodopsin (NpHR) and subsequent illumination with yellow light (~580 nm), causing these neurons to hyperpolarize and inhibit their firing (Gradinaru, Thompson, & Deisseroth, 2008; Han & Boyden, 2007; F. Zhang et al., 2007).

The power and utility of optogenetics as a tool is rooted in its ability to efficiently deliver and express opsin genes in distinct neuronal cell types. This can be achieved through a few methods. The first method is through stereotactic delivery of a viral vector, which is encoded with an opsin gene driven by a cell-type specific promoter, into a discrete brain region. Using this method, an optical fiber (Sparta et al., 2011) can be implanted directly above the infected cell bodies or a downstream target region, allowing for pathway-specific modulation of neural activity. For example, to selectively target glutamatergic fibers from the basolateral amygdala (BLA) to the NAc, Stuber and colleagues stereotactically delivered an adeno-associated viral vector encoded with either ChR2-eYFP or NpHR3.0-eYFP driven by the  $\text{Ca}^{2+}$ /calmodulin-dependent kinase II alpha (CaMKII $\alpha$ ) promoter into the BLA and positioned optical fibers above the NAc (Stuber et al., 2011a). Several other studies have used the same approach to target specific projections from the BLA to other brain regions, including the central nucleus of the

amygdala (CeA) (Tye et al., 2011), ventral hippocampus (vHPC) (Felix-Ortiz et al., 2013; Felix-Ortiz & Tye, 2014), and NAc shell (Britt et al., 2012).

Targeting neuronal cell types has also been achieved by using transgenic animals that express an opsin under a cell-type specific neuronal promoter. For example, several mouse lines have been created expressing ChR2 in specific subsets of neurons in several regions across the brain (Arenkiel et al., 2007; H. Wang et al., 2007; S. Zhao et al., 2011). Although this approach provides genetic specificity and millisecond temporal resolution, the spatial specificity is no longer there. The final approach provides a higher degree of spatial targeting by coupling the use of transgenic animals that express Cre recombinase in genetically distinct neurons with the use of Cre-inducible viral constructs. To illustrate, the experiments outlined in Chapter 2 of this dissertation utilize transgenic rats that express Cre recombinase under the control of the tyrosine hydroxylase (TH) gene promoter (Witten et al., 2011). To selectively activate dopaminergic neurons within the ventral midbrain, rats were microinjected with an adeno-associated virus (AAV) carrying a Cre-inducible expression cassette encoding ChR2 fused to an enhanced yellow fluorescent protein (eYFP) under the control of the EF1 $\alpha$  promoter into the VTA. Importantly, the Cre-inducible AAV viral vector construct was designed to have the ChR2-eYFP gene inverted and flanked by two loxP sites (Tsai et al., 2009). Although the virus will be transduced by all cells, only those cells expressing Cre recombinase will be able to invert ChR2-eYFP into its functional state. Thus, the opsin will only be functional in the cell type expressing Cre recombinase, which for these experiments are in those neurons that express TH.

Each method described above has its own advantages and disadvantages in their abilities to selectively manipulate neuronal activity, thus it is important to consider the specific aims of every experiment in order to choose the approach that is most appropriate.

## **OPTOGENETIC fMRI**

Global maladaptation in the structure and function of the brain are associated with the onset and progression of several neuropsychiatric disorders, including drug addiction. Although optogenetic strategies have revolutionized the field of neuroscience by providing a means to identify specific circuit components that underlie complex behaviors, it has been difficult to understand how manipulating specific neuronal subpopulations affects network activity dynamics across the whole brain. With the recent development of optogenetic fMRI, it is now possible to observe macroscale patterns of activity across the whole brain in response to modulation of genetically distinct cell groups. In the first report to combine optogenetics with fMRI, Lee and colleagues found that selective optogenetic stimulation of excitatory neurons in the primary motor cortex (M1) elicited a positive blood oxygen level-dependent (BOLD) response at the site of optical stimulation, whereas in control animals that received laser light delivery but were injected with saline instead of the opsin encoded viral vector, no BOLD signal was detected (Lee et al., 2010). Notably, the optically-driven BOLD signal dynamics and hemodynamic response function were very similar to those observed in the motor cortices of rodents and humans following the use of more traditional sensory-evoked fMRI procedures (Buxton, Wong, & Frank, 1998). Lee et al. also showcased the important capability of optogenetic fMRI to resolve brain-wide macroscale patterns of activity by stimulating M1 and showing robust BOLD responses in long range projection target regions such as the thalamus. Collectively, these findings suggest that modulating genetically distinct cell types can impact global brain dynamics and underscore the utility of optogenetic fMRI in providing a means to detect these changes. Technical considerations and limitations of optogenetic fMRI are further discussed in the **General Discussion**.

## **OVERVIEW OF FUNCTIONAL MRI (fMRI): TASK-BASED VERSUS RESTING STATE fMRI**

Functional MRI (fMRI) is a neuroimaging technique used to indirectly measure large-scale brain network activity by detecting associated hemodynamic changes in blood oxygenation. The non-invasive nature of fMRI and its ability to resolve brain-wide macroscale patterns of activity are two key advantages that have contributed to its widespread use and versatility as both a diagnostic tool in the clinic and in basic research (Logothetis, 2008). First described by Seiji Ogawa in 1990, blood-oxygen-level-dependent (BOLD) contrast imaging has become the mainstay of fMRI as a means to indirectly detect brain activity (Ogawa & Lee, 1990; Ogawa, Lee, Kay, & Tank, 1990; Ogawa, Lee, Nayak, & Glynn, 1990). When neurons become activated in response to a task or stimulus, they require an increase in oxygen and glucose consumption. This will cause local increases in cerebral metabolic rate of oxygen (CMRO<sub>2</sub>), cerebral blood volume (CBV), and cerebral blood flow (CBF). Although both CMRO<sub>2</sub> and CBF are enhanced during neuronal activation, CBF of fresh oxygenated blood to the activated region exceeds that of CMRO<sub>2</sub>, resulting in an over proportional influx of oxyhemoglobin (Buxton & Frank, 1997). The BOLD contrast is caused by the paramagnetic property differences between oxy- and deoxyhemoglobin and their local ratio differential following neuronal activation.

The two main fMRI techniques used to study global neurocircuit function are task-based (evoked) and resting state functional connectivity (intrinsic). During task-based fMRI experiments, a task or stimulus (i.e. motor task, language task, working memory task, visual stimulus, etc.) is used to elicit the BOLD hemodynamic response described above. A stimulus presentation strategy frequently used during task-based experiments is called block design (Amaro & Barker, 2006). A block design experiment consists of periods of rest alternated with periods of task performance/stimulus presentation. The block design aids in the detection of

brain-wide MR signal changes during periods of stimulation relative to baseline and/or periods of rest. Regions of the brain that show MR signal changes that coincide with the block design pattern are considered areas that alter their activity due to the task or stimulus.

In contrast to task-based fMRI, resting state fMRI (rsfMRI) provides information about neuronal connectivity through investigating temporal correlations in the BOLD signal across the brain at rest. During rest, spatially distinct regions of the brain that are interconnected display temporally synchronized spontaneous low frequency (0.01-0.1 Hz) fluctuations (Biswal, Yetkin, Haughton, & Hyde, 1995). Several studies have demonstrated that the human brain (Damoiseaux et al., 2006; De Luca, Beckmann, De Stefano, Matthews, & Smith, 2006), as well as non-human primate and rodent brains (Hutchison, Mirsattari, Jones, Gati, & Leung, 2010; Lu et al., 2012; Pawela et al., 2008; Vincent et al., 2007), are organized into distinct sets of interconnected regions that display these highly correlated spontaneous fluctuations. Examples of these resting state networks (RSNs) include those involved with sensory-related processing such as motor, visual and auditory and those involved with more higher-order cognitive function including default mode, salience and executive networks. Dysregulation within these networks has been implicated in several neuropsychiatric disorders, including schizophrenia and depression, and drug addiction. We explore these networks in the drug naïve rodent brain and characterize shifts in their connectivity patterns across the brain following cocaine exposure. We hope to provide new biomarkers that may link neural system dysregulation following cocaine exposure with the maladaptive behaviors seen in drug addiction.

## **DISSERTATION**

While it is well established that DA release events occur in terminal fields such as the NAc in response to reward predictive cues, including those associated with drugs of abuse, how DA release events affect whole-brain activity dynamics has largely been unexplored. In Chapter

2, we couple optogenetic stimulation techniques with functional magnetic resonance imaging to selectively activate TH<sup>VTA</sup> neurons in transgenic rats and measure resulting changes in whole-brain activity. Next, we investigate whether explicit pairing of midbrain DA neuron activity and a sensory stimulus can enhance the brain-wide representation of that specific sensory stimulus. In Chapter 3, we investigate changes in global functional connectivity following extended access cocaine self-administration in drug naïve rats. Taken together, our work suggests that large-scale neuronal network dynamics, measured across many distinct neuroanatomical circuit nodes, are regulated by the activity of VTA dopaminergic neurons.



## CHAPTER 2: COORDINATION OF BRAIN-WIDE ACTIVITY DYNAMICS BY DOPAMINERGIC NEURONS<sup>1</sup>

### INTRODUCTION

Midbrain dopaminergic neurons have been reported to encode reward prediction errors (Cohen, Haesler, Vong, Lowell, & Uchida, 2012; Wolfram Schultz, 1998; Steinberg et al., 2013) and signal the incentive salience (Kent C Berridge & Robinson, 1998) of sensory cues. During reward-seeking behavior, burst firing of these neurons results in phasic dopamine release (Day et al., 2007; P. E. M. Phillips et al., 2003; Stuber et al., 2008) in cortical and limbic terminal fields such as the medial prefrontal cortex (mPFC) and nucleus accumbens (NAc), which in conjunction with other neurotransmitters act to modulate postsynaptic neuronal firing (Gee et al., 2012; Surmeier, Ding, Day, Wang, & Shen, 2007) and promote changes in motivated behavioral output (Salamone et al., 2007; Stuber et al., 2011b; Tsai et al., 2009; Tye et al., 2013). The direct consequences of dopamine signaling are largely restricted to brain regions that contain appreciable presynaptic fibers that release dopamine, as well as postsynaptic dopamine receptors. However, dopaminergic signaling may also indirectly influence the activity in multiple brain regions, some of which may receive little to no direct dopamine input. By sculpting activity

---

<sup>1</sup> This chapter previously appeared as an article in the journal *Neuropsychopharmacology*. The original citation is as follows: Decot HK, Namboodiri VM, Gao W, McHenry JA, Jennings JH, Lee SH, Kantak PA, Jill Kao YC, Das M, Witten IB, Deisseroth K, Shih YI, Stuber GD (2017). Coordination of Brain-Wide Activity Dynamics by Dopaminergic Neurons. *Neuropsychopharmacology: Official Publication of the American College of Neuropsychopharmacology*, 42(3), 615–627. <https://doi.org/10.1038/npp.2016.151>.

dynamics of neurons that are polysynaptically downstream, ventral tegmental area (VTA) DAergic neurons may thus modulate a much larger functional brain circuit.

In addition to dopamine signaling by natural rewards (Cohen et al., 2012; Day et al., 2007; Roitman et al., 2004; Roitman, Wheeler, Wightman, & Carelli, 2008; Wolfram Schultz, 1998), drugs of abuse increase extracellular DA in the mesolimbic terminal fields such as the nucleus accumbens (P. E. M. Phillips et al., 2003; Stuber, Roitman, Phillips, Carelli, & Wightman, 2005; Stuber, Wightman, & Carelli, 2005) supporting the notion that aberrant dopamine signaling may play a principal role in mediating the neurobiological and behavioral maladaptation associated with addiction (Pascoli, Terrier, Hiver, & Lüscher, 2015). A hallmark feature of addiction is the enhanced salience that sensory stimuli acquire when paired with drugs of abuse, which can promote drug craving (Childress et al., 1999; Peter W. Kalivas & Volkow, 2005; Koob & Volkow, 2010; Volkow, Fowler, Wang, & Swanson, 2004). This enhanced salience triggered by drug-associative cues, likely involves phasic dopamine release as drug associated cues can directly evoke robust dopamine release events in the NAc that are modulated by the cue-drug association (P. E. M. Phillips et al., 2003; Stuber, Wightman, et al., 2005). While release of dopamine during this process would be predicted to have direct effects on striatal neuronal activity, it is also possible that dopamine release, when paired with a sensory stimulus, may modulate the salience or value of that particular stimuli via effects that occur in brain regions downstream of circuits that are directly modulated by dopamine. Indeed, a previous report demonstrated that electrical stimulation of the VTA, timed to an auditory stimulus presentation resulted in enlarged sensory representation of that particular stimulus within the auditory cortex (Bao, Chan, & Merzenich, 2001). Thus, previous work implies that dopamine signaling may modulate cue-evoked behavioral responding by acting both at the site of release in

striatal targets, as well as by changing brain activity in potentially many other brain nuclei that do not directly receive appreciable dopamine input.

To further investigate these two complementary ideas, we studied how *in vivo* modulation of VTA dopaminergic neurons altered brain-wide activity patterns using *in vivo* optogenetics coupled with fMRI (Domingos et al., 2011; Ferenczi et al., 2016; Gerits et al., 2012; Kahn et al., 2011; Lee et al., 2010). We first tested whether selective optogenetic stimulation of TH<sup>VTA</sup> neurons produced changes in fMRI signals and altered activity within multiple, anatomically distinct regions that directly receive dopamine input. This approach capitalizes on the genetic specificity offered by optogenetic strategies and the high throughput, with the capability of resolving brain wide macroscale patterns of activity afforded by fMRI. Utilizing a standard generalized linear model (GLM) analysis approach, our results indicate that selective activation of TH<sup>VTA</sup> neurons produces dopamine receptor dependent increases in CBV signals in well-established dopaminergic terminal fields such as the striatum. In contrast, whole brain voxel-based principal component analysis (PCA) of the same dataset, which allowed us to survey changes in brain-wide activity, revealed that dopaminergic modulation activates many additional anatomically defined regions throughout the brain. Using our developed PCA-fMRI approach, we also explored how DA stimulation coupled with a discrete sensory stimulus affects the representation of that stimulus throughout the entire brain. We reveal that explicit pairing of TH<sup>VTA</sup> neuron activity with forepaw stimulation dramatically alters the brain-wide sensory representation of that stimulus. These findings provide new insight into the global adaptation in neurocircuit function associated with the attribution of salience to sensory cues in the environment.

## METHODS

### Experimental Subjects and Stereotactic Surgery

All procedures were conducted in accordance with the Guide for the Care and Use of Laboratory Animals, as adopted by the National Institutes of Health, and with approval of the Institutional Animal Care and Use Committee at the University of North Carolina (UNC). Adult (400-450 g) male tyrosine hydroxylase (TH)-ires-cre Long Evans rats were group housed until surgery and were maintained on a 12-h light cycle (lights off at 19:00) with mild food restriction to maintain ~90% body weight during the duration of the study. To target dopamine (DA) neurons within the midbrain, TH-ires-cre rats were endotracheally intubated and ventilated using a small animal ventilator (CWE Inc., SAR-830/PA, Moore, PA) with ~1.5% isoflurane in medical air prior to being placed into a stereotactic frame (Model 962, Kopf Instruments, Tujunga, CA). For all experiments, rats were microinjected with quadruple injections of 1  $\mu$ l of purified and concentrated adeno-associated virus ( $\sim 10^{12}$  infections units per ml, packaged by the UNC Vector Core Facility) into the ventral tegmental area (VTA) using the following coordinates (in mm from bregma): -5.4 and -6.2 anterior/posterior,  $\pm 0.7$  medial/lateral, -8.4 and -7.4 dorsal/ventral. VTA dopaminergic neurons were transduced with an AAV5 carrying a cre-inducible expression cassette encoding channelrhodopsin-2 (ChR2) fused to an enhanced yellow fluorescent protein (eYFP) under the control of the EF1 $\alpha$  promoter (AAV5-DIO-ChR2-eYFP; TH<sup>VTA</sup>::ChR2 rats) or only eYFP (AAV5-DIO-eYFP; TH<sup>VTA</sup>::control rats). 200  $\mu$ m multimode chronic optical fibers were stereotactically implanted bilaterally at a 10° angle directly above the VTA using the following stereotactic coordinates: -5.8 mm to bregma,  $\pm 2.14$  mm lateral to midline, and -7.8 mm ventral to the skull surface. The time from virus injection to the start of the MRI experiments was 5–6 weeks for all subjects.

## fMRI Procedures

MRI was performed using a 9.4 Tesla Bruker BioSpec system with a BGA-9S gradient insert (Bruker Corp., Billerica, MA) at the UNC Biomedical Research Imaging Center (BRIC). On the day of MRI experiments, each rat was endotracheally intubated and ventilated with ~1.5% isoflurane in medical air. The ventilation rate and volume were adjusted via a capnometer (Surgivet v9004, Smith Medical, Waukesha, WI) to maintain end-tidal CO<sub>2</sub> (EtCO<sub>2</sub>) within a range of 3.0±0.2%. Non-invasive EtCO<sub>2</sub> values were previously calibrated against invasive blood-gas samplings under identical baseline conditions, resulting in an arterial pCO<sub>2</sub> of 37.6±4.7 mmHg (Yen-Yu I. Shih et al., 2013). Heart rate and oxygen saturation (SpO<sub>2</sub>) were continuously monitored by a non-invasive MouseOx Plus System with MR-compatible sensors (STARR Life Science Corp., Oakmont PA) and maintained within normal ranges (~280 bpm and above 96%, respectively). Rectal temperature was maintained at 37±0.5°C with a warm-water circulating pad. Black tape was placed over the eyes and a masking light was directed into the face of each rat to minimize visual stimulation during laser light delivery.

A home-made surface coil with an internal diameter of 1.6 cm placed directly over the head was used as a RF transceiver. Magnetic field homogeneity was optimized using standard FASTMAP shimming with first order shims on an isotropic voxel of 7x7x7 mm encompassing the imaging slices. A RARE T<sub>2</sub>-weighted image was taken in the mid-sagittal plane to localize the anatomical position by identifying the anterior commissure at 0.36 mm posterior to bregma. To ensure anatomical consistency of the imaging data, twelve coronal slices were acquired using T<sub>2</sub>-weighted imaging, with the 4<sup>th</sup> slice from the anterior direction aligned with the anterior commissure. A RARE sequence (spectral width=47 kHz, TR/TE=2500/33 ms, FOV=2.56x2.56 cm, slice thickness=1 mm, matrix=256x256, RARE factor=8, and number of averages=8) was used to confirm optical fiber position with reference to the cortical surface, midline, and the

anterior commissure. For functional scans, single shot gradient echo-EPI sequence (spectral width=300 kHz, TR/TE=1000/8.1 ms, FOV=2.56x2.56 cm<sup>2</sup>, slice thickness= 1 mm, matrix=80x80, providing temporal resolution=1 s) was used.

During fMRI, dexmedetomidine (0.1 mg/kg/hr) and pancuronium bromide (1.0 mg/kg/hr) were infused intraperitoneally and isoflurane was lowered to 0.5% 30 min after the infusion began (Fukuda, Vazquez, Zong, & Kim, 2013). Cerebral blood volume (CBV)-weighted fMRI (Mandeville et al., 1998) was achieved by injecting Feraheme (AMAG Pharmaceuticals, Lexington, MA) at a dose of 30 mg Fe/kg via a tail vein catheter. CBV-weighted fMRI was chosen over the more conventional blood oxygenation-level dependent (BOLD) fMRI due to its ability to provide significantly greater functional sensitivity (Kim et al., 2013). Optical fibers were coupled via 3-m patch cables to solid-state lasers (473 nm wavelength) located outside of the MRI room delivering ~10 mW light to each hemisphere of the VTA. Evoked fMRI scans were acquired for 100 s during which photostimulation was applied in a 20-s OFF, 10-s ON, 30-s OFF, 10-s ON, 30-s OFF pattern. Subjects underwent two to five repeated trials at each photostimulation frequency (10, 20, 30 and 40 Hz at 5 ms pulse width) in a pseudo-random manner. Dopamine D1 receptor antagonist, SCH23390 (0.6 mg/kg) (Sigma) was injected intravenously to explore its effects on stimulus-evoked CBV changes observed in TH<sup>VTA</sup>::ChR2 rats. This SCH23390 dose was chosen because it was comparable to the dose used in a similar fMRI study (Marota et al., 2000). For paired forepaw and optogenetic stimulation experiments, electrical forepaw stimulation was applied using two needle electrodes inserted under the skin of the right forepaw of each subject. The stimulation was applied in a 20-s OFF, 10-s ON, 70-s OFF pattern. To measure the frequency dependence of the stimulus-evoked activation, subjects underwent two to five repeated trials at the following frequencies: 1, 3, 9, 15, and 21 Hz with a

fixed pulse width of 0.3 ms and a current of 1.5 - 3.0 mA (pre-pairing). Then, a repeated pairing of forepaw electrical stimulation at 9 Hz with 30 Hz optogenetic stimulation of VTA DA neurons was performed with an initial 20-s OFF, followed by 20 blocks of 10-s ON and 70-s OFF. Finally, changes in CBV signals and frequency dependence in response to all forepaw stimuli frequencies were re-assessed (post-pairing).

## **Data Processing and Statistical Analysis**

### *Generalized Linear Model (GLM)-based stimulation analysis*

fMRI data analyzed using a generalized linear model (GLM) were processed using Matlab (Math-Works, Natick, MA) and Statistical Parametric Mapping (SPM) codes, with the pipeline similar to our previous publications (Lai, Albaugh, Kao, Younce, & Shih, 2015; Yen-Yu Ian Shih, Huang, et al., 2014; Yen-Yu Ian Shih, Yash, Rogers, & Duong, 2014; Younce, Albaugh, & Shih, 2014). Automatic co-registration were applied to realign time-series data within subjects to correct subtle drift of EPI images and then again across subjects to provide group-based fMRI maps. Data were analyzed using the Analysis of Functional Neuroimages (AFNI) with the framework of GLM (R. W. Cox, 1996; Worsley et al., 2002; Worsley & Friston, 1995), with false discovery rate (FDR) correction to adjust for the multiple comparisons of fMRI maps ( $p < 0.05$ ). The stimulation paradigm was convoluted with response model of Feraheme (Leite et al., 2002) injection in AFNI package in order to get an ideal model of hemodynamic response (**Figure A.2 F**). Regions of interest (ROIs) were placed on the dorsal striatum bilaterally to extract fMRI time-course data after the images were co-registered. For pairing experiments, ROI was placed on the contralateral somatosensory cortex (S1). To control for Feraheme metabolism over the course of each experiment, the following equations were used to calculate  $\Delta\text{CBV}$ : Baseline  $\Delta R_2^* = -1/\text{TE} \ln(S_{\text{prestim}}/S_0)$ , where  $S_{\text{prestim}}$  and  $S_0$  represents MR signal intensity after and before Feraheme injection. Stimulus evoked  $\Delta R_2^* = -1/\text{TE} \ln(S_{\text{stim}}/S_{\text{prestim}})$ ,

where  $S_{\text{stim}}$  and  $S_{\text{prestim}}$  are the MR signal intensities during and before stimulation, respectively. Cerebral blood volume changes were calculated by dividing stimulus-evoked  $\Delta R_2^*$  by baseline  $\Delta R_2^*$  values. The effect of optogenetic and forepaw stimulation frequency on  $\Delta \text{CBV}$  change was calculated by averaging CBV values from the first 20 s time points during each stimulation epoch. Two-way ANOVA tests followed by Bonferroni post hoc comparisons were applied for comparisons with more than two groups. All data were expressed as mean  $\pm$  SEM and significance was set at  $p < 0.05$ .

#### *Principal Component Analysis (PCA)-based stimulation analysis*

PCA analysis pipeline for data analyzed utilizing this method within this manuscript was written in python 2.7 using numpy and scikitlearn packages. Additional ipython notebooks with documented code used for this pipeline can be found at:

[https://github.com/stuberlab/PC\\_opto\\_fmri\\_analysis](https://github.com/stuberlab/PC_opto_fmri_analysis).

Raw data used for this study can be downloaded via the associated ipython notebooks. The aim of this data analysis pipeline was to analyze the activity of the whole brain (as opposed to pre-defined ROIs) in relation to the various stimulation paradigms. To this end, we employed a Principal Component Analysis (PCA) based dimensionality reduction.

Skull-stripped data from each animal was first aligned to a reference T2-weighted atlas. Subsequent masking deleted all data outside of the reference atlas in order to align voxels across all animals. To correct for variation between animals introduced by the injection of monocryalline iron oxide nanoparticles (MION), the fMRI signal from each animal was



normalized by calculating the corresponding CBV-weighted signal as:

$$CBVWS = \frac{(S_{baseline}(v) - S(v, t))}{(S_{preMION} - S_{baseline})}$$

where  $S_{baseline}(v)$  is the baseline signal for voxel  $v$ , and was calculated as the mean signal in the first 20 s of the run for that voxel.  $S_{baseline}$  was calculated as the mean  $S_{baseline}(v)$  across all voxels, and  $S_{preMION}$  was calculated as the mean signal in the first 20 s of the baseline scan prior to the injection of MION across all voxels. This analysis corrects for the average signal change introduced by the MION injection for each animal, prior to averaging the data across animals. To ensure that only shared variation across animals (likely from the stimulation) is present in the dataset on which PCA is performed, voxel traces were averaged across all animals and runs. Variability within the dataset extraneous to that introduced by stimulation was likely averaged out. As a result, the extracted PC representing stimulation effect is likely going to have minimal contribution from endogenous fluctuations within the signal. Furthermore, slow constant drifts in the signal during the imaging session could be largely isolated from the principal component representing the stimulation effect (e.g. **Figure A.3 A**). Thus, this method automatically corrects for some sources of noise.

PCA was performed on averaged data from experimental (ChR2-eYFP) and control (eYFP) animals. Spatial and temporal dimensions representing the voxels within this feature space were treated as features and samples, respectively. Dimensionality reduction was performed by limiting the number of principal components to that required in explaining 80% of the variance in the data. PCA decomposition was done using scikit-learn in Python. Sign-standardization was performed. This requires that the change in the signal at the moment of first stimulation is positive, i.e. if the change in the signal at the moment of first stimulation is

negative, we multiplied the PC vector and trace (or score) by -1. Thus, the stimulation response in all PCs are positive; the caveat being for PCs not representing stimulation effect, the change in signal at this time point might be due to random fluctuations.

The PC representing the stimulation effect was chosen and defined as the PC that showed a significant difference in the mean signal during the post-stimulation period compared to the mean signal in the baseline period (using a Welch's t-test). An additional constraint on the PC representing the stimulation effect was also applied: the post-stimulation response needed to trend towards baseline. This criterion ensured that PCs showing a stable drift across the entire session were not considered as stimulation-induced. For the VTA stimulation experiment, each experimental run had two stimulation epochs. Thus, in this case, it was required that the PC representing the stimulation response satisfied the above criteria for both stimulations, i.e. the mean post-stimulation response was higher than the mean baseline response for both post-stimulation periods, and that the response during the post-stimulation period for both stimulations trended towards baseline.

A caveat for this method is that it is possible that the stimulation effect is not entirely isolated within a single PC. In our case, it was clear looking at the traces of each PC that the post-stimulation effect was captured within the identified PC. If this was not the case, it would be appropriate to run a subsequent rotation of the axes within a subspace spanned by the first few PCs to isolate non-orthogonal components (Andersen, Gash, & Avison, 1999). Subsequently, the result of this trace could be used as a stimulation model for a GLM approach. However, since our analysis only required PCA, performing such a GLM is equivalent to identifying the significant voxels contributing to the PC of interest. Voxels that significantly contributed to the

PC representing the stimulation response were identified using the following equation:

$$w_i = \frac{\sigma_i}{\sigma_{PC}} \rho(S_i, S_{PC})$$

where  $\sigma_i$  represents the standard deviation of the  $i^{th}$  voxel trace ( $S_i$ ),  $\sigma_{PC}$  the standard deviation of the PC trace ( $S_{PC}$ ) and  $\rho$ , the Pearson correlation coefficient . Thus, the voxels that contribute significantly to the PC are the voxels that show significant Pearson's correlation with the PC (Yamamoto et al., 2014). Similar to Generalized Linear Model (GLM)-based approaches (Monti, 2011), this method extracts out the voxels that show significant correlation with a stimulation response function. However, unlike GLM, we do not have to define *a priori* models of stimulation effects using a putative hemodynamic response function (HRF). This is a significant advantage as it has been shown that HRFs are different depending on the species and region in the brain (Ferenczi et al., 2016; Handwerker, Ollinger, & D'Esposito, 2004). Crucially, the appropriate HRF for each voxel in the brain of a rat is not known and may even be impossible to reliably specify. Thus, using PCA to identify the shape of the stimulation response is data-driven and mitigates biases introduced by the specifications of the GLM model.

Voxels showing significant correlation with the PC trace representing the stimulation effect were mapped back to hand-drawn ROIs based on the reference brain atlas. Subsequently, ROIs were ranked based on their fraction of voxels that significantly contributed to the PC representing the stimulation effect. Comparing ROIs based on the fraction of significant voxels has the benefit of normalizing for the size of the ROI. However, two caveats are worth mentioning: 1) This fraction ignores the magnitude of the response for each voxel, and, 2) ROIs with fewer voxels may have spuriously high or low fractions due to their small sizes.

To analyze the effect of TH<sup>VT</sup>A pairings with paw stimulation, fMRI data from the pre-pairing epoch (averaged across animals and runs) was concatenated with the data during pairing

(averaged across animals) and the data from the post-pairing epoch (averaged across animals and runs). The PCA pipeline detailed above was run on this combined dataset. To find the PCs representing paw stimulation response for both groups, two conditions were required: 1) A positive stimulation response to every stimulation (22 in total), and 2) the post-stimulation response should show a decreasing trend following every stimulation. The traces for the PCs identified thus are shown in Figure 4a. As these traces showed variable magnitudes prior to each stimulation, the stimulation response for any stimulation was calculated by subtracting out the mean baseline response (over a 10 s period before that stimulation) from the peak response during stimulation. To test for the presence of sensory habituation, the response magnitudes for each group were divided with respect to the response magnitude pre pairing from the same group. Subsequently, the presence of a negative linear regression between the normalized response and the number of stimulations during pairing (i.e. excluding pre and post pairing responses) was investigated. To determine whether the habituation effect was comparable between ChR2-eYFP and eYFP groups, the interaction effect of pairings and the effect of group on the normalized response magnitude was also explored. Lastly, to test for an enhancement in the fMRI signal due to pairings in addition to a shared habituation, the ratio of responses for each pairing (including pre and post pairing) between the ChR2-eYFP and eYFP groups for a positive linear regression was determined.

The primary aim of this pipeline was to measure the spatial extent over which responses correlated with the stimulation. To aid in the detection of stimulation related responses in each cohort of animals, ChR2-eYFP and eYFP groups were analyzed separately by estimating the optimal principal component basis set for each group. Since the principal component vectors of these groups were not identical, their traces could not be directly compared to each other.

However, this analysis provides a means to test whether any significant post-stimulation response was present in either group and identified which voxels across the brain contributed to this response. Separate principal component basis sets were used for the TH<sup>VTA</sup> stimulation experiment and the forepaw pairing experiment.

### **Histology, Immunohistochemistry, and Microscopy**

Rats were deeply anaesthetized with pentobarbital, and transcardially perfused with phosphate buffered saline (PBS) followed by 4% (weight/volume) paraformaldehyde in PBS. Brains were post-fixed in 4% paraformaldehyde for 24 hr and transferred to 30% sucrose in ddH<sub>2</sub>O for 48 hr. 40  $\mu$ m brain sections were collected and blocked in 1:10 normal donkey serum: 0.1% Triton (200:1800  $\mu$ l) for 1 hr. Sections were then incubated in primary antibody (tyrosine hydroxylase, 1:500 Pel Freeze; made in sheep) for 48 hr at 4°C. Following 4  $\times$  10 min PBS washes, the sections were incubated in secondary antibody (Dylight 649 donkey anti-sheep, 1:800, Jackson ImmunoResearch Laboratories, Inc., West Grove, PA) for 24 hr at 4°C. All sections were coverslipped with Fluoroshield with DAPI (Sigma Aldrich, St. Louis, MO). Z-stack and tiled images of mounted brain sections were visualized using Zeiss LSM 710 confocal microscope with a 20x or 63x objective.

## **RESULTS**

### **Viral Targeting of VTA Dopaminergic Neurons in TH-Cre Rats**

To selectively stimulate TH<sup>VTA</sup> neurons *in vivo*, we introduced the light-gated cation channel, channelrhodopsin-2 conjugated to enhanced yellow fluorescent protein (ChR2-eYFP) selectively into VTA neurons in transgenic rats that express Cre recombinase under the control of the *tyrosine hydroxylase* (TH) gene promoter (Witten et al., 2011) using established viral procedures (Jennings et al., 2013) (**Figure 2.1 A**). Because of a recent report of ectopic targeting of VTA neurons in TH-Cre mouse lines (Lammel et al., 2015), we performed a detailed

quantitative assessment of viral targeting to TH<sup>+</sup> neurons in the TH-Cre rat line across the anterior/posterior and medial/lateral subregions of the midbrain (**Figure 2.1 A-C**). We quantified the location of all neurons within anterior, middle, and posterior sections expressing only eYFP (eYFP<sup>+</sup>/TH<sup>-</sup>), TH (eYFP<sup>-</sup>/TH<sup>+</sup>), and neurons that expressed both (eYFP<sup>+</sup>/TH<sup>+</sup>) (n = 9 sections in n = 3 rats). Collapsed across the anterior-posterior axis containing the VTA, we observed highly specific viral transduction of TH<sup>+</sup> neurons (97.4 +/- 1.0%, n = 9 slices from n = 3 rats, **Figure 2.1 D**). Notably, few neurons that were eYFP<sup>+</sup>, but showed TH immunoreactivity that could not be resolved above background tended to reside in the anterior VTA or ventral to the VTA in the interpeduncular nucleus (**Figure 2.1 C**). Based on stereotactic optical fiber placement directly above the VTA and predicted transmission of light power at 473 nm through brain tissue, it was unlikely that light from the optical fiber tip would spread to illuminate and activate those few neurons in the IPN that were eYFP<sup>+</sup>/TH<sup>-</sup> (Aravanis et al., 2007). In TH-Cre rats injected with AAV-DIO-ChR2-eYFP, we also observed substantial innervation of striatal subregions including the dorsal medial striatum (DMS) and the NAc (**Figure 2.1 E,F**). These results further validate the use of TH-Cre rats for targeted manipulation of TH<sup>VTA</sup> neurons, with minimal targeting to TH<sup>-</sup> neurons in and around the VTA.

### **Whole Brain Analysis of the Effect of TH<sup>VTA</sup> Neuron Stimulation**

In separate rats, we expressed ChR2-eYFP or eYFP alone in TH<sup>VTA</sup> neurons and implanted bilateral optical fibers directly above the VTA for light delivery (Sparta et al., 2011) (**Figure 2.2 and Figure A.1 A**). Following recovery from surgery and sufficient time for adequate ChR2-eYFP expression in TH<sup>VTA</sup> neurons, sedated rats were interfaced with a custom-built surface coil, placed in a 9.4 Tesla small animal MRI scanner, and the implanted optical fibers were connected to 473 nm diode pumped solid state lasers located outside of the MRI room (**Figure 2.3 A**). Following acquisition of 12, coronal T<sub>2</sub>-weighted anatomical image

sections from each animal (**Figure 2.2 B**), CBV-weighted fMRI (Kim et al., 2013; Mandeville et al., 1998; Yen-Yu I. Shih et al., 2009; Smirnakis et al., 2007) data, which indirectly measures neuronal activity by detecting changes in hemodynamic signals accompanying vascular responses, were acquired using single-shot echo planar imaging sequence at 1 s temporal resolution. In order to produce sustained, dopaminergic signaling, TH<sup>VTa</sup> neurons were optically stimulated at 10 – 40 Hz for 10 s (**Figure A.2 A and C**). With these parameters we measured CBV responses across 12 continuous coronal slices of 1 mm thickness each encompassing nearly the entire cerebrum. Using a standard generalized linear model (GLM) to compare each voxel's activity trace to a predefined stimulation template or hemodynamic response function (Ferenczi et al., 2016; Leite et al., 2002; Monti, 2011) (**Figure A.2 E**), optogenetic stimulation of TH<sup>VTa</sup> neurons produced pronounced CBV increases in striatal brain regions in a frequency dependent fashion relative to control animals that received laser-light delivery, but only expressed eYFP in TH<sup>VTa</sup> neurons (**Figure A.2**). Further, systemic administration of a dopamine D1-receptor (D1R) antagonist, SCH23390, significantly attenuated CBV signals caused by TH<sup>VTa</sup> optogenetic stimulation (**Figure A.2 B**). The D1R antagonist had no significant effect on eYFP control animals, verifying that the antagonist is specifically blocking the TH<sup>VTa</sup> neuron stimulated signal, and not causing a stimulation-independent effect on the baseline (**Figure A.2 C**). Taken together, these data show that selective activation of TH<sup>VTa</sup> neurons produces dopamine receptor dependent signaling that result in increased CBV signals in dopaminergic terminal fields.

Due to the lack of a well-defined dopamine-evoked hemodynamic response function and to mitigate the biases and assumptions imposed by traditional fMRI whole brain signal analysis, we developed an analytical pipeline by which all imaging voxels (35,182 per brain) and

associated CBV weighted time series data were subjected to principal component analysis (PCA) factorization (Andersen et al., 1999; Freeman et al., 2014) (**Figure 2.3 C**). This resulted in a substantial reduction of the dimensionality of the spatial-temporal dataset from 35,182 down to 75 PCs that explained 80% of the variance of the data. Importantly, the first PC alone explained 7% of the variance of data collected from ChR2-eYFP rats. The percent variance of the data explained by each subsequent PCs reached an asymptote by 3-4 PCs (**Figure 2.3 D**).

The first PC plotted as a function of time represented the effect of TH<sup>VTa</sup> optogenetic stimulation as it significantly increased from the baseline period (0 – 20 s) in each post-stimulation period (30 - 60 s, and 70 – 100 s) ( $t(48.0) = 11.69$ ,  $p < 0.001$ , Welch's t-test for post-stimulation period 1 and  $t(38.7) = 7.15$ ,  $p < 0.001$ , Welch's t-test for post-stimulation period 2, **Figure 2.3 E**), largely recapitulating the ROI analysis of striatal signals shown in **Figure A.2 A**. In contrast, data collected from rats only expressing eYFP in TH<sup>VTa</sup> neurons showed no significant post stimulation response. As the weight of a voxel to a given PC reflects the correlation between the voxel's and the PC time series signals (Yamamoto et al., 2014), we hypothesized that a given voxel's contribution to PC1 would highly correlate with the raw signal intensity for that voxel in the post-stimulation period exclusively in data collected from ChR2-eYFP rats. Supporting this, a highly significant positive Pearson's correlation between these two variables was observed in the ChR2-eYFP group ( $R^2 = 0.68$ ), slope = 1.12,  $p < 0.001$ ). In contrast, the eYFP group showed a slight, but significant negative correlation ( $R^2 = 0.08$ , slope = -0.28,  $p < 0.001$ ; **Figure 2.3 F**). We then ranked all voxels as a function of PC1 weight and plotted the time series for the top 500 voxels for both ChR2-eYFP and eYFP groups (**Figure 2.3 G**). Comparing these results to the top 500 voxels ranked by their mean post-stimulation



response shows a dramatic enhancement of the temporal structure of the data (**Figure A.3 B**) further supporting our PCA based analysis approach.

We then mapped the voxels that significantly contributed to the PC representing the stimulation effect back to a T2-weighted reference brain atlas (**Figure 2.3 H**). This also showed a dramatic enhancement of brain wide activation patterns evoked by the stimulation compared to standard GLM based significant voxels (**Figure A.3 C and D**). In order to then place all significant PC1 weighted voxels back to defined brain regions we annotated all 12 T2-weighted brain slices into 42 anatomical subregions based on two widely used rodent brain atlases (Lein et al., 2007) (Paxinos and Watson, 2005) taking into account the spatial resolution of fMRI (**Figure 2.4**). Extracted significant voxels (based on PCA and GLM) mapped to numerous diverse brain regions (**Figure 2.3 I**). All GLM extracted voxels largely fell into ROIs within striatal subregions and frontal cortices as predicted based on innervation patterns of TH<sup>VTA</sup> neurons (Swanson, 1982) (**Figure 2.1 E and F**). However, significant PCA extracted voxels represented a substantially larger fraction of each ROI within these subregions, further highlighting the enhanced sensitivity of this method. Furthermore, many additional brain regions were identified with a high fraction of significant voxels including basal ganglia, basal forebrain, and sensory cortical regions (**Figure 2.3 I**). Interestingly, intravenous injection of the D1R antagonist not only significantly attenuated CBV signals within striatal target regions, it also prevented stimulation-induced alterations in brain areas that do not directly receive TH<sup>VTA</sup> input (**Figure A.3 E and F**). To investigate these effects at a more physiologically relevant stimulation period, TH<sup>VTA</sup> neurons were optically stimulated at 30 Hz for 1 s in a subset of animals (**Figure A.4**). PCA-based analysis of this dataset revealed that selective stimulation of TH<sup>VTA</sup> neurons for 1 s caused activation in fewer pixels across the brain. Interestingly, while the majority of activated

pixels were in striatal target regions, some of the regions that showed enhancement at 10 s stimulation also showed slight activation at 1 s. Collectively, this analytical approach reveals for the first time that increased dopaminergic activity produces dispersed effects not only in brain regions that directly receive TH<sup>VTA</sup> input, but also in numerous accessory regions not typically associated with direct VTA DAergic modulation.

### **Whole Brain Analysis of Forepaw Stimulation Pre and Post Pairing with TH<sup>VTA</sup> Neuron Stimulation**

In pathological conditions, such as addiction and schizophrenia, aberrant dopaminergic activity may act to over-enhance the salience of particular intrinsic and extrinsic stimuli (Kent C Berridge & Robinson, 1998; Kapur, 2003). Non-specific stimulation of the VTA can also alter cortical plasticity (Bao et al., 2001; Gee et al., 2012; Lewis & O'Donnell, 2000; Otani, Daniel, Roisin, & Crepel, 2003) however it is unclear whether explicit pairing of TH<sup>VTA</sup> activity with a discrete sensory stimulus alters the brain-wide sensory representation of that stimulus. Thus, in a new cohort of rats we tested whether somatosensory representations measured with fMRI was affected by coincidental and selective TH<sup>VTA</sup> activity (**Figure A.1**). We first measured changes in CBV signals in response to a range of forepaw stimulation frequencies. We then paired a single forepaw stimulation frequency (9 Hz) with 30 Hz optogenetic stimulation of TH<sup>VTA</sup> neurons 20 times (one pairing every 70 s). Following the pairing protocol, we re-assessed changes in CBV signals in response to all forepaw stimuli frequencies (**Figure 2.5 A**). Forepaw stimulation produced timelocked CBV increases in the contralateral somatosensory cortex ROI in a frequency dependent fashion. Following pairing of 9 Hz forepaw stimulation with TH<sup>VTA</sup> activity, there was a selective enhancement in CBV signals in response to 9 Hz subsequent forepaw stimulation compared to other non-paired frequencies and data from control animals that

received laser light delivery, but did not express ChR2 in TH<sup>VTa</sup> neurons (**Figure 2.5 B-E, Figure A.6**).

To assess whole brain activity patterns before and after forepaw-TH<sup>VTa</sup> pairing, we applied the PCA pipeline described above (**Figure 2.3 C**) to this dataset. PC1 signal intensity evoked by forepaw stimulation was significantly enhanced following pairing in the ChR2-eYFP group ChR2: ( $t(18) = 19.484$ ,  $p < 0.001$ ) but not to eYFP controls ( $t(18) = 0.660$ ,  $p = 0.52$  two-tailed t-test of the mean response in the stimulation period, **Figure 2.5 F-H, Figure A.7**).

Significant voxel weights to the PC1 vector remapped back to the reference atlas revealed a striking enhancement of the fMRI measured sensory representation of forepaw stimulation induced by the pairing protocol (**Figure 2.5 I-K**). To determine whether repeated TH<sup>VTa</sup> forepaw stimulation pairing gradually enhanced the representation as a function of each pairing, we also calculated the PC fMRI signal for each TH<sup>VTa</sup> forepaw pairing (20 total). Normalized to the maximum PC signal evoked by forepaw stimulation signals after the pairing, we observed that even the first and all subsequent TH<sup>VTa</sup> forepaw stimulation pairings produced an increase in the PC signal in ChR2-eYFP rats relative to eYFP controls (**Figure 2.6 A**). This is further shown by plotting the ratio of each evoked response per pairing between ChR2-eYFP and eYFP groups (**Figure 2.6 B**). For either group, normalizing the PC signal to the respective pre-pairing forepaw response revealed a gradual habituation of the signal with increasing number of pairings (**Figure 2.6 C**). Collectively, these data suggest that forepaw stimulation paired with dopaminergic activity enhances the PC-fMRI signal gain during pairing as well as the subsequent brain wide representation of sensory stimuli.

## DISCUSSION

It is well known that midbrain dopaminergic neuronal activation produces neuronal excitation and plasticity in striatal target regions. However, it is not yet clear whether the effect

of elevated dopaminergic signaling is limited to these areas. This is an important question to address as it might shed light on the extent of anomalous activity seen in disorders such as addiction and schizophrenia. Two reports, using similar opto-fMRI methods, have shown that stimulation of VTA dopamine neurons produce BOLD signal changes locally within the VTA (Domingos et al., 2011) and the striatum (Ferenczi et al., 2016). Through our development of novel analytic methods, we extend these findings to show that fMRI related signal changes are not restricted to these regions but occur brain-wide. Our findings suggest that large-scale brain wide activity dynamics, measured across many distinct neuroanatomical regions, are also directly or indirectly regulated by activity of VTA dopaminergic neurons *in vivo*. In addition, dopaminergic activity, coincidental with a particular sensory stimulus, enhanced stimulus-specific neuronal representations brain wide. Previous work has largely focused on the timing at which dopaminergic activity occurs during ongoing behavior (Cohen et al., 2012; Day et al., 2007; P. E. M. Phillips et al., 2003; Wolfram Schultz, 1998; Stuber et al., 2008) as well as cellular mechanisms by which dopamine signaling can alter the function of individual neurons (Gee et al., 2012; Jacob, Ott, & Nieder, 2013; Lewis & O'Donnell, 2000; Marder, 2012). Although we can state that changes in the brain wide signal are a result of direct stimulation of VTA TH expressing neurons, we cannot exclude an effect from coincidental signaling by Glutamate/GABA that may also be released from VTA dopaminergic neurons (Chuhma et al., 2004; Hnasko et al., 2010; Lavin et al., 2005; Stuber, Hnasko, et al., 2010; Tritsch et al., 2012, 2014). Nevertheless, in the presence of a D1R antagonist, the extent of activation due to TH<sup>VTA</sup> stimulation reduced significantly, with only a few non-striatal voxels showing significant responses (**Figure A.3 F**). Indeed, one study (Marota et al., 2000) found that SCH23390 alone provided nearly complete blockade of cocaine-induced functional responses in rats, implicating a

major role for D1 receptor activation during cocaine administration. Thus, while a significant amount of brain-wide responses is D1R dependent, the residual striatal signal may be dependent on either D2R activation or Glutamate/GABA signaling. While our current work shows that VTA dopaminergic neuronal activity has immediate global consequences, and can remodel brain-wide neuronal activity patterns alone or in the presence of a sensory stimulus, future work is needed to assess how each specific neurotransmitter species that is released by VTA dopaminergic neurons contributes to these phenomena.

In order to detect and characterize brain-wide activity patterns measured with fMRI following TH<sup>VTA</sup> optogenetic stimulation, we developed a PCA based approach. This allowed us to reduce the dimensionality of the data in the voxel space, isolate the PC temporal trace that represents the stimulation effect, and then map voxels that contribute significant weight to this PC back to anatomical locations in the brain. The identification of brain voxels that significantly contribute to the PC representing the stimulation effect is effectively similar to the standard GLM approach (Monti, 2011) with notable distinctions. First, standard implementations of GLM require *a priori* specification of an expected stimulation effect. This is traditionally calculated using a hemodynamic response function. However, these functions vary widely across brain regions and species, and additionally are oftentimes derived from task-evoked activity, which is difficult to evaluate brain wide. Moreover, if multiple valid stimulation templates need to be compared (especially in the case with multiple regions of interest), power of the analysis can be dramatically compromised due to corrections for multiple comparisons. In contrast, our model free approach is entirely data driven and makes no assumptions of regional fMRI response specificity, thus making it highly applicable for analyzing brain wide changes in fMRI activity throughout the entire rat brain in response to timelocked stimulation. Another key

benefit of our approach is apparent in the case where the stimulation of interest is not of a sensory region but is instead of a region that releases neuromodulators (e.g. VTA). In this case, modeling the expected stimulation effect as a standard sensory stimulation based template may be inappropriate as these models assume an exponential decay of the signal immediately following stimulation offset (**Figure A.2 F**). However, extracting the stimulation response template using PCA (**Figure 2.3 E**) shows that the stimulation has a prolonged effect even after stimulation offset. Thus, in such cases, we advocate a data-driven approach to extract the stimulation response function. One caveat to our method is that a single PC representing the stimulation effect might also contain shared variation that is independent of the stimulation (for example intrinsic brain oscillations across regions). This is mitigated within our pipeline by averaging raw fMRI voxels across all animals in each group, since the shared temporal variability that remains in the data is likely only due to the stimulation. Furthermore, the voxel-wise analysis used here addresses some of the concerns and limitations inherent to cluster-based approaches more common in fMRI data analysis (Eklund, Nichols, & Knutsson, 2016). It is also possible that a single PC does not completely isolate the entire stimulation effect on brain wide activity. This in theory could be improved by additionally performing independent component analysis within the subspace formed by the top PCs. However, in the current dataset no post-stimulation effects were observed outside of the first PC. Taken together, our brain wide fMRI analysis approach was designed to be easily implemented and sensitive enough to detect stimulation-induced changes in activity across the brain, while also imposing as few assumptions as possible.

The dramatic sensory pattern emergence following TH<sup>VTA</sup>-forepaw pairing showcases the utility of optogenetic-fMRI experimentation (**Figure A.3**), as findings would have likely been

unresolvable using methods that are focused on recording activity in one particular anatomical site. Importantly, our approach can easily be applied to examine the brain wide consequences of the modulation of any particular neurocircuit node. Our data also suggest that by pairing a sensory stimulus with activation of the TH<sup>VTa</sup> neurons produces an immediate enhancement of the sensory representation (even on the first pairing) while not affecting the rate of habituation to the sensory stimulus (**Figure 2.6 A-C**). Our findings provide a foundation and roadmap for future studies that will examine the duration and/or permanence of the brain-wide sensory enhancement by TH<sup>VTa</sup> stimulation as well as examine similar phenomena at the cellular level in a particular brain region using large-scale single cell calcium imaging approaches.

It is well documented that isoflurane utilized during opto-fMRI experiments can significantly suppress evoked hemodynamic responses and do not fully reflect those observed during the awake state (Desai et al., 2011; Ferenczi et al., 2016). In the present study, animals were continuously infused with a cocktail comprised of the  $\alpha_2$ -adrenergic receptor agonist, dexmedetomidine and the paralytic agent pancuronium bromide supplemented with very light isoflurane anesthesia (0.5%) over the course of fMRI scan acquisition (Fukuda et al., 2013). While this study attempts to minimize the effects of isoflurane by coupling its use with a sedative and paralytic agent, future studies are needed to replicate our findings in awake animals. We predict we would see the same enhancement of the sensory representation to an even greater extent if these experiments were performed on awake animals. We also predict we would still see an enhanced response, albeit to a slightly lesser extent, while utilizing shorter optogenetic stimulation epochs during the TH<sup>VTa</sup>-forepaw pairing, which would better resemble physiologically relevant dopaminergic signaling seen during normal reward processing. Future studies using unpaired stimulations or utilizing another sensory input of another modality

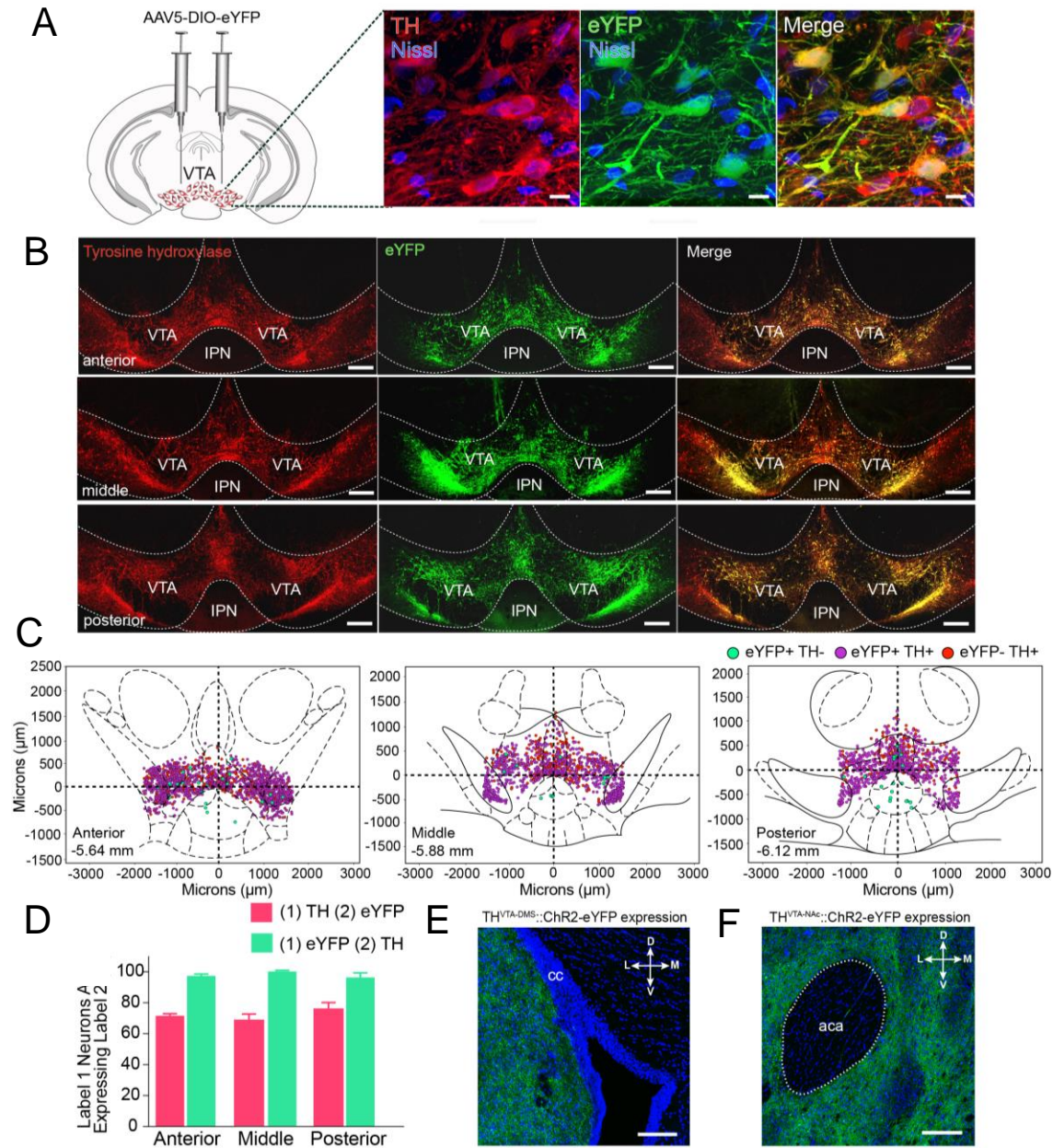
following pairing would also be ideal to further investigate whether explicit pairing of dopaminergic signaling and a sensory stimulus is necessary for this effect. It is also important to consider the results of a recent report showing that non-specific stimulation of the VTA can induce reanimation from general anesthesia, including isoflurane (Solt et al., 2014), making it possible that enhanced response to sensory stimuli in the ChR2-eYFP group may be due to reduced depth of anesthesia. Although not recorded, there were no observable changes in autonomic responses (i.e. heart rate, end tidal CO<sub>2</sub>, O<sub>2</sub> saturation) that would indicate animals were becoming more conscious during photostimulation of TH<sup>VTA</sup> neurons.

A hallmark feature of both adaptive learning and addiction is the enhanced salience that sensory stimuli acquire when paired with natural rewards or drugs of abuse. Consistent with this, direct activation of VTA dopaminergic neurons promotes stimulus driven learning (Steinberg et al., 2013; Tsai et al., 2009; Witten et al., 2011), but can also result in addiction-like phenotypes in animals (Pascoli et al., 2015). It has been proposed that drugs of abuse and cues that predict these drugs, by increasing dopaminergic activity, will be processed as salient stimuli, thus promoting motivated behavior to obtain more drug (Robinson & Berridge, 2003). Although this is true for the initial drug experience, many have argued that over the course of addiction, neural control of drug taking behaviors shifts to become dependent on non-dopaminergic mechanisms (Peter W. Kalivas & Volkow, 2005). In support of this, human and animal studies have shown that extensive drug experience decreases dopaminergic signaling in response to both drug and drug associated cues over time despite increased salience and behavioral responses (i.e. drug seeking/taking) to those cues (Volkow et al., 2014; Willuhn, Burgeno, Groblewski, & Phillips, 2014). By elucidating the brain wide activity pattern evoked by TH<sup>VTA</sup> stimulation paired with a sensory stimulus, we show that dopamine-driven plasticity in this experiment is not



limited to sensory cortices, but instead recruits numerous extrasensory brain regions, even in the absence of further dopaminergic signaling (i.e. as seen during the post-pairing paw stimulation). Taken together, our findings reveal a putative mechanism whereby drugs and drug-associated cues become pathologically salient, particularly through dopamine-mediated recruitment of non-dopaminergic mechanisms during early drug use, such that these cues remain salient despite subsequent hypoactivity in the dopamine system as seen during later phases of addiction.

## FIGURES

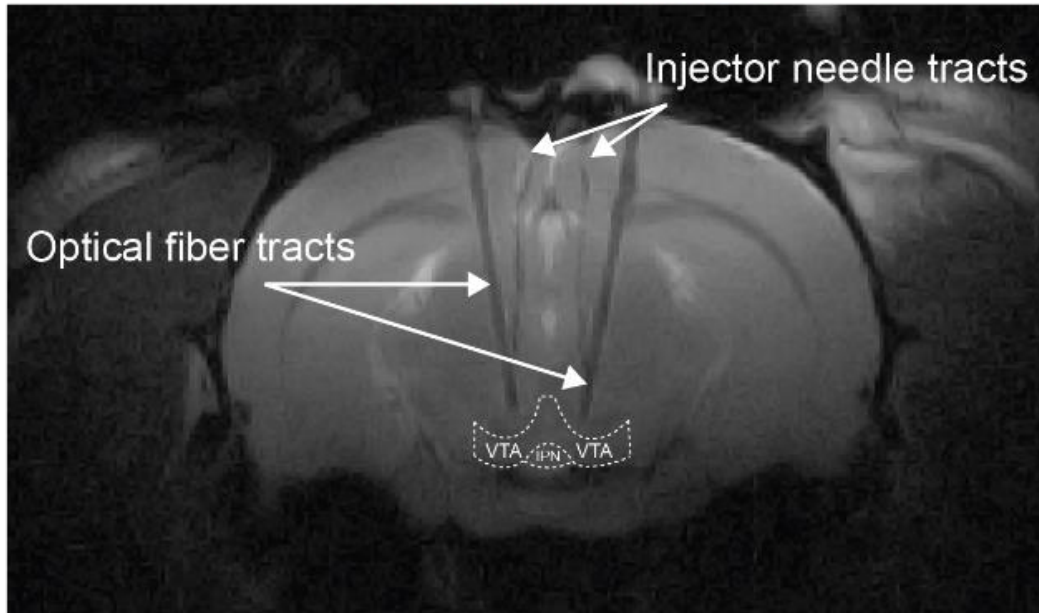


**Figure 2.1: Viral targeting of VTA dopaminergic neurons in TH-cre rats.**

(A) 63x and (B) 20x confocal images depicting eYFP expression (green) following injection of a Cre-inducible virus into the VTA in TH-cre rats. Merged images reveal co-localization of eYFP and TH; red = TH; blue = Nissl stain; VTA: Ventral Tegmental Area, IPN: Interpeduncular Nucleus. (C,D) Quantification of the location of all neurons within anterior, middle, and posterior slices of the VTA expressing only eYFP (eYFP+/TH-), TH (eYFP-/TH+), and neurons that expressed both (eYFP+/TH+) ( $n = 9$  sections in  $n = 3$  rats). Collapsed across the anterior-posterior axis,  $71.9 \pm 2.1\%$  of TH+ neurons within the VTA also expressed eYFP and  $97.4 \pm 1.0\%$  of eYFP positive cells also expressed TH. Error bars represent SEM. (E,F) Confocal images showing expression of ChR2-eYFP fibers in downstream target regions of the VTA including the dorsomedial striatum (DMS) and nucleus accumbens (NAc) of a TH<sup>VTA</sup>::ChR2 rat. cc: corpus callosum, aca: anterior commissure. Scale bars, 200 and 500  $\mu$ m, respectively.

**A**

T2-weighted MRI image



**Figure 2.2: Optical fiber placement in the VTA of TH-cre rats.**

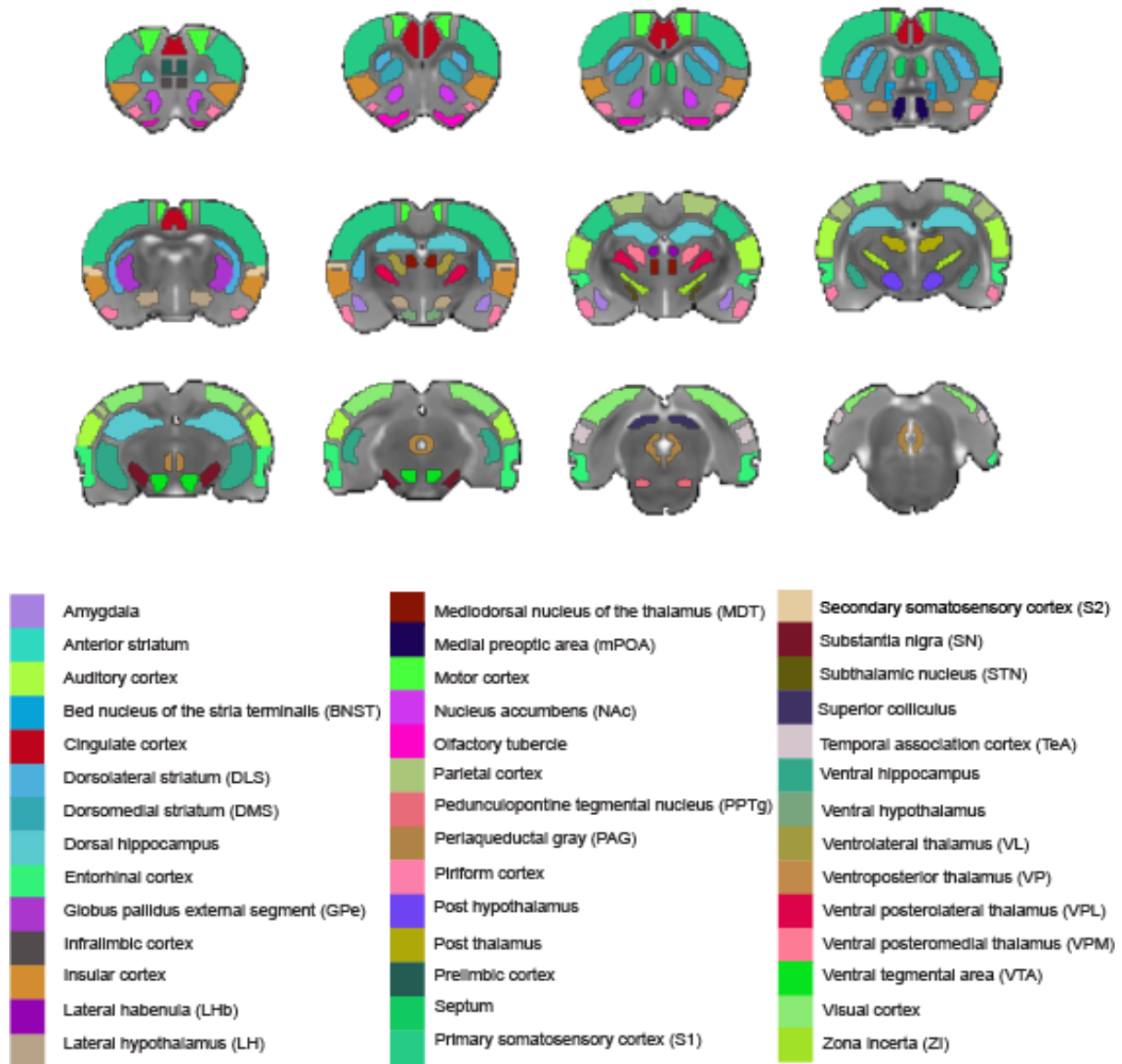
(A) RARE T2-weighted sequences were used to confirm optical fiber placements.



scatter plot showing the correlation between the weight of a voxel to the first PC and its mean post-stimulation response for both groups. **(G)** The raw voxel traces for the top 500 voxels contributing to the first PC for both groups. **(H)** The map showing the significant voxels contributing to the first PC vector for the experimental group, for which a significant post-stimulation response was identified (see Supplementary information). There was no PC for the control group that represented any significant post-stimulation effect. PC weights were divided by the maximum PC weight for normalization. **(I)** Individual ROIs and their fractional contribution (see Supplementary information) to the PC representing the stimulation effect is shown in cyan. Red and green show the fraction of significant voxels that shows significant GLM coefficients for the experimental and control group, respectively.

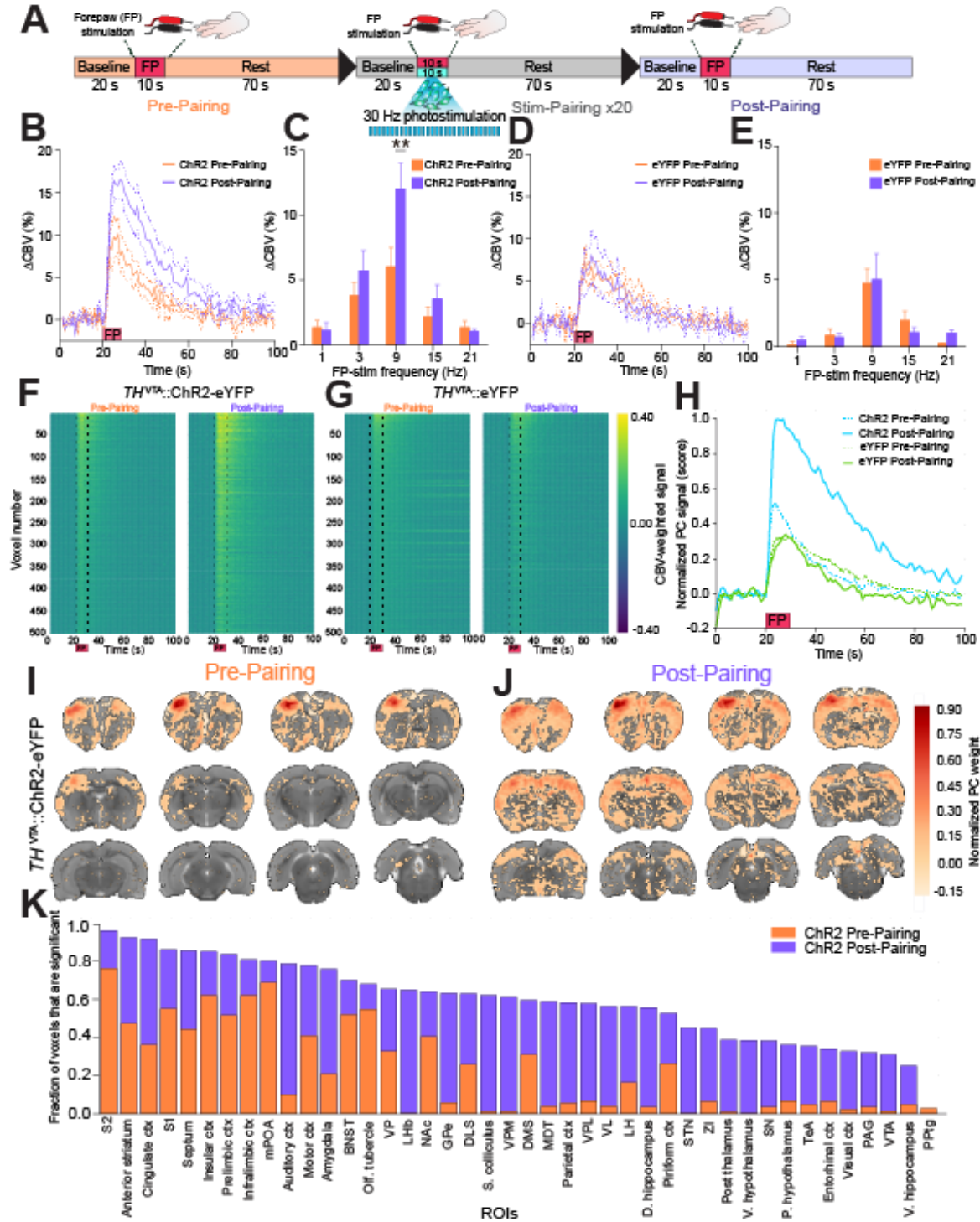


A



**Figure 2.4: Map of defined regions of interest.**

(A) 42 anatomical subregions are shown across the 12 slices of the brain.

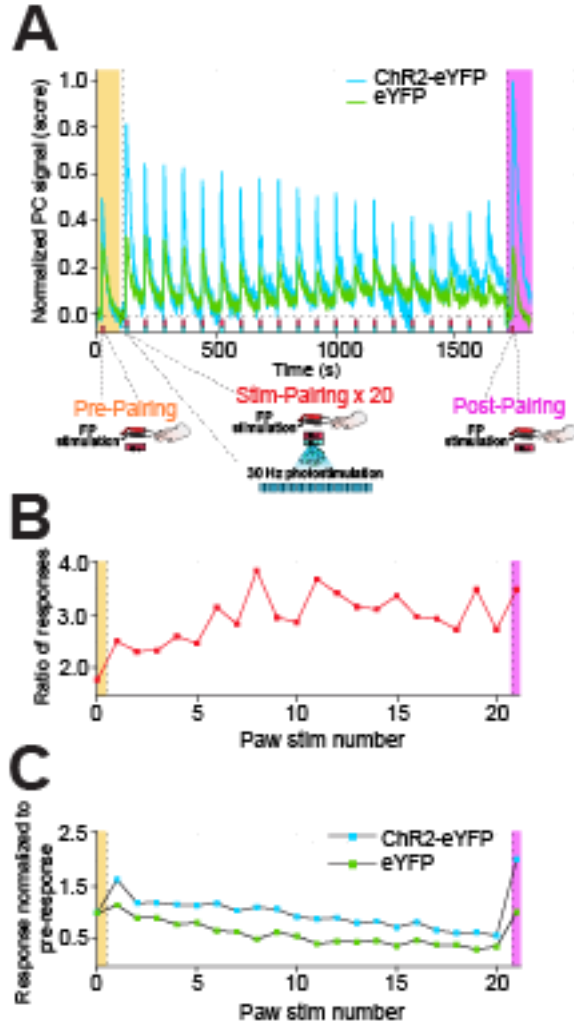


**Figure 2.5: Whole brain analysis of forepaw stimulation pre and post pairing with  $TH^{VTA}$  neuron stimulation.**

(A) Experimental timing diagram. (B) Following pairing of VTA dopaminergic activity with 9 Hz FP stimulation there was a significant increased somatosensory cortex CBV timecourse signals (group main effect:  $F_{1,99} = 183.7$ ,  $P < 0.0001$ ,  $n = 7$  rats per group). (C) Pairing VTA dopaminergic activity with 9 Hz FP stimulation selectively

enhanced somatosensory CBV signals at 9 Hz compared to other tested frequencies (pairing main effect:  $F_{1,50} = 5.58$ ,  $P = 0.0219$ ,  $n = 6-7$  rats per group, double asterisks denote significant ( $p < 0.01$ ) post-hoc tests between before and after pairing at each frequency). **(D)** Following pairing of VTA laser light delivery with 9 Hz FP in rats only expressing eYFP did significantly change CBV responses in somatosensory cortex although the postpairing effect was slightly lower than prepairing (group main effect:  $F_{1,99} = 3.976$ ,  $P = 0.0465$ ,  $n = 5$  rats per group). **(E)** Pairing VTA laser light delivery with 9 Hz FP stimulation in rats only expressing eYFP did not alter somatosensory CBV frequency tuning signals (pairing main effect:  $F_{1,50} = 0.02$ ,  $P = 0.8785$ ,  $n = 5$  rats). **(F,G)** Raw voxel traces pre and post pairing around the forepaw stimulation (FP) for experimental and control groups, respectively. Post-pairing FP shows an enhancement of responses only for the experimental group. The voxels are sorted according to their pre-pairing FP response. The same row represents the same voxels across pre and post-pairing for both groups. **(H)** PC traces (scores) for all conditions. **(I,J)** The PC vectors capturing the FP response for pre and post pairing in the experimental group, showing a dramatic enhancement of voxels that significantly contribute to the PC representing the FP response. **(K)** Individual ROIs showing fractional contribution to the PCs representing FP response.





**Figure 2.6: Evolution of forepaw stimulation pairing response over the course of pairings.**

(A) The PCs identified (see Supplementary information) as the ones representing forepaw stimulation response for both groups. The plots show pre-pairing and post-pairing forepaw stimulation responses, along with 20 responses during the pairing. (B) The ratio of forepaw stimulation response (difference between the peak response during stimulation and the mean response during a 10 s baseline period prior to stimulation) for each stimulation between the ChR2-eYFP group and the eYFP group. There is a significant enhancement (positive linear regression) in this ratio as a function of the forepaw stimulation number ( $slope = 0.044$ ,  $P = 0.005$ ,  $R^2 = 0.33$ ). (C) When the forepaw stimulation response for either group is normalized to the pre-pairing response for the same group, there is significant habituation (negative linear regression) with the number of stimulations during pairing for both groups (ChR2-eYFP:  $slope = -0.041$ ,  $R^2 = 0.895$ ; eYFP:  $slope = -0.034$ ,  $P < 0.001$ ,  $R^2 = 0.831$ ). Importantly, the magnitude of habituation, as measured by the slope of response with respect to pairing number, is statistically indistinguishable for both groups ( $F_{1, 19} = 2.10$ ,  $P = 0.156$ , interaction term in ANCOVA).

## **CHAPTER 3: BRAIN-WIDE FUNCTIONAL CONNECTIVITY CHANGES FOLLOWING SELF-ADMINISTRATION OF COCAINE AND ABSTINENCE**

### **INTRODUCTION**

Cocaine is a powerfully addictive stimulant drug that exerts its reinforcing effects, at least in part, through the mesolimbic dopamine (DA) system (Aragona et al., 2008; Di Chiara & Imperato, 1988; Stuber, Roitman, et al., 2005). The direct consequences of DA signaling are classically thought to be largely restricted to brain regions that contain appreciable presynaptic fibers that release DA. However, dopaminergic signaling may also indirectly influence many brain regions, some of which receive little to no direct dopamine input, by directly modulating the activity dynamics of neurons that are embedded within a more widespread functional brain circuit. For instance, we recently found using optogenetic fMRI that selective activation of ventral tegmental area (VTA) DA neurons recruits several anatomically distinct regions throughout the brain, not typically associated with DA release events, as discussed in **Chapter 2** (Decot et al., 2017). Considering this, we investigated whether cocaine exposure can alter functional connectivity, not only in dopamine-related circuits, but on a global scale.

While our understanding of the molecular, cellular and structural drug-induced changes following repeated cocaine exposure has advanced (Conrad et al., 2008; Muñoz-Cuevas, Athilingam, Piscopo, & Wilbrecht, 2013; Stuber, Hopf, Tye, Chen, & Bonci, 2010; Ungless et al., 2001), much less is known about the circuit-level neuroadaptations that occur. Resting state functional connectivity magnetic resonance imaging (rsfMRI) has emerged as a powerful neuroimaging tool as it provides researchers with a means to investigate large-scale brain network function. rsfMRI provides information about neuronal connectivity across the brain, as

spatially distinct regions that are interconnected display temporally synchronized spontaneous fluctuations at rest (Biswal et al., 1995). Previous human neuroimaging studies have revealed that cocaine dependence is associated with functional connectivity alterations in the brain (Gu et al., 2010; Tomasi et al., 2010; Wilcox, Teshiba, Merideth, Ling, & Mayer, 2011). However, confounding factors inherent to human subject research make it difficult to isolate the direct impact of cocaine exposure on the brain (Compton, Thomas, Stinson, & Grant, 2007; Greenland, Pearl, & Robins, 1999). Animal models of addiction not only allow researchers to probe the effect of chronic cocaine exposure in a more controlled manner but on the drug naïve brain, something that would not be possible in human research. Here, we used a standard, yet powerful pre-post, treatment-control design, which allowed us to measure brain-wide functional connectivity before and after cocaine exposure in the same animal and to compare these findings to a control group. This research may provide critical insight into the circuit-level maladaptations that underlie the escalation from voluntary use of the drug to the compulsive drug-seeking behavior, and chronic cycles of abstinence and relapse that characterize addiction in humans.

Here, we evaluated changes in global functional connectivity across the brain following self-administration of cocaine. Using a whole brain, data-driven independent component analysis (ICA) (Beckmann, DeLuca, Devlin, & Smith, 2005) and dual regression approach (Beckmann et al., 2009), we show that cocaine self-administration orchestrates dynamic shifts in functional connectivity across many anatomically defined neuronal networks and nodes, several of which that do not directly receive dopamine input. These findings provide new insight into the global adaptation in neurocircuit function associated with cocaine exposure and identifies novel neuroanatomical circuit nodes associated with phases of addiction.

## **METHODS**

### **Experimental Subjects**

All procedures were conducted in accordance with the Guide for the Care and Use of Laboratory Animals, as adopted by the National Institutes of Health, and with approval of the Institutional Animal Care and Use Committee at the University of North Carolina (UNC). Adult (initially weighing ~300 g) male Sprague Dawley rats (Charles River Laboratories) were individually housed and maintained on a 12-h light cycle. All animals were mildly water restricted to ~20 ml/d during the self-administration portion of the experiment. Animals also underwent mild food restriction during the 30d abstinence period to maintain ~90% body weight during this portion of the study. A schematic of the experimental set-up and timing of surgical procedures and scans appears in **Figure 3.1** and detailed descriptions of the experimental procedures are outlined below.

### **fMRI Procedures**

All animals underwent 6 consecutive 5-minute rsfMRI scans prior to self-administration, immediately following self-administration (within 24-48 hr following last session) and after 30d of abstinence. On the day of rsfMRI experiments, each rat was endotracheally intubated and initially ventilated with 2% isoflurane mixed with medical air. Each rat was then placed on a custom-built MR cradle lined with a warm-water circulating pad and rectal temperature was maintained at  $37 \pm 0.5^{\circ}\text{C}$ . The ventilation rate and volume were adjusted via a capnometer to maintain end-tidal CO<sub>2</sub> (EtCO<sub>2</sub>) within a range of  $3.0 \pm 0.2\%$ . Heart rate and oxygen saturation (SpO<sub>2</sub>) were continuously monitored by a non-invasive MouseOx Plus System with MR-compatible sensors and maintained within normal ranges (~280 b.p.m. and >96%, respectively). During fMRI acquisition, 2% isoflurane anesthesia was substituted with sedation, using dexmedetomidine (0.05 mg/kg/hr) and pancuronium bromide (0.5 mg/kg/hr) with 0.5%

isoflurane. All fMRI data were acquired using a 9.4 Tesla Bruker BioSpec MR scanner with a 72 mm volume coil and four-channel phased array receiver. BOLD functional resting state scans were acquired using a single shot gradient echo-EPI sequence (spectral width=150 kHz, TR/TE=2000/11.2 ms, FOV=2.88x2.88x1.28 cm, slices = 32, matrix=72x72 and spatial resolution=0.4 mm isotropic).

### **Cocaine Self-Administration**

Following the baseline rsfMRI scans, rats were surgically implanted with MR compatible intrajugular catheters and allowed to recover for one week prior to being randomly assigned to either the intravenous cocaine self-administration group (n = 7) or water self-administration (n = 6) control group. Catheter implantation surgeries were conducted as previously described (Carelli & Deadwyler, 1994). Each animal underwent daily 6h self-administration sessions for 10 days and were mildly water restricted to 20 ml/d over the duration of the training. At the beginning of each session, rats were placed into a standard self-administration chamber (25 x 25 x 30 cm, stainless steel rod floor; MED Associates) and connected via their intrajugular catheter to tubing that interfaced with a syringe containing either cocaine (1.67 mg/ml in 0.9% saline) or saline (0.9% saline). At the onset of each session, a cue light would become illuminated within the nosepoke port. We trained rats on a fixed-ratio of 1 (FR1) schedule where each nosepoke resulted in intravenous cocaine delivery (0.33 mg/infusion) over 6 s. Each infusion was signaled by the cue light turning off and the onset of a tone-house light stimulus over a 20 s interval. Nosepokes made during the 20 s post-response interval were recorded but had no consequences. Following this 20 s interval, the tone-house light stimulus turned off and cue light turned back on. For control animals, nosepokes delivered a 200  $\mu$ l water reward into a food cup to control for potential learning effects by the cocaine animals during a self-administration operant

behavior task. Control animals also received yoked saline infusions (0.9% saline, 0.2 mL, 6 s) contingent upon the delivery schedule of a paired rat in the cocaine self-administration group.

### **Data Pre-Processing**

Functional scans were preprocessed using the Analysis of Functional NeuroImages software suite (AFNI v2011-12-21-1014, Bethesda, MD) following standard pipelines. Briefly, the steps included skull-stripping, slice-timing correction, rigid-body motion correction, alignment to a high resolution template space (Valdés-Hernández et al., 2011), high-pass filtering ( $>0.01$  Hz) , and spatial smoothing (Gaussian kernel full width at half maximum, FWHM = 0.5 mm). Six motion parameters were regressed out of the data to minimize motion effects on the BOLD signal (AFNI 3dTproject).

### **Functional Connectivity Analysis**

#### *Multi-subject Independent Component Analysis (ICA)*

Following data pre-processing, rsfMRI connectivity analyses were carried out using FMRIB Software Library (FSL v5.0, University of Oxford, Oxford, UK) using a group-level, multi-session independent component analysis (ICA) temporal concatenation approach. FSL Multivariate Exploratory Linear Optimized Decomposition into Independent Components (Melodic) was used to extract 30 group-level components on the baseline scans collected from all subjects. Each IC was visually inspected and classified as either a component that represented a resting state network (RSN) or noise. Components exhibiting artifacts and noise were discarded while the components selected for further analyses were classified as a specific RSN, defined by the brain regions found within each network and RSNs defined previously in existing literature.

## Dual Regression Analysis

To further analyze whether cocaine exposure alters brain-wide functional connectivity, we used a dual regression analysis approach (Beckmann et al., 2005; Filippini et al., 2009). First, using the spatial IC maps that were classified as a RSN in the initial gICA, we performed regression on all rsfMRI subject data along the time axis to estimate the subject level oscillation of each IC. Using this estimated subject level oscillation time-course data, we then performed regression again on subject rsfMRI data (including every trial performed on each subject) to extract the subject and trial specific IC map. Bayesian Ridge estimator of scikit-learning module in Python was used for this analysis. Finally, group analysis was performed to compare the between group and within group effect with repeated-measures ANOVA using 3dMVM in AFNI package (G. Chen, Adleman, Saad, Leibenluft, & Cox, 2014). Spatial maps were created showing the significant group differences between their respective pre- and post- condition.

### *Seed-based Connectivity Analysis*

First, seed regions chosen for this analysis were those areas showing statistical significance in the cocaine pre- and post-condition difference maps following the dual regression analysis. Using 0.01 Hz – 0.1 Hz bandpass filtering, we extracted the subject level time course from each seed. Seed-based whole brain connectivity maps were generated by calculating the Pearson correlation coefficient between the seed time course and the time course of every other voxel across the brain. These values underwent Fisher's z-transformation and subjected to one-sample t-tests. Group analysis was performed using repeated-measures ANOVA ( $p < 0.01$ ).

### *Multiple Comparison Correction*

The noise spatial autocorrelation of the rsfMRI data were estimated using a mixed model (AFNI 3dFWMx software). We applied family wise error rate (FWER) correction using

3dClustSim acf function to estimate the cluster size at  $p\text{-value} = 0.01$  and  $\alpha = 0.05$  (Robert W. Cox, Chen, Glen, Reynolds, & Taylor, 2017; Eklund et al., 2016).

## RESULTS

Following the baseline rsfMRI scans, rats were intravenously catheterized and allowed to recover for one week prior to being randomly assigned to either the intravenous cocaine self-administration group ( $n = 7$ ) or water self-administration ( $n = 6$ ) control group. Each rat was mildly water restricted and trained to self-administer either cocaine (0.33 mg/infusion over 6s) or a water reward (200  $\mu$ l). Control animals also received yoked saline infusions (0.9% saline, 0.2 mL over 6 s) contingent upon the delivery schedule of a paired rat in the cocaine self-administration group (**Figure 3.1 A**). Due to poor physiology, primarily because of weight gain, data collected from the abstinence scan sessions was not analyzed. Results of self-administration behavior are displayed in **Figure 3.1 B**. There was no significant difference in main effect of Drug type,  $F_{(1, 11)} = 0.7524$ ,  $P = 0.4043$ , and a significant Day x Drug interaction,  $F_{(9, 99)} = 9.395$ ,  $P < 0.0001$ .

We first used multi-subject ICA to derive resting state networks (RSNs) from the baseline scans acquired from all subjects ( $n = 13$ ). Each component was mapped onto a T2-weighted reference brain atlas and anatomical regions within each component were identified. Following visual inspection of the 30 extracted components, 11 of them were excluded due to noise artifacts (**Figure A.8 A**). The remaining 19 components were each classified as a RSN, representing a group of brain regions that exhibit spontaneous BOLD fluctuations at rest that are highly correlated with each other (**Figure 3.2**). We used the findings from several previous reports, across species, using similar analytical methods to classify them appropriately (Becerra, Pendse, Chang, Bishop, & Borsook, 2011; Buckner, Andrews-Hanna, & Schacter, 2008; Hutchison et al., 2010; Lu et al., 2012; Seeley et al., 2007; Vincent et al., 2007). The 19



networks were classified as follows: sensorimotor and somatosensory networks (**Figure 3.2 A**), striatal and hippocampal networks (**Figure 3.2 B**), fronto-insular and thalamocortical networks (**Figure 3.2 C**), visual and auditory networks (**Figure 3.2 D**), anterior default mode and posterior default mode networks (**Figure 3.2 E**), cerebellar networks (**Figure 3.2 F**), and olfactory networks (**Figure 3.2 G**).

We used a dual regression analysis approach to investigate whether correlated activity between these networks and other brain structures was altered following cocaine exposure. This analysis revealed significant increases in correlated activity between the anterior cingulate cortex and the visual network (IC #14) (FWER-corrected,  $p$ -value = 0.01,  $\Delta Z = -1.94 \pm 0.43$ ; **Figure 3.3**) and between the somatosensory cortex and the sensorimotor network (IC #8) (FWER-corrected,  $p$ -value = 0.01,  $\Delta Z = -2.31 \pm 0.43$ ; **Figure 3.4**) following exposure to cocaine in drug naïve rats. Although trending but not passing FWER-correction at  $p = 0.01$ , we also observed an increase in correlated activity between the cingulate cortex and somatosensory network (IC #3) following cocaine exposure (not FWER-corrected,  $p$ -value = 0.05,  $\Delta Z = -1.32 \pm 0.35$ ; **Figure 3.5**) as well as a reduction in correlated activity between the insular cortex and the hippocampal network (IC #18) (not FWER-corrected,  $p$ -value = 0.05,  $\Delta Z = 1.73 \pm 0.40$ ; **Figure 3.6**). No significant differences were observed between these regions and their respective networks in the yoked-saline control animals (**Figures 3.3 – 3.6**).

Finally, since the four regions derived from the dual regression analysis indicate areas in the brain that significantly altered their correlated activity with a specific network following cocaine exposure, we used a seed-based connectivity analysis to further investigate whether these regions altered their connectivity strength with other brain structures. Following cocaine exposure, the two anterior cingulate cortex seeds that showed greater coactivation with the

somatosensory (IC #3, Seed 1) and visual networks (IC #14, Seed 2) (**Figure 3.7 A, Figure A.9**) showed significant reduction in functional connectivity strength with the dorsal striatum (FWER corrected, p-value = 0.01; Seed 1:  $\Delta Z = 0.135 \pm 0.03$ , Seed 2:  $\Delta Z = 0.143 \pm 0.03$ ; **Figure 3.7 B**). No significant differences in functional connectivity with these two anterior cingulate cortex seed regions were observed in the control animals (**Figure 3.7 C**).

## DISCUSSION

Our findings characterize the effect of high levels of cocaine exposure on the drug naïve brain. Through our use of an unbiased, data-driven analysis approach, we show that cocaine exposure caused significant, large-scale neuronal network changes in functional connectivity across several distinct brain regions. Specifically, we found that cocaine exposure caused an increase in functional connectivity between the anterior cingulate cortex with the visual and somatosensory networks, and local strengthening within the sensorimotor network with the somatosensory cortex in drug naïve rats. We also found a reduction in functional connectivity between the insular cortex and the hippocampal network in these animals. These changes were not present in the yoked-saline control animals, suggesting these alterations are specific to drug exposure in the cocaine animals. Previous preclinical work has largely focused on the effect of acute cocaine exposure on functional connectivity in animals during forced abstinence that have had a prior history of cocaine self-administration (Lu et al., 2014; Murnane et al., 2015). To our knowledge, this is the first study to assess the network-level effects of cocaine exposure on the drug naïve brain in rodents. Our findings may begin to provide a critical mechanistic link between neural system dysregulation following cocaine exposure and the maladaptive behaviors that ensue in drug addiction.

Our first main finding was that cocaine exposure caused corticocortical projection strengthening between the anterior cingulate cortex and visual and somatosensory cortices, and

local strengthening within the sensorimotor network. The rat cingulate cortex has been shown to be neuroanatomically connected with the visual and sensorimotor cortices (Carmichael & Price, 1995; Hoover & Vertes, 2007; Vogt & Miller, 1983) and sensory stimuli, including those that are visual and auditory, have been shown to cause evoked responses within the cingulate cortex in non-human primates (Cuénod, Casey, & MacLean, 1965). It has been shown that the neuronal firing rate in the rat cingulate cortex in response to a sensory stimulus increases when the stimulus has been paired with a positive reward (Segal, 1973). Drug addiction is marked by enhanced salience and hypervigilance for sensory stimuli that have previously been paired with the drug of abuse. Intriguingly, several human neuroimaging studies using PET and fMRI to investigate brain activation in cocaine dependent individuals in response to exposure of a drug-associated cue show robust activation in the anterior cingulate cortex (Childress et al., 1999; Kilts, Gross, Ely, & Drexler, 2004; Maas et al., 1998; Wexler et al., 2001). Thus, the strengthening in functional connectivity between sensory cortical regions and the anterior cingulate cortex following cocaine exposure may act to over-enhance the salience of an environmental stimulus that had previously been paired with drug, which may promote drug craving and relapse.

We also found a reduction in functional connectivity between the hippocampal network and the insular cortex following cocaine exposure. Mounting evidence suggests that the insular cortex is important in drug addiction. It has been shown that lesioning the insular cortex can extinguish previously established conditioned place preference for nicotine in mice (Scott & Hiroi, 2011). Importantly, it has also been shown that damage to the insular cortex following stroke in humans disrupts addiction to cigarette smoking (Naqvi, Rudrauf, Damasio, & Bechara, 2007; Suñer-Soler et al., 2012). There are conflicting reports on whether there are direct

projections from the insular cortex to the hippocampus, with one study reporting their existence (Barbas & Blatt, 1995) while others do not (Aggleton, Wright, Rosene, & Saunders, 2015; Carmichael & Price, 1995). Nonetheless, defined circuits do not exist in isolation to one another, thus network activity dynamics can be altered by neurons that are polysynaptically downstream from one another. Whether these changes reflect network-level alterations underlying the maladaptive behavioral outcomes seen in addiction is a question that remains to be answered and would need to be addressed in future studies.

Finally, we performed a seed-based functional connectivity analysis approach on the seed regions derived from the dual regression analysis, and found a significant decrease in functional connectivity between the anterior cingulate cortex and the striatum (ventral portion of the caudate putamen (CPu) and NAc) following cocaine exposure. The CPu has been heavily implicated in habit learning, including playing a significant role in the habitual, automated drug-seeking behavior seen in addiction, whereas the NAc is integral for reward-related behaviors (Day & Carelli, 2007; T. W. Robbins & Everitt, 1999; Vanderschuren, Di Ciano, & Everitt, 2005). The anterior cingulate cortex sends projections mainly to the rostral striatum, including the NAc (both core and shell), caudate and putamen (Brog, Salyapongse, Deutch, & Zahm, 1993; Haber, Kim, Mailly, & Calzavara, 2006). Decreased functional connectivity between the prefrontal cortex and striatum following cocaine exposure in drug naïve rats may cause a loss of top-down inhibitory control over striatal activity, contributing to the impaired response inhibition seen in addiction. Indeed, human neuroimaging studies indicate that chronic cocaine use is associated with deficits in prefrontal cortical function (Goldstein & Volkow, 2002, 2011). Several preclinical studies have also shown a reduction in prefrontal cortex activity following prolonged cocaine self-administration (B. T. Chen et al., 2013; Jasinska, Chen, Bonci, & Stein,

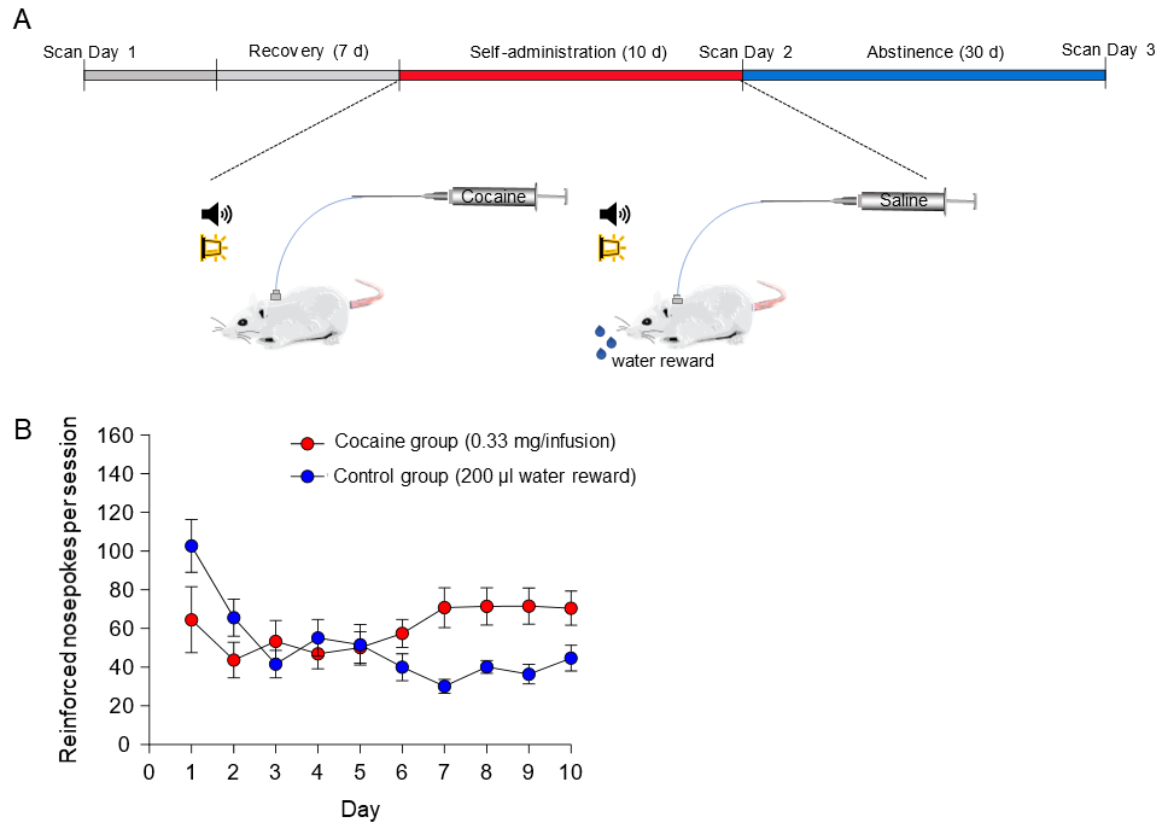
2015). In fact, using optogenetic stimulation techniques to rescue the cocaine-induced hypoactivity of the prefrontal cortex significantly inhibited compulsive cocaine seeking (B. T. Chen et al., 2013). Two recent studies found that acute cocaine exposure following a period of abstinence in animals who had previously undergone cocaine self-administration, caused a significant reduction in functional connectivity between the dorsolateral prefrontal cortex and NAc (Lu et al., 2014; Murnane et al., 2015), and degree of impairment between these two regions reliably predicted cocaine intake during the resumption of cocaine use (Murnane et al., 2015). These results suggest that our findings may not be transient and continue to persist following a period of abstinence. Thus, our findings provide further evidence that frontostriatal dysregulation may reflect a key biomarker underlying compulsive drug-seeking and the high relapse susceptibility found in cocaine dependence (Hanlon, Beveridge, & Porrino, 2013).

To detect and characterize brain-wide functional connectivity alterations that occur following exposure to cocaine in drug naïve rats, we coupled multi-subject ICA with a dual regression approach (Beckmann et al., 2005). This allowed us to derive multiple independent components which corresponded to globally, distributed resting state networks, to identify the associated temporal dynamics within the fMRI dataset that correspond with these networks, and to then characterize the within-group and between-group differences across condition, i.e. pre- versus post- cocaine or saline exposure. The results observed in this study showcase the utility of this unbiased, data-driven approach, as several of our findings identify regions of the brain that have not been extensively studied in relation to drug addiction. These data most likely would have been lost had we limited our search to a specific number of seed regions chosen *a priori*, as done with alternative methods, such as the seed-based analysis approach. Technical

considerations and limitations of the studies performed here, as well as future directions will be discussed in further detail in Chapter 4: General Discussion.

Together, these data suggest that cocaine exposure causes significant global network remodeling in the drug naïve brain. These findings may reflect key network-level alterations underlying the maladaptive behavioral outcomes seen in cocaine dependence. Importantly, this research provides a means to identify novel neuroanatomical circuit nodes associated with phases of addiction, and for future experiments to explore whether network-based interventions such as deep brain stimulation (DBS) and repetitive transcranial magnetic stimulation (rTMS) can normalize maladaptive network activity.

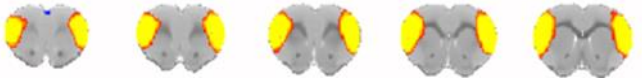
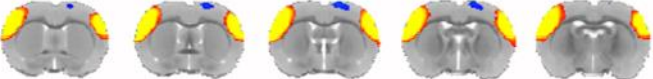

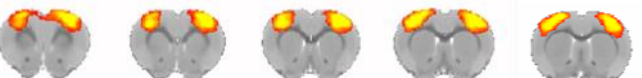
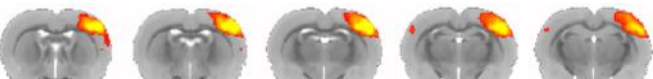
## FIGURES



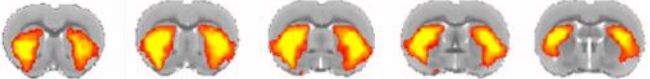
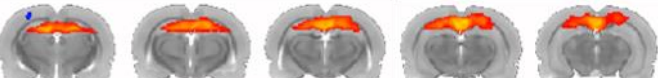
**Figure 3.1: Experimental timing diagram and self-administration training data.**

(A) All animals underwent 6 consecutive 5-minute rsfMRI scans prior to self-administration, immediately following self-administration (within 24-48 hr following last session) and after 30d of abstinence. Self-administration sessions were 6 h per day for 10 days. Cocaine rats were trained to nosepoke to self-administer intravenous cocaine (0.33 mg/infusion). Control rats were trained to nosepoke for a water reward and received yoked intravenous 0.9% saline infusions. All infusions were accompanied by a 20 s tone/house light stimulus. (B) Mean self-administration rates over the 10 days of training for rats nosepoking for cocaine ( $n=7$ ) or for water ( $n=6$ ). Error bars represent  $\pm$ SEM.



**A**

IC#	RSN	Anatomical regions within network	Network connectivity maps
2	Somatosensory	Insular cortex, S1, S2	
3	Somatosensory	S1, S2	
4	Sensorimotor	M1, M2, S1, Cingulate cortex, Parietal cortex	
8	Sensorimotor	M1, M2, S1, Cingulate cortex	
16	Sensorimotor	M1, M2, S1, S2	

**B**

IC#	RSN	Anatomical regions within network	Network connectivity maps
12	Striatal	Dorsal striatum, NAc	
18	Hippocampal	Dorsal hippocampus, Retrosplenial cortex	

**C**

IC#	RSN	Anatomical regions within network	Network connectivity maps
7	Fronto-insular	Olfactory bulb, OFC, PrL cortex, Cingulate cortex, Insular cortex	
9	Thalamocortical	PrL cortex, IL cortex, BNST, Thalamus, NAc, Cingulate cortex	



**D**

IC#	RSN	Anatomical regions within network	Network connectivity maps
14	Visual	Visual cortex, TeAC, Auditory cortex	
15	Auditory	Thalamus, Inferior Colliculus	

**E**

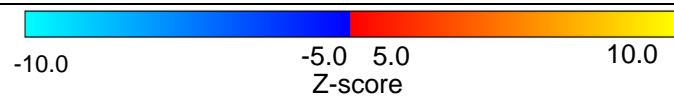
IC#	RSN	Anatomical regions within network	Network connectivity maps
5	Anterior Default Mode	PrL cortex, Cingulate cortex, Motor cortex, S1	
11	Anterior Default Mode	OFC, Cingulate cortex, PrL cortex, IL cortex	
13	Posterior Default Mode	M1, M2, S1, Cingulate cortex, Parietal cortex	
17	Posterior Default Mode	Cingulate cortex, Retrosplenial cortex, Hippocampus	

**F**

IC#	RSN	Anatomical regions within network	Network connectivity maps
6	Cerebellar	Olfactory bulb, TeAC, V1, Cerebellum	
26	Cerebellar	Cerebellum	

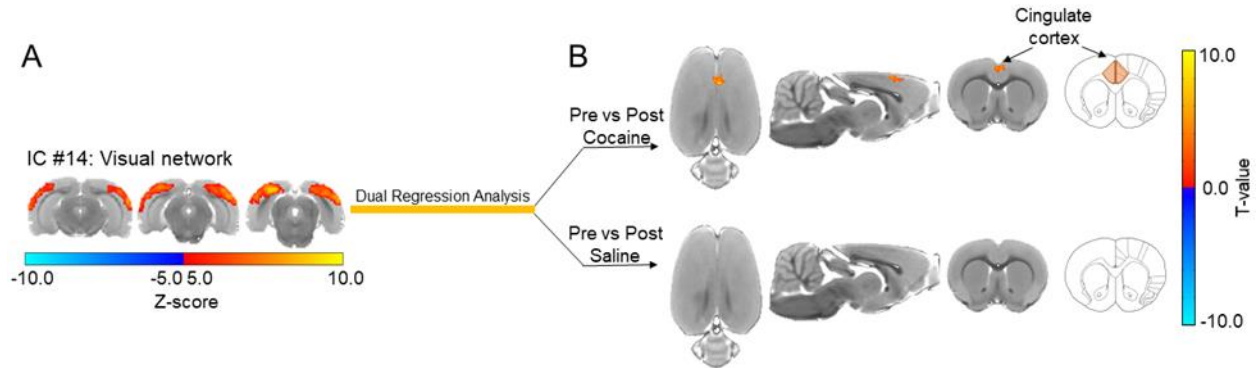
**G**

IC#	RSN	Anatomical regions within network	Network connectivity maps
10	Olfactory	Olfactory tubercle, Piriform cortex	
24	Olfactory	Piriform cortex	



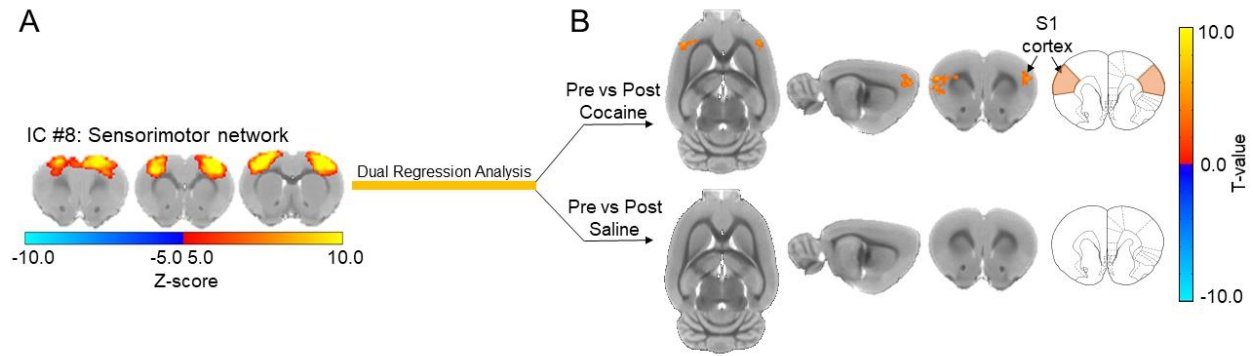
**Figure 3.2: Resting state networks derived from the multi-subject ICA analysis.**

(A) Somatosensory (IC# 2,3) and sensorimotor networks (IC# 4, 8,16). (B) Striatal network (IC# 12) and hippocampal network (IC# 18). (C) Fronto-insular network (IC# 7) and thalamocortical network (IC# 9). (D) Visual and auditory networks (IC# 14,15). (E) Anterior default mode networks (IC# 5, 11) and posterior default mode networks (IC# 13, 17). (F) Cerebellar networks (IC# 6, 26). (G) Olfactory networks (IC# 10, 24).



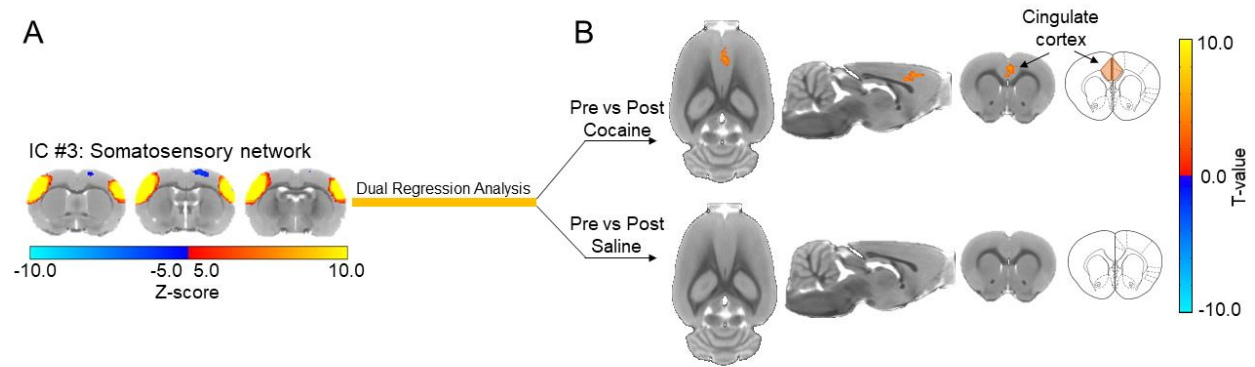
**Figure 3.3: Cocaine exposure causes a significant increase in functional connectivity between the visual network and the anterior cingulate cortex in drug naïve rats.**

(A) Visual resting state network (IC #14) spatial map derived from all subjects. Regions found within this network include visual cortex, temporal association cortex (TeAC) and auditory cortex. (B) Axial, sagittal and coronal slices showing brain areas that showed significant increases (orange) in coactivation with the visual resting state network following exposure to cocaine (FWER-corrected,  $p$ -value = 0.01,  $\Delta Z = -1.94 \pm 0.43$ ).



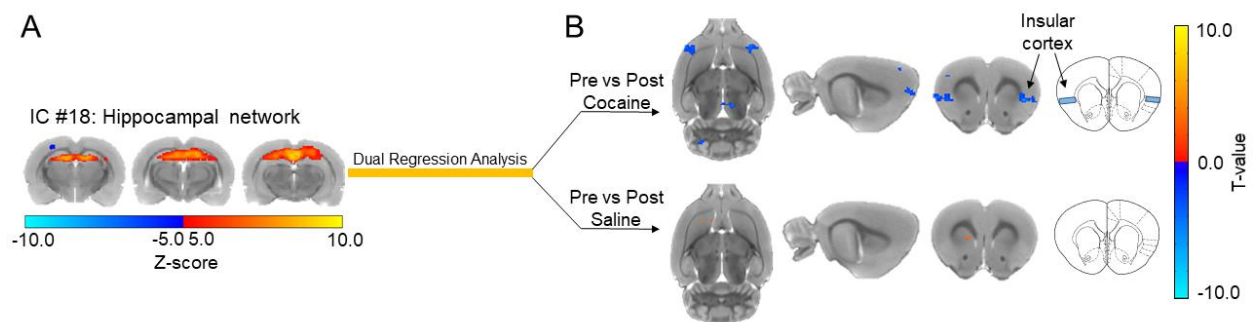
**Figure 3.4: Cocaine exposure causes a significant increase in functional connectivity between the sensorimotor network and the primary somatosensory cortex in drug naïve rats.**

(A) Sensorimotor resting state network (IC #8) spatial map derived from all subjects. Regions found within this network include primary motor cortex (M1), secondary motor cortex (M2), primary somatosensory cortex (S1) and cingulate cortex. (B) Axial, sagittal and coronal slices showing brain areas that showed significant increases (orange) in coactivation with the somatosensory resting state network following exposure to cocaine (FWER-corrected,  $p$ -value = 0.01,  $\Delta Z = -2.31 \pm 0.43$ ).



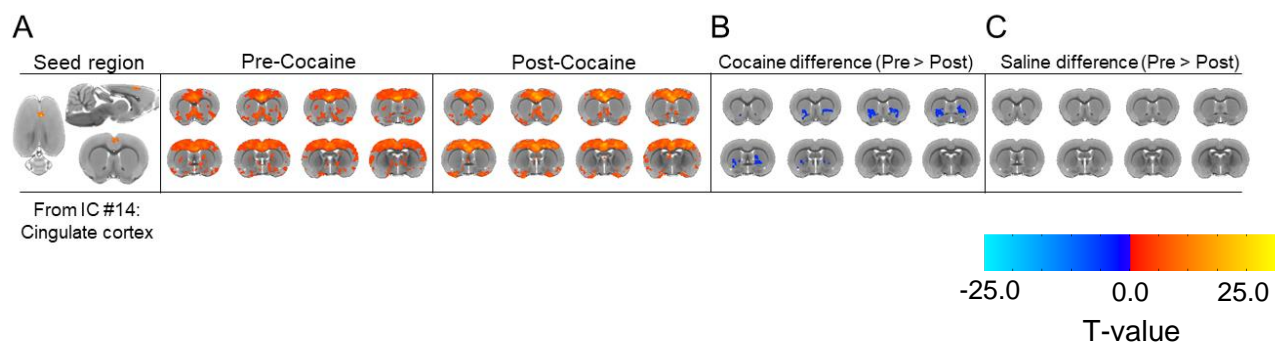
**Figure 3.5: Cocaine exposure causes an increase in functional connectivity between the somatosensory network and the anterior cingulate cortex in drug naïve rats.**

(A) Somatosensory resting state network (IC #3) spatial map derived from all subjects. Regions found within this network include primary somatosensory cortex (S1) and secondary somatosensory cortex (S2). (B) Axial, sagittal and coronal slices showing brain areas that showed significant increases (orange) in coactivation with the sensorimotor resting state network following exposure to cocaine (not FWER-corrected,  $p$ -value = 0.05,  $\Delta Z = -1.32 \pm 0.35$ ).



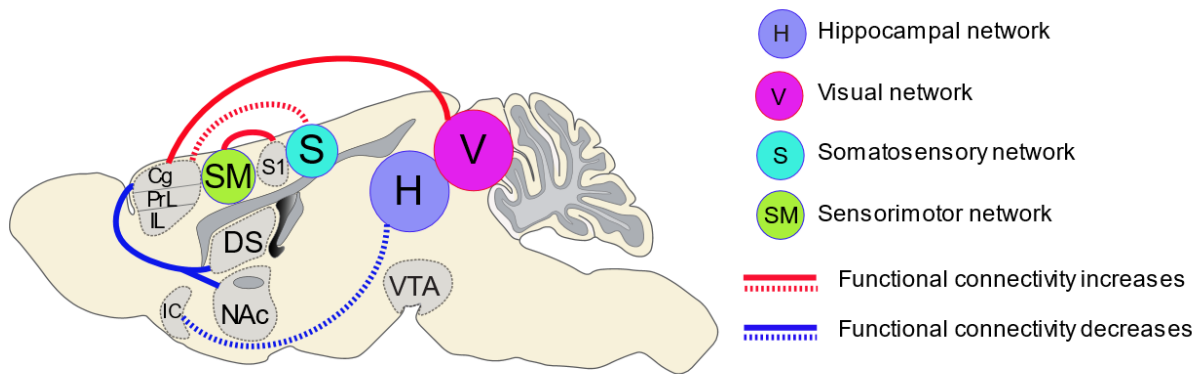
**Figure 3.6: Cocaine exposure causes a decrease in functional connectivity between the hippocampal network and the insular cortex in drug naïve rats.**

(A) Hippocampal resting state network (IC #18) spatial map derived from all subjects. Regions found within this network include dorsal hippocampus and retrosplenial cortex. (B) Axial, sagittal and coronal slices showing brain areas that showed significant decreases (blue) in correlated activity with the hippocampal resting state network following exposure to cocaine (not FWER-corrected,  $p$ -value = 0.05,  $\Delta Z = 1.73 \pm 0.40$ ).



**Figure 3.7: Seed-based whole brain connectivity maps of pre-cocaine and post-cocaine rsfMRI data.**

(A) Anterior cingulate cortex seed was derived from the dual regression analysis. (B) Group analysis was performed to compare between group effects and revealed a significant reduction in functional connectivity between the anterior cingulate cortex and the striatum (NAc and ventral portion of CPu) following exposure to cocaine in drug naïve animals (FWER corrected,  $p$ -value = 0.01;  $\Delta Z = 0.143 \pm 0.03$ ). (C) No differences between condition were observed in the control group.



**Figure 3.8: Functional connectivity changes following cocaine exposure in drug naïve rats.**

Sagittal view of the rat brain showing the statistically significant (FWER-corrected,  $p$ -value = 0.01) increases (red lines) and decreases (blue lines) in functional connectivity across the brain following cocaine exposure in drug naïve rats. The dashed lines indicate the functional connectivity increases and decreases that were trending towards significance but did not pass FWER-correction (not FWER-corrected,  $p$ -value = 0.05).

## CHAPTER 4: GENERAL DISCUSSION

### SUMMARY OF FINDINGS

The studies described in this dissertation reveal that midbrain dopaminergic modulation can orchestrate large-scale shifts in functional dynamics across several highly diverse regions throughout the brain, many of which receiving little to no direct dopaminergic input.

In Chapter 2, we coupled optogenetic stimulation techniques with fMRI in an *in vivo* transgenic rat model to investigate how the selective activation of DA neurons affects large-scale brain-wide function. By first applying a standard GLM analysis approach, our findings indicated that selective optogenetic stimulation of VTA DA neurons enhanced cerebral blood volume signals in striatal target regions in a DA receptor-dependent manner. However, through our development of a novel PCA approach, we demonstrated that dopaminergic modulation activates several additional anatomically distinct regions throughout the brain, not typically associated with DA release events. We also showed that explicit pairing of midbrain DA neuron activation and a sensory stimulus dramatically enhanced the sensory representation of that specific sensory stimulus. Taken together, these data suggest that VTA dopaminergic neuronal activity has immediate global consequences, and can modulate brain-wide neuronal activity patterns alone or in the presence of a sensory stimulus.

In Chapter 3, we presented evidence suggesting that extended exposure to cocaine for 10 days can cause significant global network remodeling in the drug naïve brain. Multi-subject independent component analysis performed on baseline rsfMRI datasets revealed several resting state networks distributed across the rat brain. Next, we used a dual regression analysis to

examine whether regions in the brain altered their correlated activity with these networks following cocaine exposure. We found significant increases in correlated activity between the anterior cingulate cortex and the visual network and between the somatosensory cortex and the sensorimotor network following exposure to cocaine in drug naïve rats. Although trending but not passing FWER-correction at  $p = 0.01$ , we also observed an increase in correlated activity between the anterior cingulate cortex and somatosensory network following cocaine exposure as well as a reduction in correlated activity between the insular cortex and the hippocampal network. No significant differences were observed between these regions and their respective networks in the yoked-saline control animals. Finally, using the seed regions derived from the dual regression analysis, we found that cocaine exposure causes a significant reduction in functional connectivity between the anterior cingulate cortex and the striatum (caudate putamen and NAc). These findings may reflect key neurobiological underpinnings to the maladaptive behaviors observed in cocaine dependence.

## **GENERAL IMPLICATIONS OF FINDINGS**

Considerable evidence suggests that drug addiction may arise in part from dysregulated activity of VTA DA neurons, as well as from more global maladaptation in neurocircuit function (Volkow, Fowler, Wang, & Swanson, 2004). Therefore, the first aim of this dissertation was to understand how activity within genetically distinct circuits contributes to shifts in large-scale brain network activity. Through our use of optogenetic-fMRI and our developed principal component analysis-based approach, we demonstrated that DA-mediated effects were not restricted to well-established DAergic terminal fields such as the striatum, but occur brain-wide. Our data imply that genetically distinct cells, like VTA DAergic neurons, have the ability to modulate global network effects. This is an important finding as direct consequence of DA signaling have classically thought to be largely restricted to brain regions that contain



appreciable presynaptic fibers that release DA. Furthermore, we show that the activity of DA neurons timelocked to a discrete sensory stimulus can dramatically enhance the brain-wide representation of that specific sensory stimulus. These findings first illustrate the utility of optogenetic-fMRI, as the exaggerated response to the forepaw stimulation following its pairing with DA activity was not confined to the somatosensory cortex but was brain-wide. These findings would have likely been lost had we been using another experimental strategy that is focused on recording activity within one specific site.

Our finding that dopaminergic neuron stimulation dramatically enhances brain-wide representation of sensory stimuli has important implications for both adaptive learning and addiction. In addition to dopaminergic signaling during natural reward-seeking behavior (Cohen et al., 2012; Day et al., 2007; Roitman et al., 2004, 2008; Wolfram Schultz, 1998), drugs of abuse also increase extracellular DA in the NAc (Di Chiara & Imperato, 1988; P. E. M. Phillips et al., 2003; Stuber, Roitman, et al., 2005; Stuber, Wightman, et al., 2005). The exaggerated dopaminergic activity that occurs during drug use is thought to underlie why drug-predictive cues become pathologically salient (K. C. Berridge & Robinson, 1998). Indeed, drug-associated cues have also been shown to directly evoke robust DA release in the NAc (P. E. M. Phillips et al., 2003; Stuber, Roitman, et al., 2005). Our findings suggest that DA signaling, timelocked to a sensory stimulus, may modulate cue-evoked behavioral responding, by not only controlling plasticity in direct target regions, but effectively modulating brain-wide network plasticity as well.

We next characterized the effect of high levels of cocaine exposure on the drug naïve brain through resting state functional connectivity fMRI. Interpretation of results from human neuroimaging studies that have investigated functional connectivity alterations in cocaine

dependence can be challenging. For instance, whether the differences reflect inherited genetic vulnerability that precede onset of cocaine use or are a direct reflection of cocaine use is a question that would be difficult to answer. Through our use of an animal model of addiction and a pre-post, treatment-control design, our results provide direct evidence that cocaine exposure causes significant global network remodeling in the drug naïve brain. The increases in correlated activity between the anterior cingulate cortex and the visual and somatosensory network, as well as the local strengthening seen between the somatosensory cortex and the sensorimotor network, following exposure to cocaine may reflect important neuroadaptations underlying salience attribution to sensory stimuli in the environment that become associated with the drug. We also found a significant reduction in functional connectivity between the anterior cingulate cortex and the striatum (ventral portion of the caudate putamen (CPu) and NAc) and hippocampal network and insular cortex following cocaine exposure. Decreased functional connectivity between the prefrontal cortex and striatum following cocaine exposure in drug naïve rats may cause a loss of top-down inhibitory control over striatal activity, which may contribute to the impulsivity and impaired decision-making found in addiction. These findings may reflect critical network-level alterations underlying the maladaptive behavioral outcomes seen in cocaine dependence. Alarming high relapse rates seen in cocaine dependence are a reflection of the powerful grip that these drug-induced neuroadaptations have on the brain, and future studies need to be done to further understand how these modifications shift or evolve after drug discontinuation.

## TECHNICAL CONSIDERATIONS AND LIMITATIONS

### Anesthesia

All of the fMRI scans described here were performed on animals receiving the  $\alpha_2$ -adrenergic receptor agonist, dexmedetomidine and the paralytic agent pancuronium bromide supplemented with 0.5% isoflurane anesthesia to limit motion and stress-related artifacts during scans (Fukuda et al., 2013). Isoflurane anesthesia has been shown to significantly suppress evoked BOLD response during optogenetic fMRI experiments, as well as diminish the correlated fluctuations in BOLD signal observed across the brain during resting state fMRI (Desai et al., 2011; Ferenczi et al., 2016). Since its debut as a viable sedative and anesthetic for longitudinal neuroimaging studies in rodents (Weber, Ramos-Cabrera, Wiedermann, van Camp, & Hoehn, 2006), dexmedetomidine has demonstrated its utility in several functional MRI studies that have used it independently or coupled its use with light isoflurane. For instance, Zhao and colleagues demonstrated robust and reliable forepaw stimulation-evoked BOLD signal as well as synchronized low frequency fluctuations of the BOLD signal during resting state in rats under dexmedetomidine (F. Zhao, Zhao, Zhou, Wu, & Hu, 2008). Further, in the first study to report that rats have a default mode network (DMN) analogous to the DMNs observed in humans and non-human primates, Lu and colleagues combined dexmedetomidine with a low dose of isoflurane (Lu et al., 2012). Taken together, these studies demonstrate that robust BOLD signaling, whether stimulation-evoked or intrinsic, is readily detected in rodents under dexmedetomidine sedation, whether it is administered independently or supplemented with low doses of isoflurane. Nonetheless, as these signals do not fully reflect those that would be observed during the awake state, future studies are needed to replicate our findings in fully conscious animals.

Performing awake fMRI imaging in rodents has its share of technical considerations and challenges as well. As these experiments require restraint and immobilization, as well as exposure to loud noise from the scanner, stress and fear circuitry is likely engaged in these animals during scan acquisition. Indeed, plasma corticosterone levels have been shown to spike on scan day in rodents who had been undergoing acclimation in a mock scanner (Chang et al., 2016). These results suggest that changing environments on scan day, even when effort has been made to make the mock scanner as similar as possible to what the rats will experience on scan day, can induce significant stress-related physiological responses. Thus, proper acclimation procedures, preferably within the same scanner that experiments will be performed, is critical in order to lessen stress-related confounds.

### **Light and Heating Artifacts During Opto-fMRI Experiments**

It has been shown that laser light delivery during opto-fMRI experiments has the potential to cause light and heating artifacts in the naïve brain (Christie et al., 2013; Rungta, Osmanski, Boido, Tanter, & Charpak, 2017). These findings highlight the importance of utilizing an appropriate laser power and stimulation frequency as well as utilizing a proper control group. Intracranial optogenetic stimulation during opto-fMRI experiments has also been shown to evoke visual responses that have the potential to introduce confounds into these datasets (Schmid et al., 2017). We found through our experiments described in Chapter 2 that placing black tape over the eyes of the rats as well as directing a masking light into their faces ablated this response.

### **Imaging Resolution**

The relatively low spatial resolution imposed by fMRI is a limitation of this study that makes it challenging to differentiate between small, neighboring yet discrete structures in the brain. For example, the NAc is divided into two distinct subregions, the core and shell. Previous

studies indicate that the core and shell have distinct molecular profiles (Zahm, 2000) as well as unique afferent and efferent projections (Brog et al., 1993; Salgado & Kaplitt, 2015). Prefrontal innervation patterns indicate that the core primarily receives inputs from the prelimbic cortex and lateral portions of the OFC while the shell is innervated predominantly by the infralimbic cortex and medial lateral OFC (Berendse, Galis-de Graaf, & Groenewegen, 1992). Importantly, DA release dynamics in the NAc have been shown to vary greatly between core and shell and seem to reflect signaling events that underlie the two dominant theories of dopamine function in the brain, with dopaminergic signaling in the shell important for tracking motivationally salient stimuli whereas signaling in the core is more associated with tracking prediction error (Saddoris, Cacciapaglia, Wightman, & Carelli, 2015). The core and shell subregions of the NAc have also been shown to have differential control over cocaine-seeking behavior. Ito and colleagues found that lesioning of the NAc core significantly impaired the acquisition of drug-seeking behavior when it was contingent on a drug-associated conditioned reinforcer, whereas lesions in the shell did not (Ito, Robbins, & Everitt, 2004). Considered in the context of the current work, these findings suggest that being able to differentiate between the core and shell and to explore how their functional connectivity changes with other brain structures following cocaine exposure is important and would further our understanding of their respective roles in the addicted brain. Future experiments using higher resolution imaging will help in doing so.

## **FUTURE DIRECTIONS**

### **To Explore the Permanence of our Findings**

In Chapter 2, we found that pairing a sensory stimulus with activation of VTA DA neurons produces an immediate enhancement of the neuronal representation of that specific stimulus throughout the brain. A future study should explore the duration of this brain-wide sensory enhancement following the presentation of the stimulus that was paired with the VTA

DA neuron activity. Would we still see the same global enhancement following exposure to the paired-stimulus after a day, a week or a month? The exaggerated dopaminergic activity that accompanies drug use is thought to underlie why drug-predictive cues become highly salient. This research may provide important clues as to why relapse rates are so high, and why relapse can occur even after years of abstinence.

Our initial design for the experiments carried out in Chapter 3 included a resting state functional connectivity scan performed after 30d of abstinence. However, due to poor physiology, primarily because of weight gain, data collected from these scans was not analyzed. Data has shown that pathologic forms of neuroplasticity underlie addiction, leading to high relapse susceptibility even following long periods of abstinence. In fact, throughout abstinence drug cravings and the associated neuropathology becomes more pronounced, a process known as incubation (Grimm, Hope, Wise, & Shaham, 2001; Hollander & Carelli, 2005; Pickens et al., 2011; Wolf, 2016). Thus, it would be so interesting to see whether the drug-evoked functional connectivity modifications we saw immediately following discontinuation of the drug continue to evolve long after the onset of drug abstinence. Another future experiment could be to allow these animals to again engage in cocaine self-administration following the abstinence scan to explore whether the degree of impairment between specific regions of the brain is correlated with cocaine intake.

### **To Explore Sex- and Age-Based Brain Functional Connectivity Differences Following Cocaine Exposure**

All rats used in the studies described here were adult males. Several studies have demonstrated that there are distinct sex differences in sensitivity to the addictive properties of cocaine. For instance, a human neuroimaging study revealed that cocaine-dependent females report more robust drug craving towards the presentation of a drug-related cue in comparison to

males (S. J. Robbins, Ehrman, Childress, & O'Brien, 1999). While males do make up a larger percentage of individuals who struggle with cocaine addiction in our society, it has been shown that if both male and female rats are given the opportunity to take cocaine, female rats will acquire cocaine self-administration faster and will self-administer more cocaine once acquisition is established (Lynch & Carroll, 1999). To explore potential causes for these findings, a follow-up study from the same group found that both surgical (i.e. ovariectomized (OVX)) and pharmacological (i.e. the antiestrogen, tamoxifen) blockade of estrogen impeded acquisition of cocaine self-administration when compared to intact females and OVX females that underwent estrogen replacement (Lynch, Roth, Mickelberg, & Carroll, 2001). These findings suggest that estrogen is a key contributor to enhancing the reinforcing effects of cocaine in females. In fact, a recent study found that during estrus, the phase of the menstrual cycle that occurs shortly after estradiol peaks, basal activity of VTA DA neurons is enhanced (Calipari et al., 2017). This increase in VTA DA activity during estrus was shown to elicit downstream posttranslational modifications of the DAT receptor, causing the affinity of cocaine for DAT to be enhanced. These findings offer a putative mechanism as to why females are more susceptible to addiction and struggle more with drug craving and relapse.

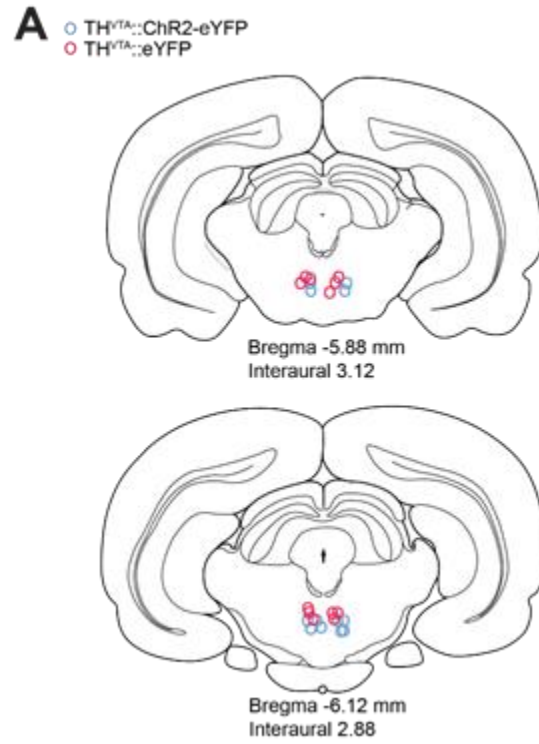
Drug use that starts during adolescence, as opposed to early adulthood, significantly increases the likelihood that an individual will go on to develop a substance use disorder. Thus, another future aim that should be explored is the effect of age of initiation of cocaine use on functional connectivity in adulthood. A recent neuroimaging study found more profound brain structural abnormalities in adult mice when exposure to cocaine occurred during adolescence than during young adulthood (Wheeler et al., 2013). Repeated cocaine exposure during adolescence, and not adulthood has also been shown to cause long term impairment in prefrontal

fast-spiking GABAergic interneuron function (Cass, Thomases, Caballero, & Tseng, 2013). Adolescent rodents have also been shown to exhibit heightened dopaminergic activity in the dorsal striatum in response to cues that predict a reward (Sturman & Moghaddam, 2012). Collectively, this evidence suggests that cocaine exposure on the adolescent brain would most likely cause significant shifts in functional connectivity and it would be interesting to see whether the results we report are enhanced in rats exposed to cocaine at an earlier age. As mentioned in the introduction, the CDC recently reported a dramatic rise in infants being born dependent on drugs (Ko et al., 2016). Thus, another important future aim would be to explore whether functional connectivity is altered in rats that were prenatally exposed to cocaine.

Collectively, our findings provide a direct link between maladaptive changes in dopaminergic activity to remodeling of whole brain activity. We demonstrate that global revision in functional connectivity can occur due to direct changes in the activity of VTA dopaminergic neurons. In a broader context, we hope our findings begin to provide mechanistic insight into the maladaptive network activity that underlies all disorders that have been linked to dysregulated dopaminergic signaling, including schizophrenia and depression. We hope future studies can expand upon our findings to determine whether the changes we found here reflect network-level alterations that underlie the maladaptive behavior seen in these disorders and for future experiments to explore whether network-based interventions, such as deep brain stimulation or repetitive transcranial magnetic stimulation can improve these outcomes.

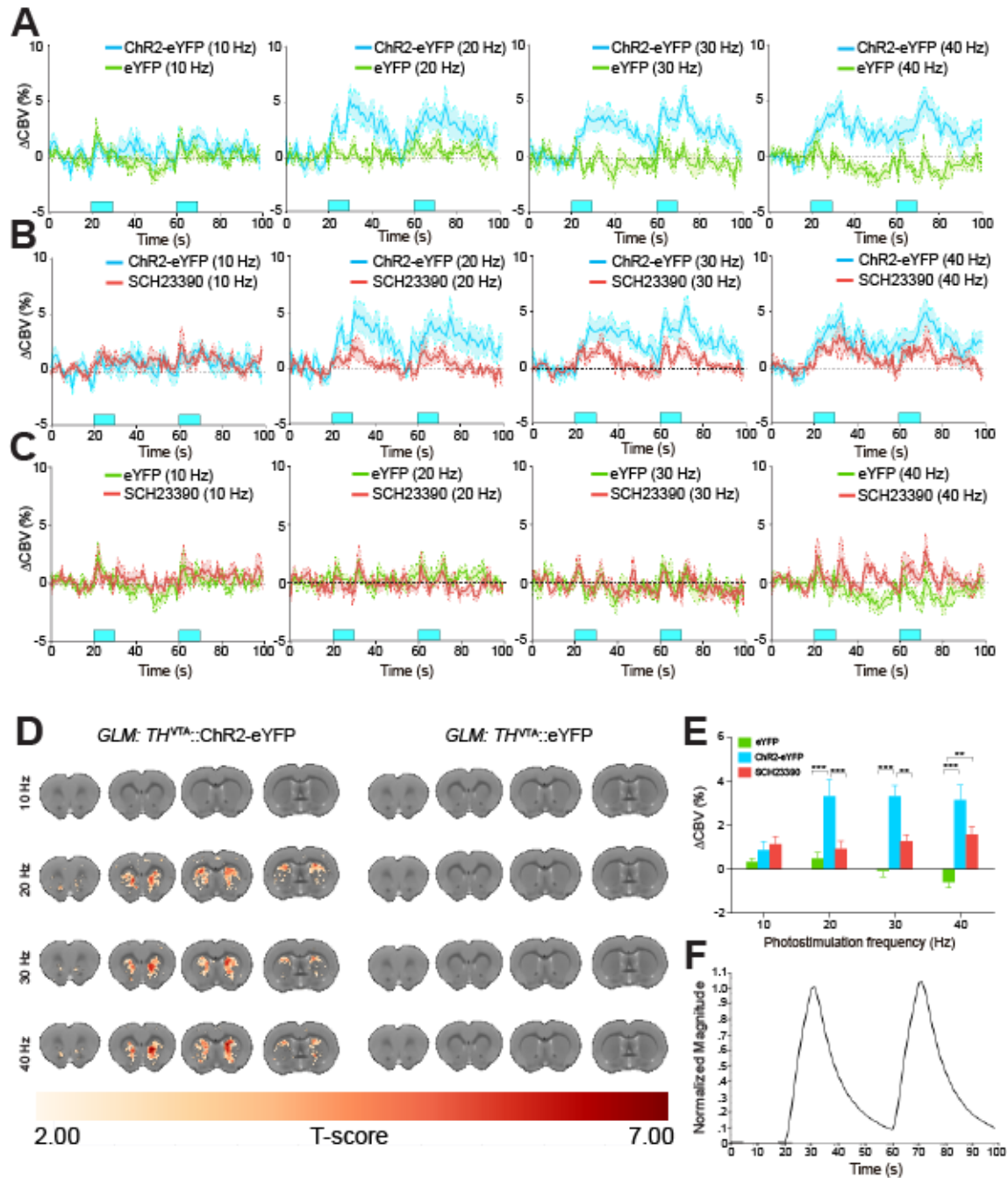


## APPENDIX 1: SUPPLEMENTAL MATERIALS FOR CHAPTER 2



### Figure A.1: Optical fiber placements in the VTA of TH-cre rats.

(A) Location of bilateral optical fibers within the VTA of TH<sup>VTA</sup>::ChR2-eYFP and TH<sup>VTA</sup>::eYFP rats based on T2-weighted image examination and histological verification of 40- $\mu$ m brain slices following experiments.



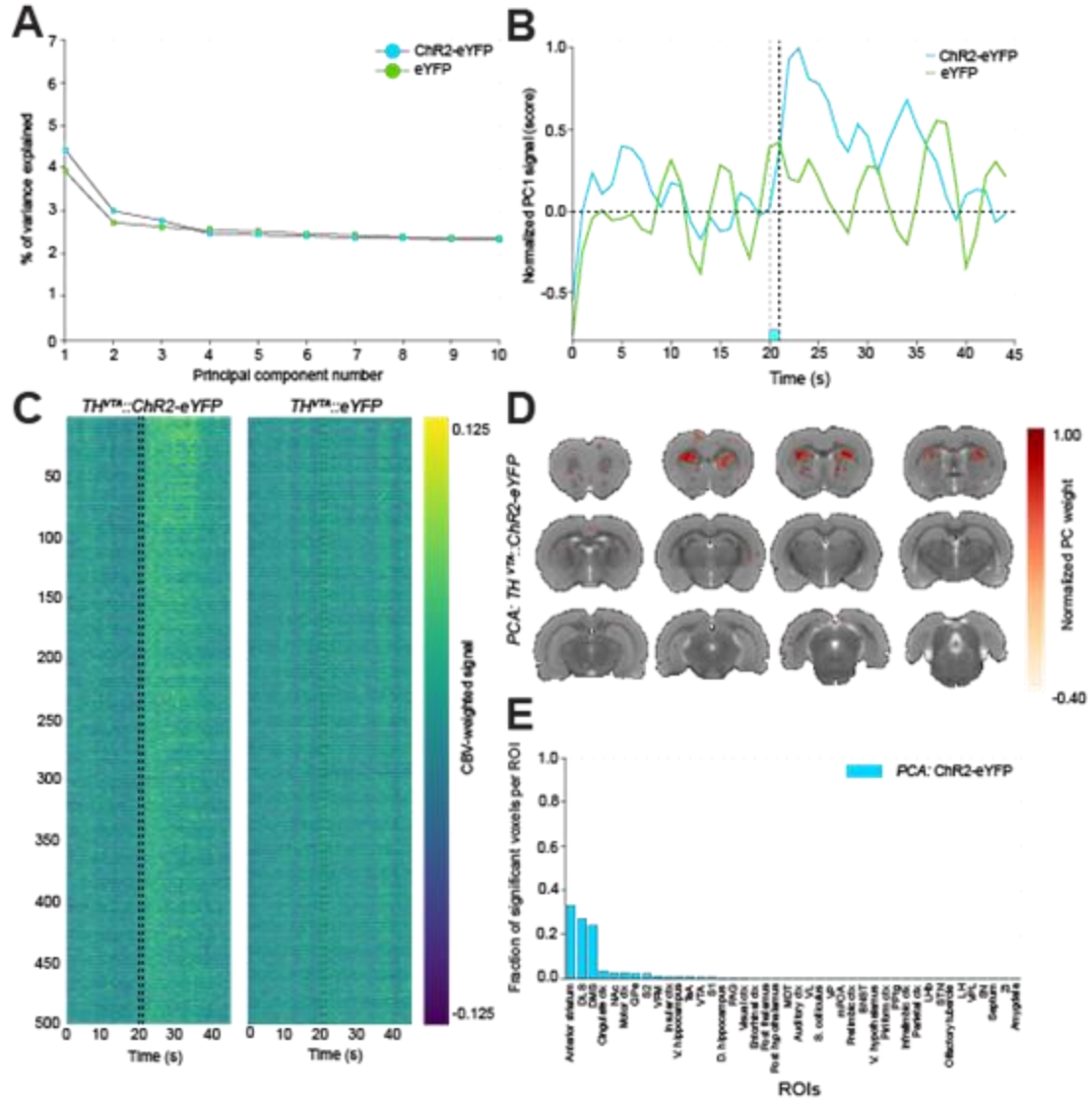
**Figure A.2: Activation of VTA dopaminergic neurons increases CBV signals in striatal target regions.**

(A) Activation of VTA dopaminergic neurons increases striatal CBV signals compared to control rats, 20 Hz (group main effect:  $F_{1,99} = 204.6$ ,  $P < 0.0001$ ,  $n = 6$  rats per group), 30 Hz (group main effect:  $F_{1,99} = 479.0$ ,  $P < 0.0001$ ,  $n = 6$  rats per group) and 40 Hz (group main effect:  $F_{1,99} = 506.4$ ,  $P < 0.0001$ ,  $n = 6$  rats per group). (B) Intravenous administration of SCH23390 significantly attenuates optically-evoked changes in  $\text{TH}^{\text{VTA}}::\text{ChR2-eYFP}$  animal striatal CBV timecourse signals at 20 and 40 Hz, 10 Hz (group main effect:  $F_{1,99} = 1.874$ ,  $P = 0.1714$ ,  $n = 5 - 6$  rats per group), 20 Hz (group main effect:  $F_{1,99} = 191.2$ ,  $P < 0.0001$ ,  $n = 5 - 6$  rats per group), 30 Hz (group main effect:

$F_{1,99} = 226.7$ ,  $P < 0.0001$ ,  $n = 5 - 6$  rats per group), and 40 Hz (group main effect:  $F_{1,99} = 92.76$ ,  $P < 0.0001$ ,  $n = 5 - 6$  rats per group). (C) Intravenous administration of SCH23390 does not significantly affect striatal CBV timecourse signals of control rats, 10 Hz (interaction main effect:  $F_{1,99} = 0.7032$ ,  $P = 0.9862$ ,  $n = 5 - 6$  rats per group), 20 Hz (interaction main effect:  $F_{1,99} = 0.6696$ ,  $P = 0.9937$ ,  $n = 5 - 6$  rats per group), 30 Hz (interaction main effect:  $F_{1,99} = 0.5658$ ,  $P = 0.9998$ ,  $n = 5 - 6$  rats per group), and 40 Hz (interaction main effect:  $F_{1,99} = 1.005$ ,  $P = 0.4708$ ,  $n = 5 - 6$  rats per group). (D) Group-averaged CBV activation maps following optogenetic stimulation of VTA dopaminergic neurons. (E) Activation of VTA dopaminergic neurons increases striatal CBV signals in a frequency dependent fashion compared to SCH23390 and eYFP groups (interaction main effect:  $F_{6,124} = 3.573$ ,  $P = 0.0027$ ,  $n = 5 - 6$  rats per group), double and triple asterisks denote significance ( $p < 0.01$  and  $p < 0.001$ , respectively) by two-way ANOVA followed by Bonferroni post hoc comparisons between each group at each frequency. For all average data figures, mean and SEM are shown. (F) Stimulation template assumed for the GLM analysis (Leite, F.P. et al., 2002).

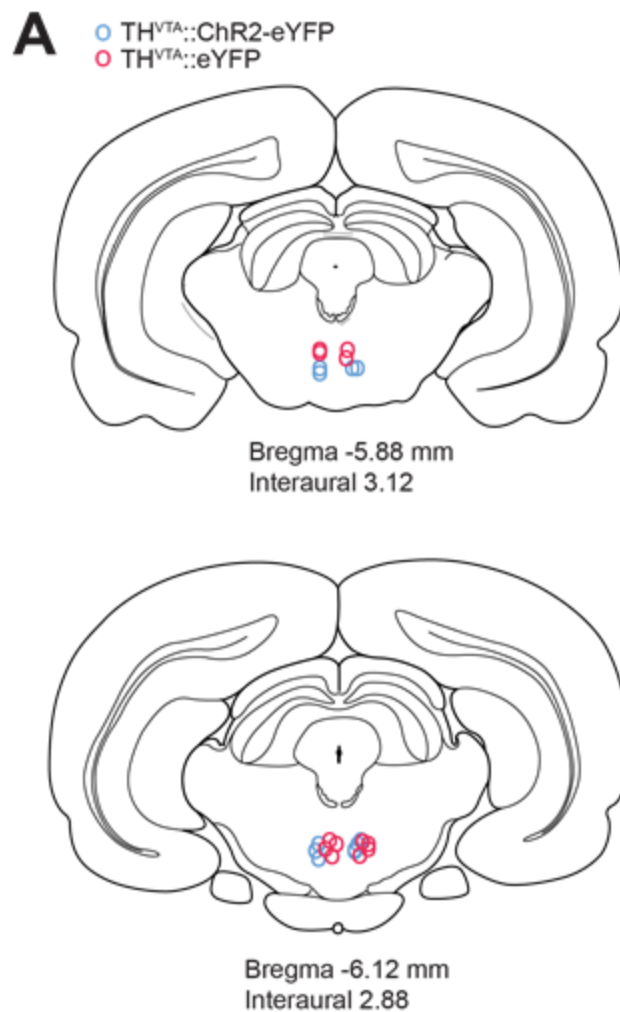


assessed by a GLM of the fMRI response. The GLM coefficients are shown only for significant voxels following Benjamini-Hochberg false discovery rate correction. **(E)** The normalized traces (scores) of the first PC for the TH<sup>VTA</sup>::ChR2-eYFP group before (cyan trace) and after (red trace) intravenous injection of the D1 antagonist, SCH23390. **(F)** Individual ROIs and their fractional contribution to the PC representing the stimulation effect in TH<sup>VTA</sup>::ChR2-eYFP animals before (cyan bars) and after (red bars) intravenous administration of the D1 antagonist.



**Figure A.4: Whole brain analysis of the effect of 1 s  $TH^{VT_A}$  neuron stimulation.**

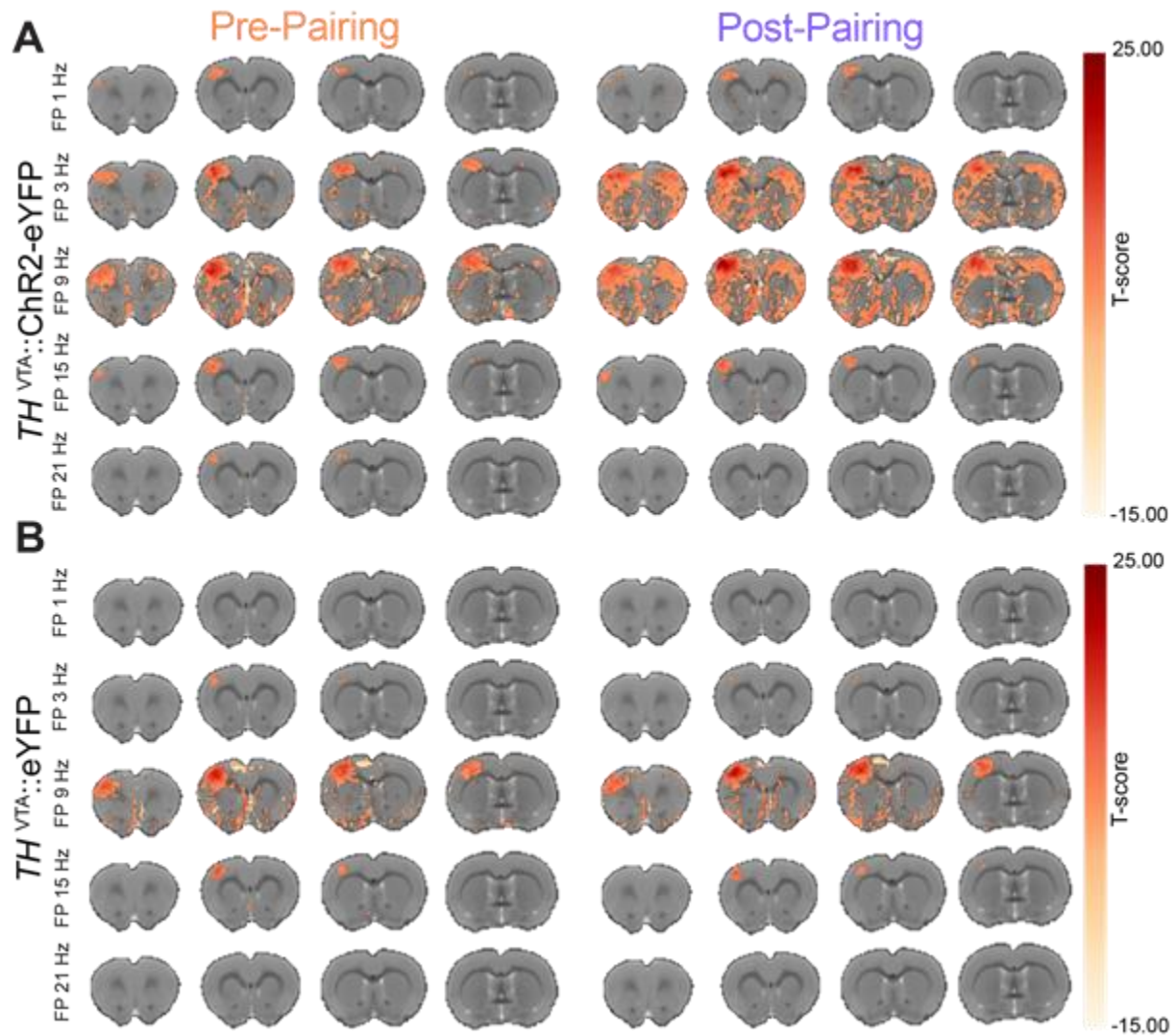
(A) The percentage of variance captured by each principal component (PC) for the top 10 PCs for both groups. (B) The normalized trace (score) of the first PC for both experimental ( $n = 4$ ) and control ( $n = 3$ ) groups. (C) The raw voxel traces for the top 500 voxels contributing to the first PC for both groups. (D) The map showing the significant voxels contributing to the first PC vector for the ChR2-eYFP group, for which a significant post-stimulation response was identified. There was no PC for the control group that represented any significant post-stimulation effect. PC weights were divided by the maximum PC weight for normalization. (E) Individual ROIs and their fractional contribution to the PC representing the stimulation effect.



**Figure A.5: Optical fiber placements in the VTA of TH-cre rats for the pairing experiments.**

(A) Location of bilateral optical fibers within the VTA of TH<sup>VTA::</sup>ChR2-eYFP and TH<sup>VTA::</sup>eYFP rats based on T2-weighted image examination and histological verification of 40- $\mu$ m brain slices following experiments.

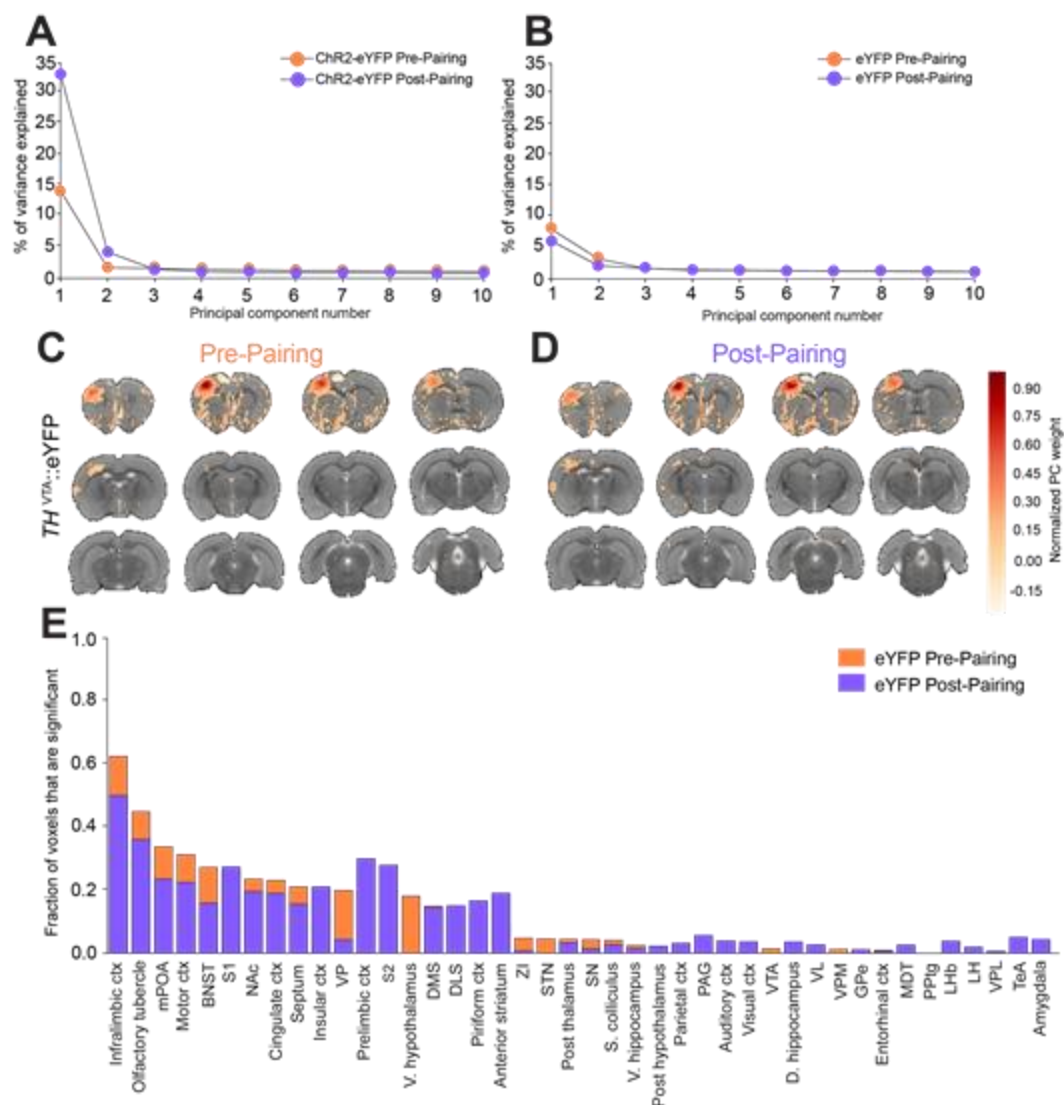




**Figure A.6: Pairing VTA dopamine neuronal activity with somatosensory stimuli enhances the neuronal representation of the sensory stimulus.**

(A,B) Group averaged CBV activation maps in response to forepaw (FP) stimulation before and after pairing 30 Hz optogenetic stimulation of VTA dopaminergic neurons with 9 Hz FP stimulation for  $TH^{VTA::ChR2-eYFP}$  and control rats.





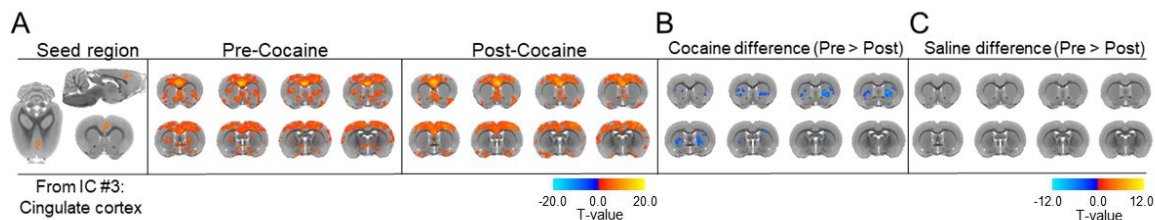
**Figure A.7: Additional results for the forepaw stimulation pre and post pairing with THVTA stimulation.**

(A, B) Percentage variance explained per PC is plotted for the top 10 PCs for both groups pre and post pairing. The first PC represented the stimulation effect in all conditions. (C, D) Significant voxels contributing to the PC vector representing stimulation effect are shown for the eYFP group pre and post pairing with THVTA stimulation. (E) Ranked ROIs based on the fractional contribution of significant voxels to the PC representing stimulation effect for the eYFP group pre and post pairing.

## APPENDIX 2: SUPPLEMENTAL MATERIALS FOR CHAPTER 3

IC#	RSN	Anatomical regions within network	Network connectivity maps
0	N/A	N/A	
1	N/A	N/A	
19	N/A	N/A	
20	N/A	N/A	
21	N/A	N/A	
22	N/A	N/A	
23	N/A	N/A	
25	N/A	N/A	
27	N/A	N/A	
28	N/A	N/A	
29	N/A	N/A	

**Figure A.8:** The independent components derived from the multi-subject ICA analysis that were excluded from further analysis due to noise artifacts.



**Figure A.9: Seed-based whole brain connectivity maps of pre-cocaine and post-cocaine rsfMRI data**

(A) The anterior cingulate cortex seed was derived from the dual regression analysis (From IC #3). (B) Group analysis was performed to compare between group effects and revealed a significant reduction in functional connectivity between the anterior cingulate cortex and the striatum (NAc and ventral portion of CPu) following exposure to cocaine in drug naïve animals (FWER corrected,  $p$ -value = 0.01;  $\Delta Z = 0.135 \pm 0.03$ ). (C) No differences between condition were observed in the control group.

## REFERENCES

- Adamantidis, A. R., Tsai, H.-C., Boutrel, B., Zhang, F., Stuber, G. D., Budygin, E. A., ... de Lecea, L. (2011). Optogenetic interrogation of dopaminergic modulation of the multiple phases of reward-seeking behavior. *The Journal of Neuroscience: The Official Journal of the Society for Neuroscience*, 31(30), 10829–10835. <https://doi.org/10.1523/JNEUROSCI.2246-11.2011>
- Adell, A., & Artigas, F. (2004). The somatodendritic release of dopamine in the ventral tegmental area and its regulation by afferent transmitter systems. *Neuroscience and Biobehavioral Reviews*, 28(4), 415–431. <https://doi.org/10.1016/j.neubiorev.2004.05.001>
- Afonso-Oramas, D., Cruz-Muros, I., Alvarez de la Rosa, D., Abreu, P., Giráldez, T., Castro-Hernández, J., ... González-Hernández, T. (2009). Dopamine transporter glycosylation correlates with the vulnerability of midbrain dopaminergic cells in Parkinson's disease. *Neurobiology of Disease*, 36(3), 494–508. <https://doi.org/10.1016/j.nbd.2009.09.002>
- Aggleton, J. P., Wright, N. F., Rosene, D. L., & Saunders, R. C. (2015). Complementary Patterns of Direct Amygdala and Hippocampal Projections to the Macaque Prefrontal Cortex. *Cerebral Cortex (New York, N.Y.: 1991)*, 25(11), 4351–4373. <https://doi.org/10.1093/cercor/bhv019>
- Amaro, E., & Barker, G. J. (2006). Study design in fMRI: basic principles. *Brain and Cognition*, 60(3), 220–232. <https://doi.org/10.1016/j.bandc.2005.11.009>
- Anand, B. K., & Brobeck, J. R. (1951a). Hypothalamic control of food intake in rats and cats. *The Yale Journal of Biology and Medicine*, 24(2), 123–140.
- Anand, B. K., & Brobeck, J. R. (1951b). Localization of a “feeding center” in the hypothalamus of the rat. *Proceedings of the Society for Experimental Biology and Medicine. Society for Experimental Biology and Medicine (New York, N.Y.)*, 77(2), 323–324.
- Andersen, A. H., Gash, D. M., & Avison, M. J. (1999). Principal component analysis of the dynamic response measured by fMRI: a generalized linear systems framework. *Magnetic Resonance Imaging*, 17(6), 795–815.
- Anstrom, K. K., & Woodward, D. J. (2005). Restraint increases dopaminergic burst firing in awake rats. *Neuropsychopharmacology: Official Publication of the American College of Neuropsychopharmacology*, 30(10), 1832–1840. <https://doi.org/10.1038/sj.npp.1300730>
- Apicella, P., Ljungberg, T., Scarnati, E., & Schultz, W. (1991). Responses to reward in monkey dorsal and ventral striatum. *Experimental Brain Research*, 85(3), 491–500.
- Aragona, B. J., Cleaveland, N. A., Stuber, G. D., Day, J. J., Carelli, R. M., & Wightman, R. M. (2008). Preferential enhancement of dopamine transmission within the nucleus accumbens shell by cocaine is attributable to a direct increase in phasic dopamine release events. *The Journal of*

*Neuroscience: The Official Journal of the Society for Neuroscience*, 28(35), 8821–8831.  
<https://doi.org/10.1523/JNEUROSCI.2225-08.2008>

Aravanis, A. M., Wang, L.-P., Zhang, F., Meltzer, L. A., Mogri, M. Z., Schneider, M. B., & Deisseroth, K. (2007). An optical neural interface: in vivo control of rodent motor cortex with integrated fiberoptic and optogenetic technology. *Journal of Neural Engineering*, 4(3), S143–156. <https://doi.org/10.1088/1741-2560/4/3/S02>

Arenkiel, B. R., Peca, J., Davison, I. G., Feliciano, C., Deisseroth, K., Augustine, G. J., ... Feng, G. (2007). In vivo light-induced activation of neural circuitry in transgenic mice expressing channelrhodopsin-2. *Neuron*, 54(2), 205–218. <https://doi.org/10.1016/j.neuron.2007.03.005>

Bao, S., Chan, V. T., & Merzenich, M. M. (2001). Cortical remodelling induced by activity of ventral tegmental dopamine neurons. *Nature*, 412(6842), 79–83.  
<https://doi.org/10.1038/35083586>

Barbas, H., & Blatt, G. J. (1995). Topographically specific hippocampal projections target functionally distinct prefrontal areas in the rhesus monkey. *Hippocampus*, 5(6), 511–533.  
<https://doi.org/10.1002/hipo.450050604>

Beart, P. M., & McDonald, D. (1982). 5-Hydroxytryptamine and 5-hydroxytryptaminergic-dopaminergic interactions in the ventral tegmental area of rat brain. *The Journal of Pharmacy and Pharmacology*, 34(9), 591–593.

Becerra, L., Pendse, G., Chang, P.-C., Bishop, J., & Borsook, D. (2011). Robust reproducible resting state networks in the awake rodent brain. *PloS One*, 6(10), e25701.  
<https://doi.org/10.1371/journal.pone.0025701>

Beckmann, C. F., DeLuca, M., Devlin, J. T., & Smith, S. M. (2005). Investigations into resting-state connectivity using independent component analysis. *Philosophical Transactions of the Royal Society of London. Series B, Biological Sciences*, 360(1457), 1001–1013.  
<https://doi.org/10.1098/rstb.2005.1634>

Beier, K. T., Steinberg, E. E., DeLoach, K. E., Xie, S., Miyamichi, K., Schwarz, L., ... Luo, L. (2015). Circuit Architecture of VTA Dopamine Neurons Revealed by Systematic Input–Output Mapping. *Cell*, 162(3), 622–634. <https://doi.org/10.1016/j.cell.2015.07.015>

Berendse, H. W., Galis-de Graaf, Y., & Groenewegen, H. J. (1992). Topographical organization and relationship with ventral striatal compartments of prefrontal corticostriatal projections in the rat. *The Journal of Comparative Neurology*, 316(3), 314–347.  
<https://doi.org/10.1002/cne.903160305>

Bernardini, G. L., Gu, X., Viscardi, E., & German, D. C. (1991). Amphetamine-induced and spontaneous release of dopamine from A9 and A10 cell dendrites: an in vitro

electrophysiological study in the mouse. *Journal of Neural Transmission. General Section*, 84(3), 183–193.

Berridge, K. C., & Robinson, T. E. (1998). What is the role of dopamine in reward: hedonic impact, reward learning, or incentive salience? *Brain Research. Brain Research Reviews*, 28(3), 309–369.

Berridge, K. C., & Robinson, T. E. (1998). What is the role of dopamine in reward: hedonic impact, reward learning, or incentive salience? *Brain Research Reviews*, 28(3), 309–369. [https://doi.org/10.1016/S0165-0173\(98\)00019-8](https://doi.org/10.1016/S0165-0173(98)00019-8)

Berridge, K. C., Venier, I. L., & Robinson, T. E. (1989). Taste reactivity analysis of 6-hydroxydopamine-induced aphagia: implications for arousal and anhedonia hypotheses of dopamine function. *Behavioral Neuroscience*, 103(1), 36–45.

Bertler, A., & Rosengren, E. (1959). Occurrence and distribution of dopamine in brain and other tissues. *Experientia*, 15(1), 10–11.

Birkmayer, W., & Hornykiewicz, O. (1961). [The L-3,4-dioxyphenylalanine (DOPA)-effect in Parkinson-akinesia]. *Wiener Klinische Wochenschrift*, 73, 787–788.

Biswal, B., Yetkin, F. Z., Haughton, V. M., & Hyde, J. S. (1995). Functional connectivity in the motor cortex of resting human brain using echo-planar MRI. *Magnetic Resonance in Medicine*, 34(4), 537–541.

Björklund, A., & Dunnett, S. B. (2007). Dopamine neuron systems in the brain: an update. *Trends in Neurosciences*, 30(5), 194–202. <https://doi.org/10.1016/j.tins.2007.03.006>

Bock, R., Shin, J. H., Kaplan, A. R., Dobi, A., Markey, E., Kramer, P. F., ... Alvarez, V. A. (2013). Strengthening the accumbal indirect pathway promotes resilience to compulsive cocaine use. *Nature Neuroscience*, 16(5), 632–638. <https://doi.org/10.1038/nn.3369>

Bocklisch, C., Pascoli, V., Wong, J. C. Y., House, D. R. C., Yvon, C., de Roo, M., ... Lüscher, C. (2013). Cocaine disinhibits dopamine neurons by potentiation of GABA transmission in the ventral tegmental area. *Science (New York, N.Y.)*, 341(6153), 1521–1525. <https://doi.org/10.1126/science.1237059>

Borgland, S. L., Malenka, R. C., & Bonci, A. (2004). Acute and chronic cocaine-induced potentiation of synaptic strength in the ventral tegmental area: electrophysiological and behavioral correlates in individual rats. *The Journal of Neuroscience: The Official Journal of the Society for Neuroscience*, 24(34), 7482–7490. <https://doi.org/10.1523/JNEUROSCI.1312-04.2004>

- Boyden, E. S., Zhang, F., Bamberg, E., Nagel, G., & Deisseroth, K. (2005). Millisecond-timescale, genetically targeted optical control of neural activity. *Nature Neuroscience*, 8(9), 1263–1268. <https://doi.org/10.1038/nn1525>
- Brinschwitz, K., Dittgen, A., Madai, V. I., Lommel, R., Geisler, S., & Veh, R. W. (2010). Glutamatergic axons from the lateral habenula mainly terminate on GABAergic neurons of the ventral midbrain. *Neuroscience*, 168(2), 463–476. <https://doi.org/10.1016/j.neuroscience.2010.03.050>
- Brischoux, F., Chakraborty, S., Brierley, D. I., & Ungless, M. A. (2009). Phasic excitation of dopamine neurons in ventral VTA by noxious stimuli. *Proceedings of the National Academy of Sciences of the United States of America*, 106(12), 4894–4899. <https://doi.org/10.1073/pnas.0811507106>
- Britt, J. P., Benaliouad, F., McDevitt, R. A., Stuber, G. D., Wise, R. A., & Bonci, A. (2012). Synaptic and behavioral profile of multiple glutamatergic inputs to the nucleus accumbens. *Neuron*, 76(4), 790–803. <https://doi.org/10.1016/j.neuron.2012.09.040>
- Brog, J. S., Salyapongse, A., Deutch, A. Y., & Zahm, D. S. (1993). The patterns of afferent innervation of the core and shell in the “accumbens” part of the rat ventral striatum: immunohistochemical detection of retrogradely transported fluoro-gold. *The Journal of Comparative Neurology*, 338(2), 255–278. <https://doi.org/10.1002/cne.903380209>
- Brown, M. T. C., Tan, K. R., O’Connor, E. C., Nikonenko, I., Muller, D., & Lüscher, C. (2012). Ventral tegmental area GABA projections pause accumbal cholinergic interneurons to enhance associative learning. *Nature*, 492(7429), 452–456. <https://doi.org/10.1038/nature11657>
- Buckner, R. L., Andrews-Hanna, J. R., & Schacter, D. L. (2008). The brain’s default network: anatomy, function, and relevance to disease. *Annals of the New York Academy of Sciences*, 1124, 1–38. <https://doi.org/10.1196/annals.1440.011>
- Burgess, N., Maguire, E. A., & O’Keefe, J. (2002). The human hippocampus and spatial and episodic memory. *Neuron*, 35(4), 625–641.
- Buxton, R. B., & Frank, L. R. (1997). A model for the coupling between cerebral blood flow and oxygen metabolism during neural stimulation. *Journal of Cerebral Blood Flow and Metabolism: Official Journal of the International Society of Cerebral Blood Flow and Metabolism*, 17(1), 64–72. <https://doi.org/10.1097/00004647-199701000-00009>
- Buxton, R. B., Wong, E. C., & Frank, L. R. (1998). Dynamics of blood flow and oxygenation changes during brain activation: the balloon model. *Magnetic Resonance in Medicine*, 39(6), 855–864.

- Calipari, E. S., Juarez, B., Morel, C., Walker, D. M., Cahill, M. E., Ribeiro, E., ... Nestler, E. J. (2017). Dopaminergic dynamics underlying sex-specific cocaine reward. *Nature Communications*, 8, 13877. <https://doi.org/10.1038/ncomms13877>
- Carelli, R. M., & Deadwyler, S. A. (1994). A comparison of nucleus accumbens neuronal firing patterns during cocaine self-administration and water reinforcement in rats. *The Journal of Neuroscience: The Official Journal of the Society for Neuroscience*, 14(12), 7735–7746.
- Carlsson, A. (1959). The occurrence, distribution and physiological role of catecholamines in the nervous system. *Pharmacological Reviews*, 11(2, Part 2), 490–493.
- Carlsson, A., Lindqvist, M., & Magnusson, T. (1957). 3,4-Dihydroxyphenylalanine and 5-hydroxytryptophan as reserpine antagonists. *Nature*, 180(4596), 1200.
- Carlsson, A., Lindqvist, M., Magnusson, T., & Waldeck, B. (1958). On the presence of 3-hydroxytyramine in brain. *Science (New York, N.Y.)*, 127(3296), 471.
- Carmichael, S. T., & Price, J. L. (1995). Limbic connections of the orbital and medial prefrontal cortex in macaque monkeys. *The Journal of Comparative Neurology*, 363(4), 615–641. <https://doi.org/10.1002/cne.903630408>
- Carr, D. B., & Sesack, S. R. (2000a). GABA-containing neurons in the rat ventral tegmental area project to the prefrontal cortex. *Synapse (New York, N.Y.)*, 38(2), 114–123. [https://doi.org/10.1002/1098-2396\(200011\)38:2<114::AID-SYN2>3.0.CO;2-R](https://doi.org/10.1002/1098-2396(200011)38:2<114::AID-SYN2>3.0.CO;2-R)
- Carr, D. B., & Sesack, S. R. (2000b). Projections from the rat prefrontal cortex to the ventral tegmental area: target specificity in the synaptic associations with mesoaccumbens and mesocortical neurons. *The Journal of Neuroscience: The Official Journal of the Society for Neuroscience*, 20(10), 3864–3873.
- Cass, D. K., Thomases, D. R., Caballero, A., & Tseng, K. Y. (2013). Developmental disruption of gamma-aminobutyric acid function in the medial prefrontal cortex by noncontingent cocaine exposure during early adolescence. *Biological Psychiatry*, 74(7), 490–501. <https://doi.org/10.1016/j.biopsych.2013.02.021>
- Chang, P.-C., Procissi, D., Bao, Q., Centeno, M. V., Baria, A., & Apkarian, A. V. (2016). Novel method for functional brain imaging in awake minimally restrained rats. *Journal of Neurophysiology*, 116(1), 61–80. <https://doi.org/10.1152/jn.01078.2015>
- Chaudhury, D., Walsh, J. J., Friedman, A. K., Juarez, B., Ku, S. M., Koo, J. W., ... Han, M.-H. (2013). Rapid regulation of depression-related behaviours by control of midbrain dopamine neurons. *Nature*, 493(7433), 532–536. <https://doi.org/10.1038/nature11713>
- Chen, B. T., Bowers, M. S., Martin, M., Hopf, F. W., Guillory, A. M., Carelli, R. M., ... Bonci, A. (2008). Cocaine but not natural reward self-administration nor passive cocaine infusion



produces persistent LTP in the VTA. *Neuron*, 59(2), 288–297.  
<https://doi.org/10.1016/j.neuron.2008.05.024>

Chen, B. T., Yau, H.-J., Hatch, C., Kusumoto-Yoshida, I., Cho, S. L., Hopf, F. W., & Bonci, A. (2013). Rescuing cocaine-induced prefrontal cortex hypoactivity prevents compulsive cocaine seeking. *Nature*, 496(7445), 359–362. <https://doi.org/10.1038/nature12024>

Chen, G., Adleman, N. E., Saad, Z. S., Leibenluft, E., & Cox, R. W. (2014). Applications of multivariate modeling to neuroimaging group analysis: a comprehensive alternative to univariate general linear model. *NeuroImage*, 99, 571–588.  
<https://doi.org/10.1016/j.neuroimage.2014.06.027>

Childress, A. R., Mozley, P. D., McElgin, W., Fitzgerald, J., Reivich, M., & O'Brien, C. P. (1999). Limbic activation during cue-induced cocaine craving. *The American Journal of Psychiatry*, 156(1), 11–18. <https://doi.org/10.1176/ajp.156.1.11>

Christie, I. N., Wells, J. A., Southern, P., Marina, N., Kasparov, S., Gourine, A. V., & Lythgoe, M. F. (2013). fMRI response to blue light delivery in the naïve brain: implications for combined optogenetic fMRI studies. *NeuroImage*, 66, 634–641.  
<https://doi.org/10.1016/j.neuroimage.2012.10.074>

Christoph, G. R., Leonzio, R. J., & Wilcox, K. S. (1986). Stimulation of the lateral habenula inhibits dopamine-containing neurons in the substantia nigra and ventral tegmental area of the rat. *Journal of Neuroscience*, 6(3), 613–619.

Chuhma, N., Zhang, H., Masson, J., Zhuang, X., Sulzer, D., Hen, R., & Rayport, S. (2004). Dopamine neurons mediate a fast excitatory signal via their glutamatergic synapses. *The Journal of Neuroscience: The Official Journal of the Society for Neuroscience*, 24(4), 972–981.  
<https://doi.org/10.1523/JNEUROSCI.4317-03.2004>

Cohen, J. Y., Haesler, S., Vong, L., Lowell, B. B., & Uchida, N. (2012). Neuron-type-specific signals for reward and punishment in the ventral tegmental area. *Nature*, 482(7383), 85–88.  
<https://doi.org/10.1038/nature10754>

Compton, W. M., Thomas, Y. F., Stinson, F. S., & Grant, B. F. (2007). Prevalence, correlates, disability, and comorbidity of DSM-IV drug abuse and dependence in the United States: results from the national epidemiologic survey on alcohol and related conditions. *Archives of General Psychiatry*, 64(5), 566–576. <https://doi.org/10.1001/archpsyc.64.5.566>

Conrad, K. L., Tseng, K. Y., Uejima, J. L., Reimers, J. M., Heng, L.-J., Shaham, Y., ... Wolf, M. E. (2008). Formation of accumbens GluR2-lacking AMPA receptors mediates incubation of cocaine craving. *Nature*, 454(7200), 118–121. <https://doi.org/10.1038/nature06995>

- Cox, R. W. (1996). AFNI: software for analysis and visualization of functional magnetic resonance neuroimages. *Computers and Biomedical Research, an International Journal*, 29(3), 162–173.
- Cox, R. W., Chen, G., Glen, D. R., Reynolds, R. C., & Taylor, P. A. (2017). FMRI Clustering in AFNI: False-Positive Rates Redux. *Brain Connectivity*, 7(3), 152–171. <https://doi.org/10.1089/brain.2016.0475>
- Cuénod, M., Casey, K. L., & MacLean, P. D. (1965). Unit analysis of visual input to posterior limbic cortex. I. Photic stimulation. *Journal of Neurophysiology*, 28(6), 1101–1107.
- Damoiseaux, J. S., Rombouts, S. a. R. B., Barkhof, F., Scheltens, P., Stam, C. J., Smith, S. M., & Beckmann, C. F. (2006). Consistent resting-state networks across healthy subjects. *Proceedings of the National Academy of Sciences of the United States of America*, 103(37), 13848–13853. <https://doi.org/10.1073/pnas.0601417103>
- Davey, C. G., Yücel, M., & Allen, N. B. (2008). The emergence of depression in adolescence: development of the prefrontal cortex and the representation of reward. *Neuroscience and Biobehavioral Reviews*, 32(1), 1–19. <https://doi.org/10.1016/j.neubiorev.2007.04.016>
- Davis, M. (1992). The role of the amygdala in fear and anxiety. *Annual Review of Neuroscience*, 15, 353–375. <https://doi.org/10.1146/annurev.ne.15.030192.002033>
- Davis, M., Walker, D. L., Miles, L., & Grillon, C. (2010). Phasic vs sustained fear in rats and humans: role of the extended amygdala in fear vs anxiety. *Neuropsychopharmacology: Official Publication of the American College of Neuropsychopharmacology*, 35(1), 105–135. <https://doi.org/10.1038/npp.2009.109>
- Day, J. J., & Carelli, R. M. (2007). The nucleus accumbens and Pavlovian reward learning. *The Neuroscientist: A Review Journal Bringing Neurobiology, Neurology and Psychiatry*, 13(2), 148–159. <https://doi.org/10.1177/1073858406295854>
- Day, J. J., Roitman, M. F., Wightman, R. M., & Carelli, R. M. (2007). Associative learning mediates dynamic shifts in dopamine signaling in the nucleus accumbens. *Nature Neuroscience*, 10(8), 1020–1028. <https://doi.org/10.1038/nn1923>
- De Luca, M., Beckmann, C. F., De Stefano, N., Matthews, P. M., & Smith, S. M. (2006). fMRI resting state networks define distinct modes of long-distance interactions in the human brain. *NeuroImage*, 29(4), 1359–1367. <https://doi.org/10.1016/j.neuroimage.2005.08.035>
- Decot, H. K., Namboodiri, V. M. K., Gao, W., McHenry, J. A., Jennings, J. H., Lee, S.-H., ... Stuber, G. D. (2017). Coordination of Brain-Wide Activity Dynamics by Dopaminergic Neurons. *Neuropsychopharmacology: Official Publication of the American College of Neuropsychopharmacology*, 42(3), 615–627. <https://doi.org/10.1038/npp.2016.151>

- Delgado, J. M. R., & Anand, B. K. (1953). Increase of food intake induced by electrical stimulation of the lateral hypothalamus. *The American Journal of Physiology*, 172(1), 162–168.
- Desai, M., Kahn, I., Knoblich, U., Bernstein, J., Atallah, H., Yang, A., ... Boyden, E. S. (2011). Mapping brain networks in awake mice using combined optical neural control and fMRI. *Journal of Neurophysiology*, 105(3), 1393–1405. <https://doi.org/10.1152/jn.00828.2010>
- Di Chiara, G., & Imperato, A. (1988). Drugs abused by humans preferentially increase synaptic dopamine concentrations in the mesolimbic system of freely moving rats. *Proceedings of the National Academy of Sciences of the United States of America*, 85(14), 5274–5278.
- Di Ciano, P., & Everitt, B. J. (2001). Dissociable effects of antagonism of NMDA and AMPA/KA receptors in the nucleus accumbens core and shell on cocaine-seeking behavior. *Neuropsychopharmacology: Official Publication of the American College of Neuropsychopharmacology*, 25(3), 341–360. [https://doi.org/10.1016/S0893-133X\(01\)00235-4](https://doi.org/10.1016/S0893-133X(01)00235-4)
- Dobi, A., Margolis, E. B., Wang, H.-L., Harvey, B. K., & Morales, M. (2010). Glutamatergic and nonglutamatergic neurons of the ventral tegmental area establish local synaptic contacts with dopaminergic and nondopaminergic neurons. *The Journal of Neuroscience: The Official Journal of the Society for Neuroscience*, 30(1), 218–229. <https://doi.org/10.1523/JNEUROSCI.3884-09.2010>
- Domingos, A. I., Vaynshteyn, J., Voss, H. U., Ren, X., Gradinaru, V., Zang, F., ... Friedman, J. (2011). Leptin regulates the reward value of nutrient. *Nature Neuroscience*, 14(12), 1562–1568. <https://doi.org/10.1038/nn.2977>
- Ehringer, H., & Hornykiewicz, O. (1960). [Distribution of noradrenaline and dopamine (3-hydroxytyramine) in the human brain and their behavior in diseases of the extrapyramidal system]. *Klinische Wochenschrift*, 38, 1236–1239.
- Eklund, A., Nichols, T. E., & Knutsson, H. (2016). Cluster failure: Why fMRI inferences for spatial extent have inflated false-positive rates. *Proceedings of the National Academy of Sciences of the United States of America*, 113(28), 7900–7905. <https://doi.org/10.1073/pnas.1602413113>
- Ellwood, I. T., Patel, T., Wadia, V., Lee, A. T., Liptak, A. T., Bender, K. J., & Sohal, V. S. (2017). Tonic or Phasic Stimulation of Dopaminergic Projections to Prefrontal Cortex Causes Mice to Maintain or Deviate from Previously Learned Behavioral Strategies. *The Journal of Neuroscience: The Official Journal of the Society for Neuroscience*, 37(35), 8315–8329. <https://doi.org/10.1523/JNEUROSCI.1221-17.2017>
- Everitt, B. J., Cador, M., & Robbins, T. W. (1989). Interactions between the amygdala and ventral striatum in stimulus-reward associations: studies using a second-order schedule of sexual reinforcement. *Neuroscience*, 30(1), 63–75.

- Faget, L., Osakada, F., Duan, J., Ressler, R., Johnson, A. B., Proudfoot, J. A., ... Hnasko, T. S. (2016). Afferent Inputs to Neurotransmitter-Defined Cell Types in the Ventral Tegmental Area. *Cell Reports*, 15(12), 2796–2808. <https://doi.org/10.1016/j.celrep.2016.05.057>
- Felix-Ortiz, A. C., Beyeler, A., Seo, C., Leppla, C. A., Wildes, C. P., & Tye, K. M. (2013). BLA to vHPC inputs modulate anxiety-related behaviors. *Neuron*, 79(4), 658–664. <https://doi.org/10.1016/j.neuron.2013.06.016>
- Felix-Ortiz, A. C., & Tye, K. M. (2014). Amygdala inputs to the ventral hippocampus bidirectionally modulate social behavior. *The Journal of Neuroscience: The Official Journal of the Society for Neuroscience*, 34(2), 586–595. <https://doi.org/10.1523/JNEUROSCI.4257-13.2014>
- Ferenczi, E. A., Zalocusky, K. A., Liston, C., Grosenick, L., Warden, M. R., Amatya, D., ... Deisseroth, K. (2016). Prefrontal cortical regulation of brainwide circuit dynamics and reward-related behavior. *Science (New York, N.Y.)*, 351(6268), aac9698. <https://doi.org/10.1126/science.aac9698>
- Filippini, N., MacIntosh, B. J., Hough, M. G., Goodwin, G. M., Frisoni, G. B., Smith, S. M., ... Mackay, C. E. (2009). Distinct patterns of brain activity in young carriers of the APOE-epsilon4 allele. *Proceedings of the National Academy of Sciences of the United States of America*, 106(17), 7209–7214. <https://doi.org/10.1073/pnas.0811879106>
- Ford, C. P., Mark, G. P., & Williams, J. T. (2006). Properties and opioid inhibition of mesolimbic dopamine neurons vary according to target location. *The Journal of Neuroscience: The Official Journal of the Society for Neuroscience*, 26(10), 2788–2797. <https://doi.org/10.1523/JNEUROSCI.4331-05.2006>
- Fouriez, G., Hansson, P., & Wise, R. A. (1978). Neuroleptic-induced attenuation of brain stimulation reward in rats. *Journal of Comparative and Physiological Psychology*, 92(4), 661–671.
- Fouriez, G., & Wise, R. A. (1976). Pimozide-induced extinction of intracranial self-stimulation: response patterns rule out motor or performance deficits. *Brain Research*, 103(2), 377–380.
- Freeman, J., Vladimirov, N., Kawashima, T., Mu, Y., Sofroniew, N. J., Bennett, D. V., ... Ahrens, M. B. (2014). Mapping brain activity at scale with cluster computing. *Nature Methods*, 11(9), 941–950. <https://doi.org/10.1038/nmeth.3041>
- Friedman, A. K., Walsh, J. J., Juarez, B., Ku, S. M., Chaudhury, D., Wang, J., ... Han, M.-H. (2014). Enhancing depression mechanisms in midbrain dopamine neurons achieves homeostatic resilience. *Science (New York, N.Y.)*, 344(6181), 313–319. <https://doi.org/10.1126/science.1249240>

- Fuchs, R. A., Weber, S. M., Rice, H. J., & Neisewander, J. L. (2002). Effects of excitotoxic lesions of the basolateral amygdala on cocaine-seeking behavior and cocaine conditioned place preference in rats. *Brain Research*, 929(1), 15–25.
- Fukuda, M., Vazquez, A. L., Zong, X., & Kim, S.-G. (2013). Effects of the  $\alpha_2$ -adrenergic receptor agonist dexmedetomidine on neural, vascular and BOLD fMRI responses in the somatosensory cortex. *The European Journal of Neuroscience*, 37(1), 80–95.  
<https://doi.org/10.1111/ejn.12024>
- Gabbott, P. L. A., Warner, T. A., Jays, P. R. L., Salway, P., & Busby, S. J. (2005). Prefrontal cortex in the rat: projections to subcortical autonomic, motor, and limbic centers. *The Journal of Comparative Neurology*, 492(2), 145–177. <https://doi.org/10.1002/cne.20738>
- Gallagher, M., & Chiba, A. A. (1996). The amygdala and emotion. *Current Opinion in Neurobiology*, 6(2), 221–227.
- Gasbarri, A., Sulli, A., & Packard, M. G. (1997). The dopaminergic mesencephalic projections to the hippocampal formation in the rat. *Progress in Neuro-Psychopharmacology & Biological Psychiatry*, 21(1), 1–22.
- Gasbarri, A., Verney, C., Innocenzi, R., Campana, E., & Pacitti, C. (1994). Mesolimbic dopaminergic neurons innervating the hippocampal formation in the rat: a combined retrograde tracing and immunohistochemical study. *Brain Research*, 668(1–2), 71–79.
- Gee, S., Ellwood, I., Patel, T., Luongo, F., Deisseroth, K., & Sohal, V. S. (2012). Synaptic Activity Unmasks Dopamine D2 Receptor Modulation of a Specific Class of Layer V Pyramidal Neurons in Prefrontal Cortex. *The Journal of Neuroscience*, 32(14), 4959–4971.  
<https://doi.org/10.1523/JNEUROSCI.5835-11.2012>
- Geisler, S., Derst, C., Veh, R. W., & Zahm, D. S. (2007). Glutamatergic afferents of the ventral tegmental area in the rat. *The Journal of Neuroscience: The Official Journal of the Society for Neuroscience*, 27(21), 5730–5743. <https://doi.org/10.1523/JNEUROSCI.0012-07.2007>
- Geisler, S., & Zahm, D. S. (2005). Afferents of the ventral tegmental area in the rat-anatomical substratum for integrative functions. *The Journal of Comparative Neurology*, 490(3), 270–294.  
<https://doi.org/10.1002/cne.20668>
- Gerber, G. J., Sing, J., & Wise, R. A. (1981). Pimozide attenuates lever pressing for water reinforcement in rats. *Pharmacology, Biochemistry, and Behavior*, 14(2), 201–205.
- Gerits, A., Farivar, R., Rosen, B. R., Wald, L. L., Boyden, E. S., & Vanduffel, W. (2012). Optogenetically induced behavioral and functional network changes in primates. *Current Biology: CB*, 22(18), 1722–1726. <https://doi.org/10.1016/j.cub.2012.07.023>

- German, D. C., Schlusberg, D. S., & Woodward, D. J. (1983). Three-dimensional computer reconstruction of midbrain dopaminergic neuronal populations: from mouse to man. *Journal of Neural Transmission*, 57(4), 243–254.
- Goldman-Rakic, P. S., & Selemon, L. D. (1997). Functional and anatomical aspects of prefrontal pathology in schizophrenia. *Schizophrenia Bulletin*, 23(3), 437–458.
- Goldstein, R. Z., & Volkow, N. D. (2002). Drug addiction and its underlying neurobiological basis: neuroimaging evidence for the involvement of the frontal cortex. *The American Journal of Psychiatry*, 159(10), 1642–1652. <https://doi.org/10.1176/appi.ajp.159.10.1642>
- Goldstein, R. Z., & Volkow, N. D. (2011). Dysfunction of the prefrontal cortex in addiction: neuroimaging findings and clinical implications. *Nature Reviews. Neuroscience*, 12(11), 652–669. <https://doi.org/10.1038/nrn3119>
- Gradinaru, V., Thompson, K. R., & Deisseroth, K. (2008). eNpHR: a Natronomonas halorhodopsin enhanced for optogenetic applications. *Brain Cell Biology*, 36(1–4), 129–139. <https://doi.org/10.1007/s11068-008-9027-6>
- Greenland, S., Pearl, J., & Robins, J. M. (1999). Causal diagrams for epidemiologic research. *Epidemiology (Cambridge, Mass.)*, 10(1), 37–48.
- Grimm, J. W., Hope, B. T., Wise, R. A., & Shaham, Y. (2001). Neuroadaptation. Incubation of cocaine craving after withdrawal. *Nature*, 412(6843), 141–142. <https://doi.org/10.1038/35084134>
- Grossman, S. P., Dacey, D., Halaris, A. E., Collier, T., & Routtenberg, A. (1978). Aphagia and adipsia after preferential destruction of nerve cell bodies in hypothalamus. *Science (New York, N.Y.)*, 202(4367), 537–539.
- Gu, H., Salmeron, B. J., Ross, T. J., Geng, X., Zhan, W., Stein, E. A., & Yang, Y. (2010). Mesocorticolimbic circuits are impaired in chronic cocaine users as demonstrated by resting-state functional connectivity. *NeuroImage*, 53(2), 593–601. <https://doi.org/10.1016/j.neuroimage.2010.06.066>
- Gunaydin, L. A., Grosenick, L., Finkelstein, J. C., Kauvar, I. V., Fenno, L. E., Adhikari, A., ... Deisseroth, K. (2014). Natural neural projection dynamics underlying social behavior. *Cell*, 157(7), 1535–1551. <https://doi.org/10.1016/j.cell.2014.05.017>
- Haber, S. N., Kim, K.-S., Mailly, P., & Calzavara, R. (2006). Reward-related cortical inputs define a large striatal region in primates that interface with associative cortical connections, providing a substrate for incentive-based learning. *The Journal of Neuroscience: The Official Journal of the Society for Neuroscience*, 26(32), 8368–8376. <https://doi.org/10.1523/JNEUROSCI.0271-06.2006>

- Han, X., & Boyden, E. S. (2007). Multiple-color optical activation, silencing, and desynchronization of neural activity, with single-spike temporal resolution. *PloS One*, 2(3), e299. <https://doi.org/10.1371/journal.pone.0000299>
- Handwerker, D. A., Ollinger, J. M., & D'Esposito, M. (2004). Variation of BOLD hemodynamic responses across subjects and brain regions and their effects on statistical analyses. *NeuroImage*, 21(4), 1639–1651. <https://doi.org/10.1016/j.neuroimage.2003.11.029>
- Hanlon, C. A., Beveridge, T. J. R., & Porrino, L. J. (2013). Recovering from cocaine: insights from clinical and preclinical investigations. *Neuroscience and Biobehavioral Reviews*, 37(9 Pt A), 2037–2046. <https://doi.org/10.1016/j.neubiorev.2013.04.007>
- Heimer, L., Zahm, D. S., Churchill, L., Kalivas, P. W., & Wohltmann, C. (1991). Specificity in the projection patterns of accumbal core and shell in the rat. *Neuroscience*, 41(1), 89–125.
- Herman, J. P., Guillonneau, D., Dantzer, R., Scatton, B., Semerdjian-Rouquier, L., & Le Moal, M. (1982). Differential effects of inescapable footshocks and of stimuli previously paired with inescapable footshocks on dopamine turnover in cortical and limbic areas of the rat. *Life Sciences*, 30(25), 2207–2214.
- Hernandez, L., & Hoebel, B. G. (1988). Feeding and hypothalamic stimulation increase dopamine turnover in the accumbens. *Physiology & Behavior*, 44(4–5), 599–606.
- Hjelmstad, G. O., & Fields, H. L. (2003). Kappa opioid receptor activation in the nucleus accumbens inhibits glutamate and GABA release through different mechanisms. *Journal of Neurophysiology*, 89(5), 2389–2395. <https://doi.org/10.1152/jn.01115.2002>
- Hnasko, T. S., Chuhma, N., Zhang, H., Goh, G. Y., Sulzer, D., Palmiter, R. D., ... Edwards, R. H. (2010). Vesicular glutamate transport promotes dopamine storage and glutamate corelease in vivo. *Neuron*, 65(5), 643–656. <https://doi.org/10.1016/j.neuron.2010.02.012>
- Hnasko, T. S., Hjelmstad, G. O., Fields, H. L., & Edwards, R. H. (2012). Ventral tegmental area glutamate neurons: electrophysiological properties and projections. *The Journal of Neuroscience: The Official Journal of the Society for Neuroscience*, 32(43), 15076–15085. <https://doi.org/10.1523/JNEUROSCI.3128-12.2012>
- Hoebel, B. G., Mark, G. P., & West, H. L. (1992). Conditioned release of neurotransmitters as measured by microdialysis. *Clinical Neuropharmacology*, 15 Suppl 1 Pt A, 704A–705A.
- Hollander, J. A., & Carelli, R. M. (2005). Abstinence from cocaine self-administration heightens neural encoding of goal-directed behaviors in the accumbens. *Neuropsychopharmacology: Official Publication of the American College of Neuropsychopharmacology*, 30(8), 1464–1474. <https://doi.org/10.1038/sj.npp.1300748>

- Hoover, W. B., & Vertes, R. P. (2007). Anatomical analysis of afferent projections to the medial prefrontal cortex in the rat. *Brain Structure & Function*, 212(2), 149–179. <https://doi.org/10.1007/s00429-007-0150-4>
- Hutchison, R. M., Mirsattari, S. M., Jones, C. K., Gati, J. S., & Leung, L. S. (2010). Functional networks in the anesthetized rat brain revealed by independent component analysis of resting-state fMRI. *Journal of Neurophysiology*, 103(6), 3398–3406. <https://doi.org/10.1152/jn.00141.2010>
- Ito, R., Robbins, T. W., & Everitt, B. J. (2004). Differential control over cocaine-seeking behavior by nucleus accumbens core and shell. *Nature Neuroscience*, 7(4), 389–397. <https://doi.org/10.1038/nn1217>
- Jacob, S. N., Ott, T., & Nieder, A. (2013). Dopamine regulates two classes of primate prefrontal neurons that represent sensory signals. *The Journal of Neuroscience: The Official Journal of the Society for Neuroscience*, 33(34), 13724–13734. <https://doi.org/10.1523/JNEUROSCI.0210-13.2013>
- Jalabert, M., Aston-Jones, G., Herzog, E., Manzoni, O., & Georges, F. (2009). Role of the bed nucleus of the stria terminalis in the control of ventral tegmental area dopamine neurons. *Progress in Neuro-Psychopharmacology & Biological Psychiatry*, 33(8), 1336–1346. <https://doi.org/10.1016/j.pnpbp.2009.07.010>
- Jasinska, A. J., Chen, B. T., Bonci, A., & Stein, E. A. (2015). Dorsal medial prefrontal cortex (MPFC) circuitry in rodent models of cocaine use: implications for drug addiction therapies. *Addiction Biology*, 20(2), 215–226. <https://doi.org/10.1111/adb.12132>
- Jennings, J. H., Sparta, D. R., Stamatakis, A. M., Ung, R. L., Pleil, K. E., Kash, T. L., & Stuber, G. D. (2013). Distinct extended amygdala circuits for divergent motivational states. *Nature*, 496(7444), 224–228. <https://doi.org/10.1038/nature12041>
- Jhou, T. C., Fields, H. L., Baxter, M. G., Saper, C. B., & Holland, P. C. (2009). The rostromedial tegmental nucleus (RMTg), a GABAergic afferent to midbrain dopamine neurons, encodes aversive stimuli and inhibits motor responses. *Neuron*, 61(5), 786–800. <https://doi.org/10.1016/j.neuron.2009.02.001>
- Jhou, T. C., Geisler, S., Marinelli, M., Degarmo, B. A., & Zahm, D. S. (2009). The mesopontine rostromedial tegmental nucleus: A structure targeted by the lateral habenula that projects to the ventral tegmental area of Tsai and substantia nigra compacta. *The Journal of Comparative Neurology*, 513(6), 566–596. <https://doi.org/10.1002/cne.21891>
- Ji, H., & Shepard, P. D. (2007). Lateral habenula stimulation inhibits rat midbrain dopamine neurons through a GABA(A) receptor-mediated mechanism. *The Journal of Neuroscience: The*



*Official Journal of the Society for Neuroscience*, 27(26), 6923–6930.  
<https://doi.org/10.1523/JNEUROSCI.0958-07.2007>

Johnson, S. W., & North, R. A. (1992). Two types of neurone in the rat ventral tegmental area and their synaptic inputs. *The Journal of Physiology*, 450, 455–468.

Jones, J. L., Day, J. J., Aragona, B. J., Wheeler, R. A., Wightman, R. M., & Carelli, R. M. (2010). Basolateral amygdala modulates terminal dopamine release in the nucleus accumbens and conditioned responding. *Biological Psychiatry*, 67(8), 737–744.  
<https://doi.org/10.1016/j.biopsych.2009.11.006>

Kabanova, A., Pabst, M., Lorkowski, M., Braganza, O., Boehlen, A., Nikbakht, N., ... Blaess, S. (2015). Function and developmental origin of a mesocortical inhibitory circuit. *Nature Neuroscience*, 18(6), 872–882. <https://doi.org/10.1038/nn.4020>

Kahn, I., Desai, M., Knoblich, U., Bernstein, J., Henninger, M., Graybiel, A. M., ... Moore, C. I. (2011). Characterization of the functional MRI response temporal linearity via optical control of neocortical pyramidal neurons. *The Journal of Neuroscience: The Official Journal of the Society for Neuroscience*, 31(42), 15086–15091. <https://doi.org/10.1523/JNEUROSCI.0007-11.2011>

Kalivas, P. W., Churchill, L., & Klitenick, M. A. (1993). GABA and enkephalin projection from the nucleus accumbens and ventral pallidum to the ventral tegmental area. *Neuroscience*, 57(4), 1047–1060.

Kalivas, P. W., & Volkow, N. D. (2005). The Neural Basis of Addiction: A Pathology of Motivation and Choice. *American Journal of Psychiatry*, 162(8), 1403–1413.  
<https://doi.org/10.1176/appi.ajp.162.8.1403>

Kapur, S. (2003). Psychosis as a state of aberrant salience: a framework linking biology, phenomenology, and pharmacology in schizophrenia. *The American Journal of Psychiatry*, 160(1), 13–23. <https://doi.org/10.1176/appi.ajp.160.1.13>

Kilts, C. D., Gross, R. E., Ely, T. D., & Drexler, K. P. G. (2004). The neural correlates of cue-induced craving in cocaine-dependent women. *The American Journal of Psychiatry*, 161(2), 233–241. <https://doi.org/10.1176/appi.ajp.161.2.233>

Kim, S.-G., Harel, N., Jin, T., Kim, T., Lee, P., & Zhao, F. (2013). Cerebral blood volume MRI with intravascular superparamagnetic iron oxide nanoparticles. *NMR in Biomedicine*, 26(8), 949–962. <https://doi.org/10.1002/nbm.2885>

Ko, J. Y., Patrick, S. W., Tong, V. T., Patel, R., Lind, J. N., & Barfield, W. D. (2016). Incidence of Neonatal Abstinence Syndrome - 28 States, 1999–2013. *MMWR. Morbidity and Mortality Weekly Report*, 65(31), 799–802. <https://doi.org/10.15585/mmwr.mm6531a2>

Koob, G. F., & Volkow, N. D. (2010). Neurocircuitry of addiction. *Neuropsychopharmacology: Official Publication of the American College of Neuropsychopharmacology*, 35(1), 217–238. <https://doi.org/10.1038/npp.2009.110>

Kravitz, A. V., Tye, L. D., & Kreitzer, A. C. (2012). Distinct roles for direct and indirect pathway striatal neurons in reinforcement. *Nature Neuroscience*, 15(6), 816–818. <https://doi.org/10.1038/nn.3100>

Kudo, T., Uchigashima, M., Miyazaki, T., Konno, K., Yamasaki, M., Yanagawa, Y., ... Watanabe, M. (2012). Three types of neurochemical projection from the bed nucleus of the stria terminalis to the ventral tegmental area in adult mice. *The Journal of Neuroscience: The Official Journal of the Society for Neuroscience*, 32(50), 18035–18046. <https://doi.org/10.1523/JNEUROSCI.4057-12.2012>

Kulla, A., & Manahan-Vaughan, D. (2000). Depotentiation in the dentate gyrus of freely moving rats is modulated by D1/D5 dopamine receptors. *Cerebral Cortex (New York, N.Y.: 1991)*, 10(6), 614–620.

Kumar, S., Black, S. J., Hultman, R., Szabo, S. T., DeMaio, K. D., Du, J., ... Dzirasa, K. (2013). Cortical control of affective networks. *The Journal of Neuroscience: The Official Journal of the Society for Neuroscience*, 33(3), 1116–1129. <https://doi.org/10.1523/JNEUROSCI.0092-12.2013>

Lai, H.-Y., Albaugh, D. L., Kao, Y.-C. J., Younce, J. R., & Shih, Y.-Y. I. (2015). Robust deep brain stimulation functional MRI procedures in rats and mice using an MR-compatible tungsten microwire electrode. *Magnetic Resonance in Medicine*, 73(3), 1246–1251. <https://doi.org/10.1002/mrm.25239>

Lammel, S., Hetzel, A., Häckel, O., Jones, I., Liss, B., & Roeper, J. (2008). Unique properties of mesoprefrontal neurons within a dual mesocorticolimbic dopamine system. *Neuron*, 57(5), 760–773. <https://doi.org/10.1016/j.neuron.2008.01.022>

Lammel, S., Ion, D. I., Roeper, J., & Malenka, R. C. (2011). Projection-specific modulation of dopamine neuron synapses by aversive and rewarding stimuli. *Neuron*, 70(5), 855–862. <https://doi.org/10.1016/j.neuron.2011.03.025>

Lammel, S., Lim, B. K., Ran, C., Huang, K. W., Betley, M. J., Tye, K. M., ... Malenka, R. C. (2012). Input-specific control of reward and aversion in the ventral tegmental area. *Nature*, 491(7423), 212–217. <https://doi.org/10.1038/nature11527>

Lammel, S., Steinberg, E. E., Földy, C., Wall, N. R., Beier, K., Luo, L., & Malenka, R. C. (2015). Diversity of transgenic mouse models for selective targeting of midbrain dopamine neurons. *Neuron*, 85(2), 429–438. <https://doi.org/10.1016/j.neuron.2014.12.036>

- Lavin, A., Nogueira, L., Lapish, C. C., Wightman, R. M., Phillips, P. E. M., & Seamans, J. K. (2005). Mesocortical dopamine neurons operate in distinct temporal domains using multimodal signaling. *The Journal of Neuroscience: The Official Journal of the Society for Neuroscience*, 25(20), 5013–5023. <https://doi.org/10.1523/JNEUROSCI.0557-05.2005>
- LeDoux, J. E. (2000). Emotion circuits in the brain. *Annual Review of Neuroscience*, 23, 155–184. <https://doi.org/10.1146/annurev.neuro.23.1.155>
- Lee, J. H., Durand, R., Gradinaru, V., Zhang, F., Goshen, I., Kim, D.-S., ... Deisseroth, K. (2010). Global and local fMRI signals driven by neurons defined optogenetically by type and wiring. *Nature*, 465(7299), 788–792. <https://doi.org/10.1038/nature09108>
- Lein, E. S., Hawrylycz, M. J., Ao, N., Ayres, M., Bensinger, A., Bernard, A., ... Jones, A. R. (2007). Genome-wide atlas of gene expression in the adult mouse brain. *Nature*, 445(7124), 168–176. <https://doi.org/10.1038/nature05453>
- Leite, F. P., Tsao, D., Vanduffel, W., Fize, D., Sasaki, Y., Wald, L. L., ... Mandeville, J. B. (2002). Repeated fMRI using iron oxide contrast agent in awake, behaving macaques at 3 Tesla. *NeuroImage*, 16(2), 283–294. <https://doi.org/10.1006/nimg.2002.1110>
- Lewis, B. L., & O'Donnell, P. (2000). Ventral Tegmental Area Afferents to the Prefrontal Cortex Maintain Membrane Potential 'Up' States in Pyramidal Neurons via D1 Dopamine Receptors. *Cerebral Cortex*, 10(12), 1168–1175. <https://doi.org/10.1093/cercor/10.12.1168>
- Liberzon, I., Taylor, S. F., Amdur, R., Jung, T. D., Chamberlain, K. R., Minoshima, S., ... Fig, L. M. (1999). Brain activation in PTSD in response to trauma-related stimuli. *Biological Psychiatry*, 45(7), 817–826.
- Lisman, J. E., & Grace, A. A. (2005). The hippocampal-VTA loop: controlling the entry of information into long-term memory. *Neuron*, 46(5), 703–713. <https://doi.org/10.1016/j.neuron.2005.05.002>
- Lisoprawski, A., Herve, D., Blanc, G., Glowinski, J., & Tassin, J. P. (1980). Selective activation of the mesocortico-frontal dopaminergic neurons induced by lesion of the habenula in the rat. *Brain Research*, 183(1), 229–234.
- Logothetis, N. K. (2008). What we can do and what we cannot do with fMRI. *Nature*, 453(7197), 869–878. <https://doi.org/10.1038/nature06976>
- Lu, H., Zou, Q., Chefer, S., Ross, T. J., Vaupel, D. B., Guillem, K., ... Stein, E. A. (2014). Abstinence from cocaine and sucrose self-administration reveals altered mesocorticolimbic circuit connectivity by resting state MRI. *Brain Connectivity*, 4(7), 499–510. <https://doi.org/10.1089/brain.2014.0264>

- Lu, H., Zou, Q., Gu, H., Raichle, M. E., Stein, E. A., & Yang, Y. (2012). Rat brains also have a default mode network. *Proceedings of the National Academy of Sciences of the United States of America*, 109(10), 3979–3984. <https://doi.org/10.1073/pnas.1200506109>
- Lynch, W. J., & Carroll, M. E. (1999). Sex differences in the acquisition of intravenously self-administered cocaine and heroin in rats. *Psychopharmacology*, 144(1), 77–82.
- Lynch, W. J., Roth, M. E., Mickelberg, J. L., & Carroll, M. E. (2001). Role of estrogen in the acquisition of intravenously self-administered cocaine in female rats. *Pharmacology, Biochemistry, and Behavior*, 68(4), 641–646.
- Maas, L. C., Lukas, S. E., Kaufman, M. J., Weiss, R. D., Daniels, S. L., Rogers, V. W., ... Renshaw, P. F. (1998). Functional magnetic resonance imaging of human brain activation during cue-induced cocaine craving. *The American Journal of Psychiatry*, 155(1), 124–126. <https://doi.org/10.1176/ajp.155.1.124>
- Mameli, M., Balland, B., Luján, R., & Lüscher, C. (2007). Rapid synthesis and synaptic insertion of GluR2 for mGluR-LTD in the ventral tegmental area. *Science (New York, N.Y.)*, 317(5837), 530–533. <https://doi.org/10.1126/science.1142365>
- Mandeville, J. B., Marota, J. J., Kosofsky, B. E., Keltner, J. R., Weissleder, R., Rosen, B. R., & Weisskoff, R. M. (1998). Dynamic functional imaging of relative cerebral blood volume during rat forepaw stimulation. *Magnetic Resonance in Medicine: Official Journal of the Society of Magnetic Resonance in Medicine / Society of Magnetic Resonance in Medicine*, 39(4), 615–624.
- Marder, E. (2012). Neuromodulation of neuronal circuits: back to the future. *Neuron*, 76(1), 1–11. <https://doi.org/10.1016/j.neuron.2012.09.010>
- Margolis, E. B., Hjelmstad, G. O., Bonci, A., & Fields, H. L. (2003). Kappa-opioid agonists directly inhibit midbrain dopaminergic neurons. *The Journal of Neuroscience: The Official Journal of the Society for Neuroscience*, 23(31), 9981–9986.
- Margolis, E. B., Lock, H., Hjelmstad, G. O., & Fields, H. L. (2006). The ventral tegmental area revisited: is there an electrophysiological marker for dopaminergic neurons? *The Journal of Physiology*, 577(Pt 3), 907–924. <https://doi.org/10.1113/jphysiol.2006.117069>
- Marota, J. J., Mandeville, J. B., Weisskoff, R. M., Moskowitz, M. A., Rosen, B. R., & Kosofsky, B. E. (2000). Cocaine activation discriminates dopaminergic projections by temporal response: an fMRI study in Rat. *NeuroImage*, 11(1), 13–23. <https://doi.org/10.1006/nimg.1999.0520>
- Matsumoto, M., & Hikosaka, O. (2007). Lateral habenula as a source of negative reward signals in dopamine neurons. *Nature*, 447(7148), 1111–1115. <https://doi.org/10.1038/nature05860>
- Matsumoto, M., & Hikosaka, O. (2009). Representation of negative motivational value in the primate lateral habenula. *Nature Neuroscience*, 12(1), 77–84. <https://doi.org/10.1038/nn.2233>

- Meil, W. M., & See, R. E. (1997). Lesions of the basolateral amygdala abolish the ability of drug associated cues to reinstate responding during withdrawal from self-administered cocaine. *Behavioural Brain Research*, 87(2), 139–148.
- Mercuri, N. B., Bonci, A., Calabresi, P., Stefani, A., & Bernardi, G. (1995). Properties of the hyperpolarization-activated cation current  $I_h$  in rat midbrain dopaminergic neurons. *The European Journal of Neuroscience*, 7(3), 462–469.
- Mogenson, G. J., Jones, D. L., & Yim, C. Y. (1980). From motivation to action: functional interface between the limbic system and the motor system. *Progress in Neurobiology*, 14(2–3), 69–97.
- Monti, M. M. (2011). Statistical Analysis of fMRI Time-Series: A Critical Review of the GLM Approach. *Frontiers in Human Neuroscience*, 5, 28. <https://doi.org/10.3389/fnhum.2011.00028>
- Morgan, D., Grant, K. A., Gage, H. D., Mach, R. H., Kaplan, J. R., Prioleau, O., ... Nader, M. A. (2002). Social dominance in monkeys: dopamine D2 receptors and cocaine self-administration. *Nature Neuroscience*, 5(2), 169–174. <https://doi.org/10.1038/nn798>
- Muñoz-Cuevas, F. J., Athilingam, J., Piscopo, D., & Wilbrecht, L. (2013). Cocaine-induced structural plasticity in frontal cortex correlates with conditioned place preference. *Nature Neuroscience*, 16(10), 1367–1369. <https://doi.org/10.1038/nn.3498>
- Murnane, K. S., Gopinath, K. S., Maltbie, E., Daunais, J. B., Telesford, Q. K., & Howell, L. L. (2015). Functional connectivity in frontal-striatal brain networks and cocaine self-administration in female rhesus monkeys. *Psychopharmacology*, 232(4), 745–754. <https://doi.org/10.1007/s00213-014-3709-9>
- Nair-Roberts, R. G., Chatelain-Badie, S. D., Benson, E., White-Cooper, H., Bolam, J. P., & Ungless, M. A. (2008). Stereological estimates of dopaminergic, GABAergic and glutamatergic neurons in the ventral tegmental area, substantia nigra and retrorubral field in the rat. *Neuroscience*, 152(4), 1024–1031. <https://doi.org/10.1016/j.neuroscience.2008.01.046>
- Naqvi, N. H., Rudrauf, D., Damasio, H., & Bechara, A. (2007). Damage to the insula disrupts addiction to cigarette smoking. *Science (New York, N.Y.)*, 315(5811), 531–534. <https://doi.org/10.1126/science.1135926>
- Nauta, W. J., Smith, G. P., Faull, R. L., & Domesick, V. B. (1978). Efferent connections and nigral afferents of the nucleus accumbens septi in the rat. *Neuroscience*, 3(4–5), 385–401.
- Nieh, E. H., Matthews, G. A., Allsop, S. A., Presbrey, K. N., Leppla, C. A., Wichmann, R., ... Tye, K. M. (2015). Decoding Neural Circuits that Control Compulsive Sucrose-Seeking. *Cell*, 160(3), 528–541. <https://doi.org/10.1016/j.cell.2015.01.003>

- Ogawa, S., & Lee, T. M. (1990). Magnetic resonance imaging of blood vessels at high fields: in vivo and in vitro measurements and image simulation. *Magnetic Resonance in Medicine*, 16(1), 9–18.
- Ogawa, S., Lee, T. M., Kay, A. R., & Tank, D. W. (1990). Brain magnetic resonance imaging with contrast dependent on blood oxygenation. *Proceedings of the National Academy of Sciences of the United States of America*, 87(24), 9868–9872.
- Ogawa, S., Lee, T. M., Nayak, A. S., & Glynn, P. (1990). Oxygenation-sensitive contrast in magnetic resonance image of rodent brain at high magnetic fields. *Magnetic Resonance in Medicine*, 14(1), 68–78.
- Olds, J., & Milner, P. (1954). Positive reinforcement produced by electrical stimulation of septal area and other regions of rat brain. *Journal of Comparative and Physiological Psychology*, 47(6), 419–427.
- Otani, S., Daniel, H., Roisin, M.-P., & Crepel, F. (2003). Dopaminergic modulation of long-term synaptic plasticity in rat prefrontal neurons. *Cerebral Cortex (New York, N.Y.: 1991)*, 13(11), 1251–1256.
- Pascoli, V., Terrier, J., Hiver, A., & Lüscher, C. (2015). Sufficiency of Mesolimbic Dopamine Neuron Stimulation for the Progression to Addiction. *Neuron*, 88(5), 1054–1066. <https://doi.org/10.1016/j.neuron.2015.10.017>
- Pawela, C. P., Biswal, B. B., Cho, Y. R., Kao, D. S., Li, R., Jones, S. R., ... Hyde, J. S. (2008). Resting-state functional connectivity of the rat brain. *Magnetic Resonance in Medicine*, 59(5), 1021–1029. <https://doi.org/10.1002/mrm.21524>
- Paxinos G, Watson C. The Rat Brain In Stereotaxic Coordinates, 5<sup>th</sup> edn. Elsevier Academic Press: Burlington, 2005.
- Pfaus, J. G., Damsma, G., Nomikos, G. G., Wenkstern, D. G., Blaha, C. D., Phillips, A. G., & Fibiger, H. C. (1990). Sexual behavior enhances central dopamine transmission in the male rat. *Brain Research*, 530(2), 345–348.
- Pfaus, J. G., Damsma, G., Wenkstern, D., & Fibiger, H. C. (1995). Sexual activity increases dopamine transmission in the nucleus accumbens and striatum of female rats. *Brain Research*, 693(1–2), 21–30.
- Phillips, A. G., Atkinson, L. J., Blackburn, J. R., & Blaha, C. D. (1993). Increased extracellular dopamine in the nucleus accumbens of the rat elicited by a conditional stimulus for food: an electrochemical study. *Canadian Journal of Physiology and Pharmacology*, 71(5–6), 387–393.

Phillips, P. E. M., Stuber, G. D., Heien, M. L. A. V., Wightman, R. M., & Carelli, R. M. (2003). Subsecond dopamine release promotes cocaine seeking. *Nature*, 422(6932), 614–618. <https://doi.org/10.1038/nature01476>

Phillipson, O. T. (1979). Afferent projections to the ventral tegmental area of Tsai and interfascicular nucleus: a horseradish peroxidase study in the rat. *The Journal of Comparative Neurology*, 187(1), 117–143. <https://doi.org/10.1002/cne.901870108>

Pickens, C. L., Airavaara, M., Theberge, F., Fanous, S., Hope, B. T., & Shaham, Y. (2011). Neurobiology of the incubation of drug craving. *Trends in Neurosciences*, 34(8), 411–420. <https://doi.org/10.1016/j.tins.2011.06.001>

Poulin, J.-F., Zou, J., Drouin-Ouellet, J., Kim, K.-Y. A., Cicchetti, F., & Awatramani, R. B. (2014). Defining midbrain dopaminergic neuron diversity by single-cell gene expression profiling. *Cell Reports*, 9(3), 930–943. <https://doi.org/10.1016/j.celrep.2014.10.008>

Qi, J., Zhang, S., Wang, H.-L., Barker, D. J., Miranda-Barrientos, J., & Morales, M. (2016). VTA glutamatergic inputs to nucleus accumbens drive aversion by acting on GABAergic interneurons. *Nature Neuroscience*, 19(5), 725–733. <https://doi.org/10.1038/nn.4281>

Ridderinkhof, K. R., Ullsperger, M., Crone, E. A., & Nieuwenhuis, S. (2004). The role of the medial frontal cortex in cognitive control. *Science (New York, N.Y.)*, 306(5695), 443–447. <https://doi.org/10.1126/science.1100301>

Robbins, S. J., Ehrman, R. N., Childress, A. R., & O'Brien, C. P. (1999). Comparing levels of cocaine cue reactivity in male and female outpatients. *Drug and Alcohol Dependence*, 53(3), 223–230.

Robbins, T. W., & Everitt, B. J. (1999). Drug addiction: bad habits add up. *Nature*, 398(6728), 567–570. <https://doi.org/10.1038/19208>

Robinson, T. E., & Berridge, K. C. (2003). Addiction. *Annual Review of Psychology*, 54, 25–53. <https://doi.org/10.1146/annurev.psych.54.101601.145237>

Roitman, M. F., Stuber, G. D., Phillips, P. E. M., Wightman, R. M., & Carelli, R. M. (2004). Dopamine operates as a subsecond modulator of food seeking. *The Journal of Neuroscience: The Official Journal of the Society for Neuroscience*, 24(6), 1265–1271. <https://doi.org/10.1523/JNEUROSCI.3823-03.2004>

Roitman, M. F., Wheeler, R. A., Wightman, R. M., & Carelli, R. M. (2008). Real-time chemical responses in the nucleus accumbens differentiate rewarding and aversive stimuli. *Nature Neuroscience*, 11(12), 1376–1377. <https://doi.org/10.1038/nn.2219>

- Rossato, J. I., Bevilacqua, L. R. M., Izquierdo, I., Medina, J. H., & Cammarota, M. (2009). Dopamine controls persistence of long-term memory storage. *Science (New York, N.Y.)*, 325(5943), 1017–1020. <https://doi.org/10.1126/science.1172545>
- Rudd, R. A., Seth, P., David, F., & Scholl, L. (2016). Increases in Drug and Opioid-Involved Overdose Deaths - United States, 2010-2015. *MMWR. Morbidity and Mortality Weekly Report*, 65(5051), 1445–1452. <https://doi.org/10.15585/mmwr.mm655051e1>
- Rungta, R. L., Osmanski, B.-F., Boido, D., Tanter, M., & Charpak, S. (2017). Light controls cerebral blood flow in naive animals. *Nature Communications*, 8, 14191. <https://doi.org/10.1038/ncomms14191>
- Saal, D., Dong, Y., Bonci, A., & Malenka, R. C. (2003). Drugs of abuse and stress trigger a common synaptic adaptation in dopamine neurons. *Neuron*, 37(4), 577–582.
- Saddoris, M. P., Cacciapaglia, F., Wightman, R. M., & Carelli, R. M. (2015). Differential Dopamine Release Dynamics in the Nucleus Accumbens Core and Shell Reveal Complementary Signals for Error Prediction and Incentive Motivation. *The Journal of Neuroscience: The Official Journal of the Society for Neuroscience*, 35(33), 11572–11582. <https://doi.org/10.1523/JNEUROSCI.2344-15.2015>
- Sadikot, A. F., & Parent, A. (1990). The monoaminergic innervation of the amygdala in the squirrel monkey: an immunohistochemical study. *Neuroscience*, 36(2), 431–447.
- Sajikumar, S., & Frey, J. U. (2004). Late-associativity, synaptic tagging, and the role of dopamine during LTP and LTD. *Neurobiology of Learning and Memory*, 82(1), 12–25. <https://doi.org/10.1016/j.nlm.2004.03.003>
- Salamone, J. D., Correa, M., Farrar, A., & Mingote, S. M. (2007). Effort-related functions of nucleus accumbens dopamine and associated forebrain circuits. *Psychopharmacology*, 191(3), 461–482. <https://doi.org/10.1007/s00213-006-0668-9>
- Salgado, S., & Kaplitt, M. G. (2015). The Nucleus Accumbens: A Comprehensive Review. *Stereotactic and Functional Neurosurgery*, 93(2), 75–93. <https://doi.org/10.1159/000368279>
- Schmid, F., Wachsmuth, L., Albers, F., Schwalm, M., Stroh, A., & Faber, C. (2017). True and apparent optogenetic BOLD fMRI signals. *Magnetic Resonance in Medicine*, 77(1), 126–136. <https://doi.org/10.1002/mrm.26095>
- Schultz, W. (1998). Predictive Reward Signal of Dopamine Neurons. *Journal of Neurophysiology*, 80(1), 1–27.
- Schultz, W. (2001). Reward signaling by dopamine neurons. *The Neuroscientist: A Review Journal Bringing Neurobiology, Neurology and Psychiatry*, 7(4), 293–302. <https://doi.org/10.1177/107385840100700406>



Schultz, W., Dayan, P., & Montague, P. R. (1997). A neural substrate of prediction and reward. *Science (New York, N.Y.)*, 275(5306), 1593–1599.

Scott, D., & Hiroi, N. (2011). Deconstructing craving: dissociable cortical control of cue reactivity in nicotine addiction. *Biological Psychiatry*, 69(11), 1052–1059.  
<https://doi.org/10.1016/j.biopsych.2011.01.023>

Seeley, W. W., Menon, V., Schatzberg, A. F., Keller, J., Glover, G. H., Kenna, H., ... Greicius, M. D. (2007). Dissociable intrinsic connectivity networks for salience processing and executive control. *The Journal of Neuroscience: The Official Journal of the Society for Neuroscience*, 27(9), 2349–2356. <https://doi.org/10.1523/JNEUROSCI.5587-06.2007>

Segal, M. (1973). Flow of conditioned responses in limbic telencephalic system of the rat. *Journal of Neurophysiology*, 36(5), 840–854.

Shih, Y.-Y. I., Chen, C.-C. V., Shyu, B.-C., Lin, Z.-J., Chiang, Y.-C., Jaw, F.-S., ... Chang, C. (2009). A new scenario for negative functional magnetic resonance imaging signals: endogenous neurotransmission. *The Journal of Neuroscience: The Official Journal of the Society for Neuroscience*, 29(10), 3036–3044. <https://doi.org/10.1523/JNEUROSCI.3447-08.2009>

Shih, Y.-Y. I., Huang, S., Chen, Y.-Y., Lai, H.-Y., Kao, Y.-C. J., Du, F., ... Duong, T. Q. (2014). Imaging neurovascular function and functional recovery after stroke in the rat striatum using forepaw stimulation. *Journal of Cerebral Blood Flow and Metabolism: Official Journal of the International Society of Cerebral Blood Flow and Metabolism*, 34(9), 1483–1492.  
<https://doi.org/10.1038/jcbfm.2014.103>

Shih, Y.-Y. I., Wang, L., De La Garza, B. H., Li, G., Cull, G., Kiel, J. W., & Duong, T. Q. (2013). Quantitative retinal and choroidal blood flow during light, dark adaptation and flicker light stimulation in rats using fluorescent microspheres. *Current Eye Research*, 38(2), 292–298.  
<https://doi.org/10.3109/02713683.2012.756526>

Shih, Y.-Y. I., Yash, T. V., Rogers, B., & Duong, T. Q. (2014). FMRI of deep brain stimulation at the rat ventral posteromedial thalamus. *Brain Stimulation*, 7(2), 190–193.  
<https://doi.org/10.1016/j.brs.2013.11.001>

Smirnakis, S. M., Schmid, M. C., Weber, B., Tolias, A. S., Augath, M., & Logothetis, N. K. (2007). Spatial specificity of BOLD versus cerebral blood volume fMRI for mapping cortical organization. *Journal of Cerebral Blood Flow and Metabolism: Official Journal of the International Society of Cerebral Blood Flow and Metabolism*, 27(6), 1248–1261.  
<https://doi.org/10.1038/sj.jcbfm.9600434>

Solt, K., Van Dort, C. J., Chemali, J. J., Taylor, N. E., Kenny, J. D., & Brown, E. N. (2014). Electrical stimulation of the ventral tegmental area induces reanimation from general anesthesia. *Anesthesiology*, 121(2), 311–319. <https://doi.org/10.1097/ALN.0000000000000117>

Sparta, D. R., Stamatakis, A. M., Phillips, J. L., Hovelsø, N., van Zessen, R., & Stuber, G. D. (2011). Construction of implantable optical fibers for long-term optogenetic manipulation of neural circuits. *Nature Protocols*, 7(1), 12–23. <https://doi.org/10.1038/nprot.2011.413>

Squire, L. R. (1992). Memory and the hippocampus: a synthesis from findings with rats, monkeys, and humans. *Psychological Review*, 99(2), 195–231.

Stamatakis, A. M., Jennings, J. H., Ung, R. L., Blair, G. A., Weinberg, R. J., Neve, R. L., ... Stuber, G. D. (2013). A unique population of ventral tegmental area neurons inhibits the lateral habenula to promote reward. *Neuron*, 80(4), 1039–1053. <https://doi.org/10.1016/j.neuron.2013.08.023>

Stamatakis, A. M., & Stuber, G. D. (2012). Activation of lateral habenula inputs to the ventral midbrain promotes behavioral avoidance. *Nature Neuroscience*, 15(8), 1105–1107. <https://doi.org/10.1038/nn.3145>

Steinberg, E. E., Boivin, J. R., Saunders, B. T., Witten, I. B., Deisseroth, K., & Janak, P. H. (2014). Positive reinforcement mediated by midbrain dopamine neurons requires D1 and D2 receptor activation in the nucleus accumbens. *PloS One*, 9(4), e94771. <https://doi.org/10.1371/journal.pone.0094771>

Steinberg, E. E., Keiflin, R., Boivin, J. R., Witten, I. B., Deisseroth, K., & Janak, P. H. (2013). A causal link between prediction errors, dopamine neurons and learning. *Nature Neuroscience*, 16(7), 966–973. <https://doi.org/10.1038/nn.3413>

Stricker, E. M., Swerdloff, A. F., & Zigmond, M. J. (1978). Intrahypothalamic injections of kainic acid produce feeding and drinking deficits in rats. *Brain Research*, 158(2), 470–473.

Stuber, G. D., Hnasko, T. S., Britt, J. P., Edwards, R. H., & Bonci, A. (2010). Dopaminergic terminals in the nucleus accumbens but not the dorsal striatum corelease glutamate. *The Journal of Neuroscience: The Official Journal of the Society for Neuroscience*, 30(24), 8229–8233. <https://doi.org/10.1523/JNEUROSCI.1754-10.2010>

Stuber, G. D., Hopf, F. W., Tye, K. M., Chen, B. T., & Bonci, A. (2010). Neuroplastic alterations in the limbic system following cocaine or alcohol exposure. *Current Topics in Behavioral Neurosciences*, 3, 3–27. [https://doi.org/10.1007/7854\\_2009\\_23](https://doi.org/10.1007/7854_2009_23)

Stuber, G. D., Klanker, M., de Ridder, B., Bowers, M. S., Joosten, R. N., Feenstra, M. G., & Bonci, A. (2008). Reward-predictive cues enhance excitatory synaptic strength onto midbrain dopamine neurons. *Science (New York, N.Y.)*, 321(5896), 1690–1692. <https://doi.org/10.1126/science.1160873>

Stuber, G. D., Roitman, M. F., Phillips, P. E. M., Carelli, R. M., & Wightman, R. M. (2005). Rapid dopamine signaling in the nucleus accumbens during contingent and noncontingent

cocaine administration. *Neuropsychopharmacology: Official Publication of the American College of Neuropsychopharmacology*, 30(5), 853–863. <https://doi.org/10.1038/sj.npp.1300619>

Stuber, G. D., Sparta, D. R., Stamatakis, A. M., van Leeuwen, W. A., Hardjoprajitno, J. E., Cho, S., ... Bonci, A. (2011a). Amygdala to nucleus accumbens excitatory transmission facilitates reward seeking. *Nature*, 475(7356), 377–380. <https://doi.org/10.1038/nature10194>

Stuber, G. D., Sparta, D. R., Stamatakis, A. M., van Leeuwen, W. A., Hardjoprajitno, J. E., Cho, S., ... Bonci, A. (2011b). Excitatory transmission from the amygdala to nucleus accumbens facilitates reward seeking. *Nature*, 475(7356), 377–380. <https://doi.org/10.1038/nature10194>

Stuber, G. D., Wightman, R. M., & Carelli, R. M. (2005). Extinction of cocaine self-administration reveals functionally and temporally distinct dopaminergic signals in the nucleus accumbens. *Neuron*, 46(4), 661–669. <https://doi.org/10.1016/j.neuron.2005.04.036>

Sturman, D. A., & Moghaddam, B. (2012). Striatum processes reward differently in adolescents versus adults. *Proceedings of the National Academy of Sciences of the United States of America*, 109(5), 1719–1724. <https://doi.org/10.1073/pnas.1114137109>

Substance Abuse and Mental Health Services Administration (US), & Office of the Surgeon General (US). (2016). *Facing Addiction in America: The Surgeon General's Report on Alcohol, Drugs, and Health*. Washington (DC): US Department of Health and Human Services. Retrieved from <http://www.ncbi.nlm.nih.gov/books/NBK424857/>

Suñer-Soler, R., Grau, A., Gras, M. E., Font-Mayolas, S., Silva, Y., Dávalos, A., ... Serena, J. (2012). Smoking cessation 1 year poststroke and damage to the insular cortex. *Stroke*, 43(1), 131–136. <https://doi.org/10.1161/STROKEAHA.111.630004>

Surgeon general Murthy wants America to face up to addiction. (2016, November 17). Retrieved from <https://www.npr.org/sections/health-shots/2016/11/17/502402409/surgeon-general-murthy-wants-america-to-face-up-to-addiction>

Surmeier, D. J., Ding, J., Day, M., Wang, Z., & Shen, W. (2007). D1 and D2 dopamine-receptor modulation of striatal glutamatergic signaling in striatal medium spiny neurons. *Trends in Neurosciences*, 30(5), 228–235. <https://doi.org/10.1016/j.tins.2007.03.008>

Swanson, L. W. (1982). The projections of the ventral tegmental area and adjacent regions: a combined fluorescent retrograde tracer and immunofluorescence study in the rat. *Brain Research Bulletin*, 9(1–6), 321–353.

Tan, K. R., Yvon, C., Turiault, M., Mirzabekov, J. J., Doehner, J., Labouèbe, G., ... Lüscher, C. (2012). GABA neurons of the VTA drive conditioned place aversion. *Neuron*, 73(6), 1173–1183. <https://doi.org/10.1016/j.neuron.2012.02.015>

- Taylor, S. R., Badurek, S., DiLeone, R. J., Nashmi, R., Minichiello, L., & Picciotto, M. R. (2014). GABAergic and Glutamatergic Efferents of the Mouse Ventral Tegmental Area. *The Journal of Comparative Neurology*, 522(14), 3308–3334. <https://doi.org/10.1002/cne.23603>
- Tecuapetla, F., Patel, J. C., Xenias, H., English, D., Tadros, I., Shah, F., ... Koos, T. (2010). Glutamatergic signaling by mesolimbic dopamine neurons in the nucleus accumbens. *The Journal of Neuroscience: The Official Journal of the Society for Neuroscience*, 30(20), 7105–7110. <https://doi.org/10.1523/JNEUROSCI.0265-10.2010>
- Thierry, A. M., Tassin, J. P., Blanc, G., & Glowinski, J. (1976). Selective activation of mesocortical DA system by stress. *Nature*, 263(5574), 242–244.
- Tidey, J. W., & Miczek, K. A. (1996). Social defeat stress selectively alters mesocorticolimbic dopamine release: an in vivo microdialysis study. *Brain Research*, 721(1–2), 140–149.
- Tomasi, D., Volkow, N. D., Wang, R., Carrillo, J. H., Maloney, T., Alia-Klein, N., ... Goldstein, R. Z. (2010). Disrupted functional connectivity with dopaminergic midbrain in cocaine abusers. *PloS One*, 5(5), e10815. <https://doi.org/10.1371/journal.pone.0010815>
- Tritsch, N. X., Ding, J. B., & Sabatini, B. L. (2012). Dopaminergic neurons inhibit striatal output through non-canonical release of GABA. *Nature*, 490(7419), 262–266. <https://doi.org/10.1038/nature11466>
- Tritsch, N. X., Oh, W.-J., Gu, C., & Sabatini, B. L. (2014). Midbrain dopamine neurons sustain inhibitory transmission using plasma membrane uptake of GABA, not synthesis. *ELife*, 3, e01936.
- Tsai, H.-C., Zhang, F., Adamantidis, A., Stuber, G. D., Bonci, A., de Lecea, L., & Deisseroth, K. (2009). Phasic Firing in Dopaminergic Neurons Is Sufficient for Behavioral Conditioning. *Science (New York, N.Y.)*, 324(5930), 1080–1084. <https://doi.org/10.1126/science.1168878>
- Tye, K. M., Mirzabekov, J. J., Warden, M. R., Ferenczi, E. A., Tsai, H.-C., Finkelstein, J., ... Deisseroth, K. (2013). Dopamine neurons modulate neural encoding and expression of depression-related behaviour. *Nature*, 493(7433), 537–541. <https://doi.org/10.1038/nature11740>
- Tye, K. M., Prakash, R., Kim, S.-Y., Fenno, L. E., Grosenick, L., Zarabi, H., ... Deisseroth, K. (2011). Amygdala circuitry mediating reversible and bidirectional control of anxiety. *Nature*, 471(7338), 358–362. <https://doi.org/10.1038/nature09820>
- Ungerstedt, U. (1971). Adipsia and aphagia after 6-hydroxydopamine induced degeneration of the nigro-striatal dopamine system. *Acta Physiologica Scandinavica. Supplementum*, 367, 95–122.

Ungless, M. A., Whistler, J. L., Malenka, R. C., & Bonci, A. (2001). Single cocaine exposure in vivo induces long-term potentiation in dopamine neurons. *Nature*, 411(6837), 583–587. <https://doi.org/10.1038/35079077>

Valdés-Hernández, P. A., Sumiyoshi, A., Nonaka, H., Haga, R., Aubert-Vásquez, E., Ogawa, T., ... Kawashima, R. (2011). An in vivo MRI Template Set for Morphometry, Tissue Segmentation, and fMRI Localization in Rats. *Frontiers in Neuroinformatics*, 5, 26. <https://doi.org/10.3389/fninf.2011.00026>

Van Bockstaele, E. J., & Pickel, V. M. (1995). GABA-containing neurons in the ventral tegmental area project to the nucleus accumbens in rat brain. *Brain Research*, 682(1–2), 215–221.

van Zessen, R., Phillips, J. L., Budygin, E. A., & Stuber, G. D. (2012). Activation of VTA GABA neurons disrupts reward consumption. *Neuron*, 73(6), 1184–1194. <https://doi.org/10.1016/j.neuron.2012.02.016>

Vanderschuren, L. J. M. J., Di Ciano, P., & Everitt, B. J. (2005). Involvement of the dorsal striatum in cue-controlled cocaine seeking. *The Journal of Neuroscience: The Official Journal of the Society for Neuroscience*, 25(38), 8665–8670. <https://doi.org/10.1523/JNEUROSCI.0925-05.2005>

Vincent, J. L., Patel, G. H., Fox, M. D., Snyder, A. Z., Baker, J. T., Van Essen, D. C., ... Raichle, M. E. (2007). Intrinsic functional architecture in the anaesthetized monkey brain. *Nature*, 447(7140), 83–86. <https://doi.org/10.1038/nature05758>

Vogt, B. A., & Miller, M. W. (1983). Cortical connections between rat cingulate cortex and visual, motor, and postsubicular cortices. *The Journal of Comparative Neurology*, 216(2), 192–210. <https://doi.org/10.1002/cne.902160207>

Volkow, N. D., Fowler, J. S., Wang, G.-J., & Swanson, J. M. (2004). Dopamine in drug abuse and addiction: results from imaging studies and treatment implications. *Molecular Psychiatry*, 9(6), 557–569. <https://doi.org/10.1038/sj.mp.4001507>

Volkow, N. D., Tomasi, D., Wang, G.-J., Logan, J., Alexoff, D. L., Jayne, M., ... Du, C. (2014). Stimulant-induced dopamine increases are markedly blunted in active cocaine abusers. *Molecular Psychiatry*, 19(9), 1037–1043. <https://doi.org/10.1038/mp.2014.58>

Walker, D. L., & Davis, M. (2008). Role of the extended amygdala in short-duration versus sustained fear: a tribute to Dr. Lennart Heimer. *Brain Structure & Function*, 213(1–2), 29–42. <https://doi.org/10.1007/s00429-008-0183-3>

Wang, H., Peca, J., Matsuzaki, M., Matsuzaki, K., Noguchi, J., Qiu, L., ... Augustine, G. J. (2007). High-speed mapping of synaptic connectivity using photostimulation in

- Channelrhodopsin-2 transgenic mice. *Proceedings of the National Academy of Sciences of the United States of America*, 104(19), 8143–8148. <https://doi.org/10.1073/pnas.0700384104>
- Wang, H.-L., Qi, J., Zhang, S., Wang, H., & Morales, M. (2015). Rewarding Effects of Optical Stimulation of Ventral Tegmental Area Glutamatergic Neurons. *The Journal of Neuroscience: The Official Journal of the Society for Neuroscience*, 35(48), 15948–15954. <https://doi.org/10.1523/JNEUROSCI.3428-15.2015>
- Watabe-Uchida, M., Zhu, L., Ogawa, S. K., Vamanrao, A., & Uchida, N. (2012). Whole-brain mapping of direct inputs to midbrain dopamine neurons. *Neuron*, 74(5), 858–873. <https://doi.org/10.1016/j.neuron.2012.03.017>
- Weber, R., Ramos-Cabrera, P., Wiedermann, D., van Camp, N., & Hoehn, M. (2006). A fully noninvasive and robust experimental protocol for longitudinal fMRI studies in the rat. *NeuroImage*, 29(4), 1303–1310. <https://doi.org/10.1016/j.neuroimage.2005.08.028>
- Wexler, B. E., Gottschalk, C. H., Fulbright, R. K., Prohovnik, I., Lacadie, C. M., Rounsaville, B. J., & Gore, J. C. (2001). Functional magnetic resonance imaging of cocaine craving. *The American Journal of Psychiatry*, 158(1), 86–95. <https://doi.org/10.1176/appi.ajp.158.1.86>
- Wheeler, A. L., Lerch, J. P., Chakravarty, M. M., Friedel, M., Sled, J. G., Fletcher, P. J., ... Frankland, P. W. (2013). Adolescent cocaine exposure causes enduring macroscale changes in mouse brain structure. *The Journal of Neuroscience: The Official Journal of the Society for Neuroscience*, 33(5), 1797–1803a. <https://doi.org/10.1523/JNEUROSCI.3830-12.2013>
- White, F. J., & Wang, R. Y. (1984). A10 dopamine neurons: role of autoreceptors in determining firing rate and sensitivity to dopamine agonists. *Life Sciences*, 34(12), 1161–1170.
- Wilcox, C. E., Teshiba, T. M., Merideth, F., Ling, J., & Mayer, A. R. (2011). Enhanced cue reactivity and fronto-striatal functional connectivity in cocaine use disorders. *Drug and Alcohol Dependence*, 115(1–2), 137–144. <https://doi.org/10.1016/j.drugalcdep.2011.01.009>
- Willuhn, I., Burgeno, L. M., Groblewski, P. A., & Phillips, P. E. M. (2014). Excessive cocaine use results from decreased phasic dopamine signaling in the striatum. *Nature Neuroscience*, 17(5), 704–709. <https://doi.org/10.1038/nn.3694>
- Wise, R. A. (1978). Catecholamine theories of reward: a critical review. *Brain Research*, 152(2), 215–247.
- Wise, R. A. (2004). Dopamine, learning and motivation. *Nature Reviews. Neuroscience*, 5(6), 483–494. <https://doi.org/10.1038/nrn1406>
- Wise, R. A., Leone, P., Rivest, R., & Leeb, K. (1995). Elevations of nucleus accumbens dopamine and DOPAC levels during intravenous heroin self-administration. *Synapse (New York, N.Y.)*, 21(2), 140–148. <https://doi.org/10.1002/syn.890210207>

- Wise, R. A., Newton, P., Leeb, K., Burnette, B., Pocock, D., & Justice, J. B. (1995). Fluctuations in nucleus accumbens dopamine concentration during intravenous cocaine self-administration in rats. *Psychopharmacology*, *120*(1), 10–20.
- Wise, R. A., & Raptis, L. (1986). Effects of naloxone and pimozide on initiation and maintenance measures of free feeding. *Brain Research*, *368*(1), 62–68.
- Wise, R. A., Spindler, J., deWit, H., & Gerberg, G. J. (1978). Neuroleptic-induced “anhedonia” in rats: pimozide blocks reward quality of food. *Science (New York, N.Y.)*, *201*(4352), 262–264.
- Witten, I. B., Steinberg, E. E., Lee, S. Y., Davidson, T. J., Zalocusky, K. A., Brodsky, M., ... Deisseroth, K. (2011). Recombinase-driver rat lines: tools, techniques, and optogenetic application to dopamine-mediated reinforcement. *Neuron*, *72*(5), 721–733. <https://doi.org/10.1016/j.neuron.2011.10.028>
- Wolf, M. E. (2016). Synaptic mechanisms underlying persistent cocaine craving. *Nature Reviews. Neuroscience*, *17*(6), 351–365. <https://doi.org/10.1038/nrn.2016.39>
- Worsley, K. J., & Friston, K. J. (1995). Analysis of fMRI time-series revisited--again. *NeuroImage*, *2*(3), 173–181. <https://doi.org/10.1006/nimg.1995.1023>
- Worsley, K. J., Liao, C. H., Aston, J., Petre, V., Duncan, G. H., Morales, F., & Evans, A. C. (2002). A general statistical analysis for fMRI data. *NeuroImage*, *15*(1), 1–15. <https://doi.org/10.1006/nimg.2001.0933>
- Xi, Z. X., & Stein, E. A. (1998). Nucleus accumbens dopamine release modulation by mesolimbic GABAA receptors-an in vivo electrochemical study. *Brain Research*, *798*(1–2), 156–165.
- Yamamoto, H., Fujimori, T., Sato, H., Ishikawa, G., Kami, K., & Ohashi, Y. (2014). Statistical hypothesis testing of factor loading in principal component analysis and its application to metabolite set enrichment analysis. *BMC Bioinformatics*, *15*, 51. <https://doi.org/10.1186/1471-2105-15-51>
- Yizhar, O., Fenno, L. E., Davidson, T. J., Mogri, M., & Deisseroth, K. (2011). Optogenetics in neural systems. *Neuron*, *71*(1), 9–34. <https://doi.org/10.1016/j.neuron.2011.06.004>
- You, Z. B., Chen, Y. Q., & Wise, R. A. (2001). Dopamine and glutamate release in the nucleus accumbens and ventral tegmental area of rat following lateral hypothalamic self-stimulation. *Neuroscience*, *107*(4), 629–639.
- Younce, J. R., Albaugh, D. L., & Shih, Y.-Y. I. (2014). Deep brain stimulation with simultaneous FMRI in rodents. *Journal of Visualized Experiments: JoVE*, (84), e51271. <https://doi.org/10.3791/51271>

Zahm, D. S. (2000). An integrative neuroanatomical perspective on some subcortical substrates of adaptive responding with emphasis on the nucleus accumbens. *Neuroscience and Biobehavioral Reviews*, 24(1), 85–105.

Zhang, F., Wang, L.-P., Brauner, M., Liewald, J. F., Kay, K., Watzke, N., ... Deisseroth, K. (2007). Multimodal fast optical interrogation of neural circuitry. *Nature*, 446(7136), 633–639. <https://doi.org/10.1038/nature05744>

Zhang, T. A., Placzek, A. N., & Dani, J. A. (2010). In vitro identification and electrophysiological characterization of dopamine neurons in the ventral tegmental area. *Neuropharmacology*, 59(6), 431–436. <https://doi.org/10.1016/j.neuropharm.2010.06.004>

Zhao, F., Zhao, T., Zhou, L., Wu, Q., & Hu, X. (2008). BOLD study of stimulation-induced neural activity and resting-state connectivity in medetomidine-sedated rat. *NeuroImage*, 39(1), 248–260. <https://doi.org/10.1016/j.neuroimage.2007.07.063>

Zhao, S., Ting, J. T., Atallah, H. E., Qiu, L., Tan, J., Gloss, B., ... Feng, G. (2011). Cell type-specific channelrhodopsin-2 transgenic mice for optogenetic dissection of neural circuitry function. *Nature Methods*, 8(9), 745–752.

Zhou, Q. Y., & Palmiter, R. D. (1995). Dopamine-deficient mice are severely hypoactive, adipsic, and aphagic. *Cell*, 83(7), 1197–1209.